173
3/21/80

DR. 921

GA-A15544
UC-77

POSTIRRADIATION EXAMINATION REPORT OF TRISO AND BISO COATED ThO_2 PARTICLES IRRADIATED IN CAPSULES HT-31 AND HT-33

MASTER

by
B. J. SEDLAK

Prepared under
Contract DE-AT03-76ET35300
for the San Francisco Operations Office
Department of Energy

DATE PUBLISHED: JANUARY 1980

GENERAL ATOMIC COMPANY

DISCLAIMER

NOTICE

Printed in the United States of America
Available from
National Technical Information Service
U. S. Department of Commerce
5285 Port Royal Road
Springfield, Virginia 22161
Price: Printed Copy ~~$6.00~~ 8.50 Microfiche $3.~~00~~ 5.00

GA-A15544
UC-77

POSTIRRADIATION EXAMINATION REPORT OF TRISO AND BISO COATED ThO_2 PARTICLES IRRADIATED IN CAPSULES HT-31 AND HT-33

by
B. J. SEDLAK

Prepared under
Contract DE-AT03-76ET35300
for the San Francisco Operations Office
Department of Energy

GENERAL ATOMIC PROJECT 6400
DATE PUBLISHED: JANUARY 1980

GENERAL ATOMIC COMPANY

THIS PAGE

WAS INTENTIONALLY

LEFT BLANK

ABSTRACT

Capsules HT-31 and HT-33 were uninstrumented capsule experiments irradiated in the target position of the High-Flux Isotope Reactor at Oak Ridge National Laboratory. The experiments were used to evaluate the irradiation performance of (1) fuel fabricated in a 240-mm-diameter coater for production scale-up, (2) TRISO ThO_2 and BISO ThO_2 particles, and (3) fuel with certain OPyC variables. A total of 16 BISO particle samples and 32 TRISO particle samples were irradiated to fast neutron fluences ranging from 4.0 to 11.7 x 10^{25} n/m^2 $(E > 29\ fJ)_{HTGR}$ and heavy metal burnups between 3.5% and 13.2% FIMA at temperatures from 1150° to 1530°C.

The results indicate the following:

1. Fuel coated in the 240-mm-diameter coater performs comparably to fuel fabricated in the smaller pilot plant coater.

2. TRISO and BISO ThO_2 fuel showed no significant fission product release or failure up to a burnup of 7.5% FIMA at 1250°C. At 7.5% to 9.0% FIMA and 1250°C, the BISO particles showed some failure while the TRISO particles showed no failure or fission product release. At particle surface temperatures of about 1500°C, both TRISO and BISO fuel showed very high failure levels.

3. No significant correlation between failure and the OPyC variables of coating rate, anisotropy, coating gas ratio, microporosity, or density was seen in the experiment. However, the pressure vessel performance of the TRISO particles provided support for existing models and product specifications.

THIS PAGE

WAS INTENTIONALLY

LEFT BLANK

CONTENTS

FIGURES

TABLES

1. INTRODUCTION

Capsules HT-31 and HT-33 were part of a continuing cooperative effort between General Atomic Company (GA) and Oak Ridge National Laboratory (ORNL) which was funded by the DOE-sponsored HTGR Generic Technology Program. The capsules were irradiated in the target position (HT) of the High-Flux Isotope Reactor (HFIR) at ORNL. The capsules were uninstrumented and contained relatively small sample sizes (34 to 80 particles per crucible); however, they had the advantage of low cost and achieved peak HTGR fast neutron exposures and burnups in 3 to 4 months. The very high thermal flux makes them more useful for testing fertile rather than fissile material. Consequently, these experiments are well suited as evaluation tests of HTGR fertile particle coating designs.

Each capsule contained four magazines that were designed to achieve fuel particle surface temperatures of 1200° or 1500°C. A total of 16 unbonded GA fuel particle samples were tested in two magazines in HT-31, and 32 samples were tested in the four magazines in HT-33.

The experimental test matrix for the GA fuel particle specimens was established to evaluate the relationship between fuel particle performance and (1) the size of the coater in which the particles were fabricated, (2) the coating type and particle size, and (3) OPyC variables. Some of the particle coating designs were nonconservative in order to establish failure criteria required for coated particle performance model studies. The fuel specimens in HT-31 were TRISO coated ThO_2 particles. In HT-33, half of the samples were TRISO coated ThO_2 and the other half were BISO coated ThO_2.

The capsules were irradiated for four or five HFIR cycles to fast neutron fluences ranging from 4.0 to 11.7 x 10^{25} n/m^2 $(E > 29\ fJ)_{HTGR}$ and heavy metal burnups ranging from 3.5% to 13.2% FIMA. These conditions

exceed the current HTGR peak design conditions of 6.5×10^{25} n/m^2 (E > 29 fJ)$_{HTGR}$ and 7.0% FIMA. The wide range of irradiation conditions was necessary to assess the differences in irradiation performance of the coating designs tested, and to achieve high failure probabilities in some of the particle batches. This type of data is necessary to help establish the fertile particle coating design basis.

2. DESCRIPTION OF EXPERIMENTS

2.1. OBJECTIVES

The HT-31 and HT-33 capsule tests had three primary objectives:

1. To evaluate the irradiation performance of unbonded TRISO and BISO ThO_2 fuel particles fabricated in the 240-mm-diameter pilot plant coater and compare it with the performance of particles of similar design and coating properties fabricated in the 127-mm-diameter coater. Fabricating fuel particles in the large coater was part of the planned processing scale-up. Verification of the applicability of previous specifications to the scaled-up process was desirable.

2. An equally important objective was to evaluate TRISO coated, 450-μm-diameter ThO_2 kernels as an alternate design for BISO coated ThO_2 particles. The TRISO coated particle offered a design option that was expected to be more retentive of fission products compared to BISO particles. In addition, a TRISO design with a 450-μm-diameter ThO_2 kernel was tested in an effort to reduce the performance risk associated with larger TRISO ThO_2 particles with 500-μm-diameter kernels. Empirical evidence indicated that there possibly was a particle size effect governing performance; viz., the probability of particle failure increased with particle size. Consequently, a comparative evaluation between 500-μm-diameter, TRISO coated ThO_2 kernels tested in capsules HT-28 and HT-29 and the 450-μm-diameter ThO_2 kernels tested in the HT-31 and HT-33 capsules served to help establish the expected performance benefits of the smaller particles. Capsules HT-31 and HT-33 both included a sample

from a batch of TRISO coated, 500-μm-diameter ThO_2 particles (batch 6252-05-0160) irradiated in capsules HT-28 and HT-29, which provided a benchmark for comparing results.

2. To define empirical relationships between the coating irradiation performance and the outer pyrocarbon (OPyC) coating variables of (1) density, (2) active coating gas ratio, (3) coating rate, (4) diluent gas composition, and (5) anisotropy in order to provide support for performance models and to aid in defining the permissible range of coating properties for the HTGR product specification.

2.2. DESCRIPTION OF FUEL SPECIMENS

The fuel specimens tested in capsules HT-31 and HT-33 are described in detail in Ref. 2-1. The ThO_2 kernels, fabricated at GA using the gel supported precipitation process, were nominally 450 or 500 μm in diameter. Coated parent batches numbered 6252-05-015 and 6542-27-015 were produced in the 127-mm-diameter coater and used as comparison samples for the TRISO and BISO particles made in the 240-mm-diameter pilot plant coater. A summary description of the particle batches is given in Tables 2-1 through 2-5. Photomicrographs of all the samples are shown in Ref. 2-1.

The particles for each sample were selected from the parent batch so that the particles within each individual sample had a relatively constant total coated particle density and a narrow distribution of kernel and total particle diameters. The steps used to separate the particles from their respective parent batches are outlined in Fig. 2-1 for the TRISO samples and Fig. 2-2 for the BISO samples. For the TRISO samples, coated particles were sieved to narrow the range in particle diameter. They were then further separated by selecting, using a constant density liquid (thalium mallonate) column, those particles having batch-average total coated particle density. Following density separation, particles were individually radiographed to characterize each sample. Particles were subsequently heated in a vacuum for 1 hour at 1400°C to ensure volatilization

TABLE 2-1
FABRICATION CONDITIONS FOR TRISO ThO_2 PARTICLES TESTED IN CAPSULES HT-31 AND HT-33

				Buffer			IPyC			SiC				OPyC				
Sample Number	Coater Size (mm)	Kernel Diameter (μm)	Kernel Load (kg)	Coating Rate (μm/min)	Coating Gas	Diluent Gas	Coating Rate (μm/min)	Coating Gas	Diluent Gas	Charge Load (kg)	Coating Rate (μm/min)	Coating Gas	Diluent Gas	Charge Load (kg)	Coating Rate (μm/min)	Coating Gas	Active Coating Gas Ratio[a]	Diluent Gas
6252-05-0160-005	127	511	2.0	20.74	C_2H_2	Ar	3.93	C_2H_2/C_3H_6	Ar	2.4	0.254	CH_3SiCl_3	H_2	1.2	4.48	C_2H_2/C_3H_6[a]	0.16	Ar
-006		509																
-007		509																
-008		510																
6252-06-0161-001	240	449	14.5	10.53	C_2H_2	Ar	4.09	C_2H_2/C_3H_6	Ar	18.2	0.225	CH_3SiCl_3	H_2	19.5	5.04	C_2H_2/C_3H_6	0.42	Ar
-002		448																
-003		448																
-004		450																
6252-06-0261-001	240	448	15.0	10.13	C_2H_2	Ar	4.43	C_2H_2/C_3H_6	Ar	19.4	0.169	CH_3SiCl_3	H_2	11.4	5.60	C_2H_2/C_3H_6	0.36	Ar
-002		448																
-003		448																
-004		449																
6252-07-0161-001	240	448	15.0	9.77	C_2H_2	Ar	4.43	C_2H_2/C_3H_6	Ar	19.4	0.168	CH_3SiCl_3	H_2	24.2	5.92	C_2H_2/C_3H_6	0.50	Ar
-002		448																
-003		448																
-004		447																
6252-07-0261-001	240	447	15.0	10.15	C_2H_2	Ar	4.43	C_2H_2/C_3H_6	Ar	19.4	0.165	CH_3SiCl_3	H_2	11.4	5.28	C_2H_2/C_3H_6	0.36	Ar
-002		446																
-003		446																
-004		447																
6252-08-0161-001	240	447	15.0	10.12	C_2H_2	Ar	4.43	C_2H_2/C_3H_6	Ar	19.4	0.173	CH_3SiCl_3	H_2	11.4	5.87	C_2H_2/C_3H_6	0.39	Ar
-002		447																
-003		447																
-004		448																
6252-09-0161-001	240	447	14.6	10.71	C_2H_2	Ar	4.09	C_2H_2/C_3H_6	Ar	18.2	0.223	CH_3SiCl_3	H_2	8.8	7.52	C_2H_2/C_3H_6	0.38	Ar
-002		447																
-003		448																
-004		447																
6252-10-0161-001	240	447	14.6	10.19	C_2H_2	Ar	4.09	C_2H_2/C_3H_6	Ar	18.2	0.228	CH_3SiCl_3	H_2	8.8	8.43	C_2H_2/C_3H_6	0.53	Ar
-002		446																
-003		447																
-004		445																

[a] Active coating gas volume fraction = C/(C + L + D); C = active coating gas flow rate (C_2H_2/C_3H_6); L = levitation gas flow rate (Ar or He or N_2); D = diluent gas flow rate (Ar or He or N_2 or H_2).

TABLE 2-2
GENERAL DESCRIPTION OF TRISO PARTICLES TESTED IN HT-31

Sample Number	Buffer		IPyC				SiC		OPyC				Total Coated Particle			Test Conditions				
	Thickness (μm)	Density[a] (Mg/m)	Thickness (μm)	Density[a] (Mg/m^3)	BAF$_o$[b]	Mean OPTAF[b]	Thickness (μm)	Density[a] (Mg/m^3)	Thickness (μm)	Density[a] (Mg/m^3)	BAF$_o$[b]	Microporosity[c] (μℓ/kg)	Coating Thickness (μm)	Mean Diameter (μm)	Mean Density[d] (Mg/m^3)	Number of Particles Tested	Sample Position	Design Test Temp. (°C)	Design Peak Fast Fluence ($E > 29$ fJ)$_{HTGR}$ (10^{25} n/m^2)	Design Burnup (% FIMA)
6252-05-0160-005	69	1.04	30	1.84	ND	1.18	35	3.20	48	1.85	ND	32.9	176	872	3.59	34	43	1200	5.6	6.2
6252-05-0160-006	68	1.04	30	1.84	ND	1.18	34	3.20	50	1.85	ND	32.9	176	873	3.59	51	27	1500	7.7	8.4
6252-06-0161-001	69	1.07	34	1.90	1.076	1.30	41	3.22	45	1.74	1.022	49	181	819	3.39	53	49	1200	4.4	5.0
6252-06-0161-002	68	1.07	34	1.90	1.076	1.30	41	3.22	44	1.74	1.022	49	181	823	3.39	78	38	1500	7.0	7.7
6252-06-0261-001	60	1.12	39	1.93	1.088	1.30	39	3.21	47	1.70	1.028	59	190	813	3.26	52	48	1200	4.7	5.2
6252-06-0261-002	59	1.12	39	1.93	1.088	1.30	39	3.21	46	1.70	1.028	59	190	812	3.26	77	36	1500	7.3	7.9
6252-07-0161-001	57	1.12	39	1.93	1.079	1.32	39	3.20	50	1.81	1.027	59	191	816	3.23	54	46	1200	5.0	5.6
6252-07-0161-002	58	1.12	39	1.93	1.079	1.32	40	3.20	52	1.81	1.027	59	191	823	3.23	80	35	1500	7.4	8.0
6252-07-0261-001	63	1.12	39	1.93	1.098	1.31	39	3.21	46	1.80	1.030	48	187	820	3.32	53	45	1200	5.2	5.8
6252-07-0261-002	62	1.12	39	1.93	1.098	1.31	39	3.21	47	1.80	1.030	48	187	821	3.32	78	33	1500	7.5	8.2
6252-08-0161-001	60	1.12	39	1.93	1.065	1.29	39	3.20	49	1.89	1.034	46	194	836	3.30	54	51	1200	3.9	4.5
6252-08-0161-002	60	1.12	39	1.93	1.065	1.29	39	3.20	50	1.89	1.034	46	194	836	3.30	80	29	1500	7.7	8.4
6252-09-0161-001	66	1.07	34	1.90	1.095	1.28	41	3.22	47	1.78	1.018	62	185	823	3.34	53	42	1200	5.9	6.4
6252-09-0161-002	63	1.07	34	1.90	1.095	1.28	42	3.22	48	1.78	1.018	62	185	819	3.34	78	32	1500	7.6	8.2
6252-10-0161-001	63	1.07	34	1.90	1.074	1.24	42	3.22	53	1.98	1.036	46	189	829	3.31	53	40	1200	6.2	6.8
6252-10-0161-002	62	1.07	34	1.90	1.074	1.24	42	3.22	51	1.98	1.036	46	189	824	3.31	79	30	1500	7.6	8.3

[a] Measured on parent batch prior to density separation.

[b] Measured on nonheat-treated parent batch. Bacon Anisotropy Factor measured using 24-μm-diameter spot.

[c] Measured by Hg intrusion at 68.9 MPa.

[d] Determined using Hg-porosimetry.

TABLE 2-3
GENERAL DESCRIPTION OF TRISO PARTICLES TESTED IN HT-33

Sample Number	Buffer		IPyC				SiC		OPyC				Total Coated Particle			Test Conditions				
	Thickness (μm)	Density[a] (Mg/m³)	Thickness (μm)	Density[a] (Mg/m³)	BAF$_o$[b]	Mean OPTAF[b]	Thickness (μm)	Density[a] (Mg/m³)	Thickness (μm)	Density[a] (Mg/m³)	BAF$_o$[b]	Microporosity[c] (μℓ/kg)	Coating Thickness (μm)	Mean Diameter (μm)	Mean Density[d] (Mg/m³)	Number of Particles Tested	Sample Position	Design Test Temp (°C)	Design Peak Fast Fluence (E > 29 fJ)$_{HTGR}$ (10^{25} n/m²)	Design Burnup (% FIMA)
6252-05-0160-007	68	1.04	30	1.84	ND	1.18	35	3.20	50	1.85	ND	32.9	176	872	3.59	34	45	1200	6.5	9.4
6252-05-0160-008	68	1.04	30	1.84	ND	1.18	34	3.20	48.	1.85	ND	32.9	176	870	3.59	51	30	1500	9.6	12.4
6252-06-0161-003	64	1.07	34	1.90	1.076	1.30	41	3.22	44	1.74	1.022	49	181	818	3.39	53	48	1200	5.9	8.0
6252-06-0161-004	68	1.07	34	1.90	1.076	1.30	41	3.22	46	1.74	1.022	49	181	824	3.39	78	33	1500	9.3	12.1
6252-06-0261-003	60	1.12	39	1.93	1.088	1.30	38	3.21	47	1.70	1.028	59	190	812	3.26	52	46	1200	6.3	8.6
6252-06-0261-004	59	1.12	39	1.93	1.088	1.30	39	3.21	48	1.70	1.028	59	190	816	3.26	77	32	1500	9.5	12.2
6252-07-0161-003	58	1.12	39	1.93	1.079	1.32	39	3.20	51	1.81	1.027	59	191	826	3.23	54	43	1200	6.9	9.5
6252-07-0161-004	58	1.12	39	1.93	1.079	1.32	38	3.20	52	1.81	1.027	59	191	821	3.23	80	36	1500	9.1	11.8
6252-07-0261-003	61	1.12	39	1.93	1.098	1.31	39	3.21	46	1.80	1.030	48	187	813	3.32	53	42	1200	7.3	9.7
6252-07-0261-004	62	1.12	39	1.93	1.098	1.31	38	3.21	46	1.80	1.030	48	187	814	3.32	78	35	1500	9.2	11.9
6252-08-0161-003	61	1.12	39	1.93	1.065	1.29	38	3.20	47	1.89	1.034	46	194	836	3.30	54	49	1200	5.5	7.5
6252-08-0161-004	61	1.12	39	1.93	1.065	1.29	38	3.20	50	1.89	1.034	46	194	836	3.30	80	27	1500	9.6	12.5
6252-09-0161-003	65	1.07	34	1.90	1.095	1.28	42	3.22	47	1.78	1.018	62	185	824	3.34	53	40	1200	7.6	10.2
6252-09-0161-004	67	1.07	34	1.90	1.095	1.28	42	3.22	49	1.78	1.018	62	185	826	3.34	78	38	1500	8.7	11.5
6252-10-0161-003	63	1.07	34	1.90	1.074	1.24	42	3.22	51	1.98	1.036	46	189	826	3.31	53	51	1200	4.9	7.0
6252-10-0161-004	62	1.07	34	1.90	1.074	1.24	42	3.22	51	1.98	1.036	46	189	818	3.31	79	29	1500	9.6	12.5

[a] Measured on parent batch prior to density separation.

[b] Measured on nonheat-treated parent batch. Bacon Anisotropy Factor measured using 24-μm-diameter spot.

[c] Measured by Hg intrusion at 68.9 MPa.

[d] Determined using Hg porosimetry.

TABLE 2-4
FABRICATION CONDITIONS OF BISO ThO_2 PARTICLES TESTED IN HT-33

Sample Number	Coater Size (mm)	Kernel Diameter (μm)	Initial Load (kg)	Buffer			OPyC			
				Coating Rate (μm/min)	Coating Gas	Diluent Gas	Coating Rate (μm/min)	Coating Gas	Active Coating Gas Ratio[a]	Diluent Gas
6542-27-0161-001	127	500	2	18.6	C_2H_2	Ar	4.6	C_2H_2/C_3H_6	0.29	Ar
6542-27-0161-002	127	503								
6542-29-0261-001	240	504	20	9.0	C_2H_2	Ar	4.3	C_2H_2/C_3H_6	0.46	N_2
6542-29-0261-002	240	503								
6542-39-0161-001	240	508	20	8.6	C_2H_2	Ar	4.1	C_2H_2/C_3H_6	0.45	N_2
6542-39-0161-002	240	508								
6542-40-0161-001	240	500	13	13.6	C_2H_2	Ar	5.8	C_2H_2/C_3H_6	0.20	H_2
6542-40-0161-002	240	502								
6542-40-0260-001	240	503	13	13.9	C_2H_2	Ar	5.8	C_2H_2/C_3H_6	0.24	H_2
6542-40-0260-002	240	500								
6542-40-0261-001	240	500								
6542-40-0261-002	240	501								
6542-41-0160-001	240	507	13	13.0	C_2H_2	Ar	5.8	C_2H_2/C_3H_6	0.45	N_2
6542-41-0160-002	240	505								
6542-41-0161-001	240	503								
6542-41-0161-002	240	503								

[a] Active coating gas volume fraction = C/(C + L + D); C = active coating gas flow rate (C_2H_2/C_3H_6); L = levitation gas flow rate (Ar or He or N_2); D = diluent gas flow rate (Ar or He or N_2 or H_2).

TABLE 2-5
GENERAL DESCRIPTION OF BISO PARTICLES TESTED IN HT-33

Sample No.	Heat Treatment	Buffer		OPyC				Total Coated Particle			Test Conditions				
		Thickness[a] (μm)	Density[b,c] (Mg/m^3)	Thickness (μm)	Density[d,e] (Mg/m^3)	BAF_o[d,f]	Microporosity[h] (ml/kg)	Coating Thickness[a] (μm)	Mean Diameter[a] (μm)	Mean Density (Mg/m^3)	Number of Particles Tested	Sample Position	Design Test Temp. (°C)	Design Peak Fast Fluence ($E > 29$ fJ) (10^{25} n/m^2)	Design Peak Burnup (% FIMA)
6542-27-0161-001	Yes	87	1.09	75	1.86[g]	1.041	23.3	162	823	3.45	40	8	1200	6.8	9.1
6542-27-0161-002	Yes	88	1.09	75	1.86[g]	1.041	23.3	164	829	3.45	57	17	1500	9.5	11.7
6542-29-0261-001	Yes	94	1.13	76	1.96	1.081	19.5	170	843	3.45	39	10	1200	7.4	9.6
6542-29-0261-002	Yes	93	1.13	72	1.96	1.081	19.5	166	833	3.45	55	15	1500	9.2	11.4
6542-39-0161-001	Yes	86	1.13	71	1.98	1.079	17.5	156	821	3.61	38	2	1200	5.1	7.2
6542-39-0161-002	Yes	86	1.13	74	1.98	1.079	17.5	161	826	3.61	54	21	1500	9.9	12.1
6542-40-0161-001	Yes	91	1.10	73	1.74	1.042	25.0	164	828	3.35	41	4	1200	5.8	7.8
6542-40-0161-002	Yes	93	1.10	71	1.74	1.042	25.0	164	827	3.35	58	23	1500	10.0	12.2
6542-40-0260-001	No	85	1.10	76	1.77	1.038	23.5	161	829	3.36	41	7	1200	6.6	8.8
6542-40-0260-002	No	88	1.10	77	1.77	1.038	23.5	164	826	3.36	58	26	1500	10.2	12.4
6542-40-0261-001	Yes	89	1.10	78	1.77	1.038	22.5	168	832	3.39	41	5	1200	6.0	8.2
6542-40-0261-002	Yes	87	1.10	76	1.77	1.038	22.5	164	828	3.39	58	24	1500	10.1	12.3
6542-41-0160-001	No	91	1.13	70	2.00	1.060	19.0	160	827	3.51	40	13	1200	8.1	10.3
6542-41-0160-002	No	88	1.13	68	2.00	1.060	19.0	155	817	3.51	56	20	1500	9.8	12.0
6542-41-0161-001	Yes	92	1.13	69	2.02	1.081	22.5	161	825	3.54	40	11	1200	7.6	9.6
6542-41-0161-002	Yes	92	1.13	69	2.02	1.081	22.5	161	823	3.54	56	18	1500	9.6	11.8

[a] Measured or calculated or capsule test samples.

[b] Determined by mathematical calculation.

[c] Measured on as-coated parent batch.

[d] Measured on heat-treated parent batches, except where noted, for the heat-treated capsule test samples; otherwise the as-coated parent batches were measured.

[e] Measured by a liquid gradient technique.

[f] Optical anisotropy measured using the Seibersdorf optical unit at GA using a 24-μm-diameter light spot at the center of the coatings.

[g] Values for as-coated parent batch; data not available for heat-treated parent batch.

[h] Measured by Hg intrusion at 58.9 MPa.

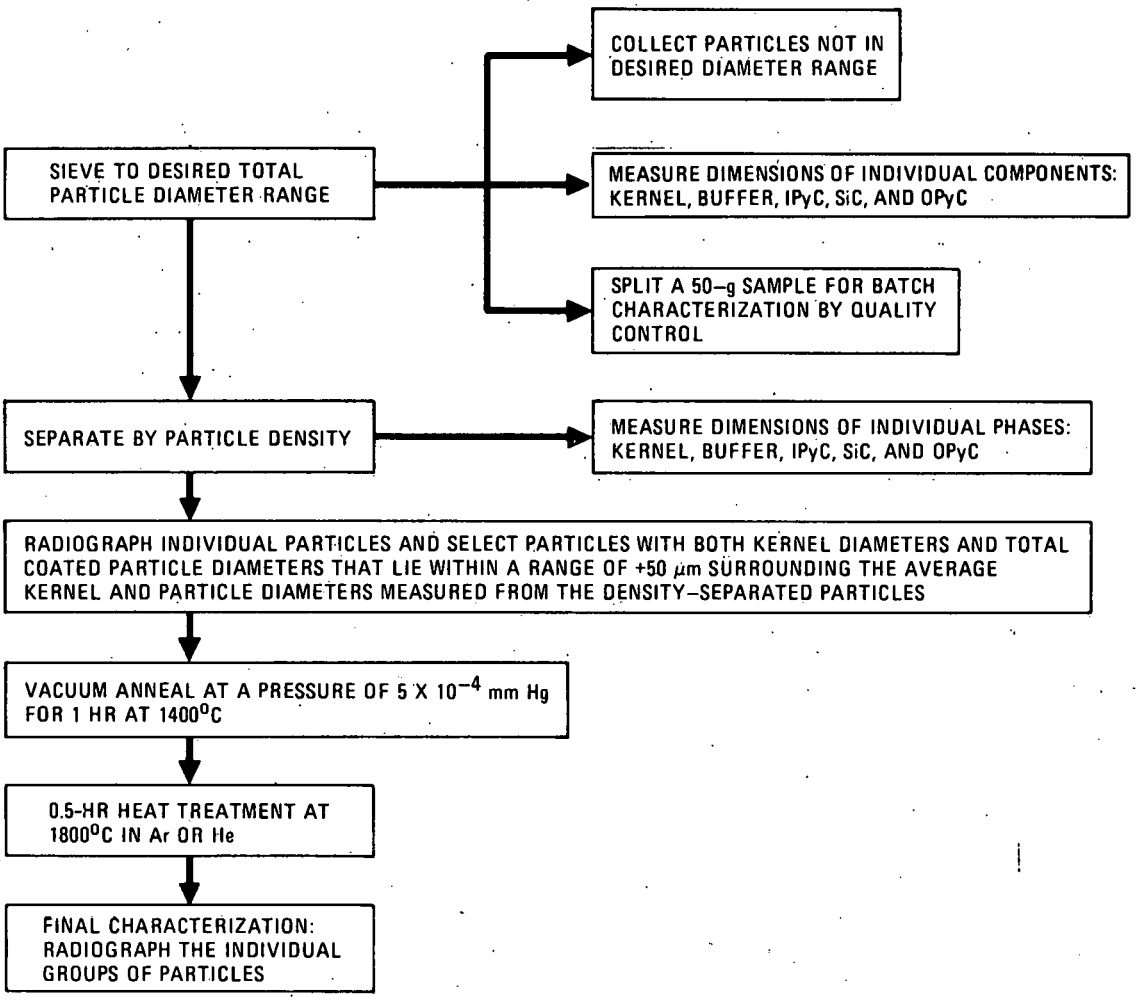

Fig. 2-1. Steps involved in selecting TRISO coated ThO_2 particles for insertion in irradiation experiments HT-31 and HT-33

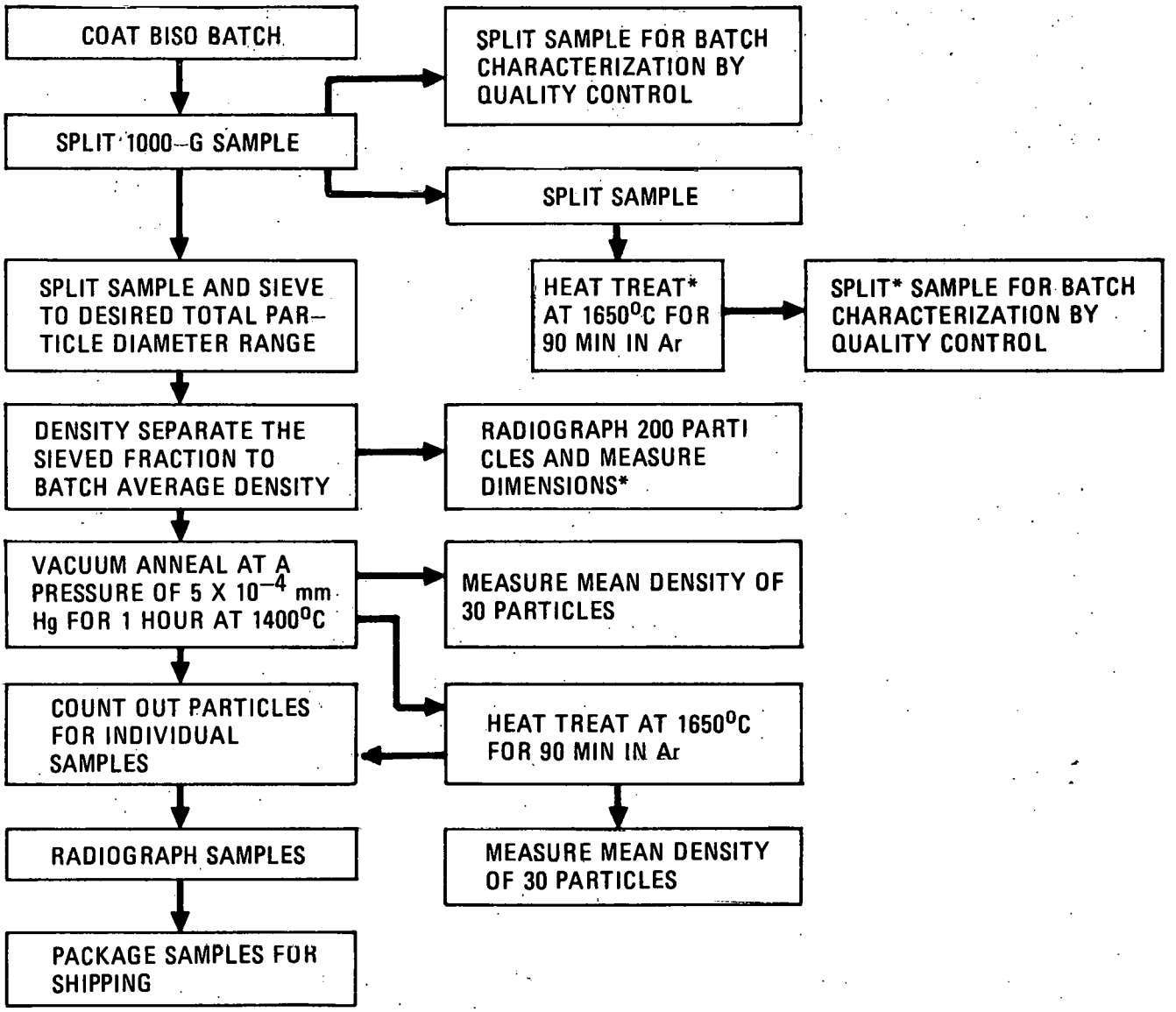

Fig. 2-2. Steps involved in obtaining the BISO coated ThO_2 particle samples for irradiation capsule HT-33. The operations marked with an asterik were not performed on parent batch 6542-27-015.

of any of the fluids used for density separation. Lastly, the particles were heat treated for 0.5 hour at 1800°C in Ar. This step was done to simulate the processing temperature that fuel particles would experience during fuel rod fabrication. As seen in Fig. 2-2, BISO samples were selected in the same manner as the TRISO samples. One additional heat treatment, for 90 min at 1650°C, was done on a split sample of each BISO parent batch coated in the large-diameter coater. The heat-treated samples are identified in Table 2-5. The purpose of the heat treatment was to determine changes in coating properties caused by heat treating and is discussed fully in Ref. 2-1.

2.3. CAPSULE DESIGN

Each HT capsule (Fig. 2-3) consisted of a metal tube with an external configuration identical to that of an HFIR target rod. After loading, the capsule was sealed with 99.995% pure Ar at a pressure of 0.14 MPa (5 psig). There was no thermocouple instrumentation for direct temperature measurement or utilization of purge gas to monitor circulating fission product activity. It was not possible to alter the temperature of fuel specimens in pile with this type of capsule design.

Each capsule contained four cylindrical graphite magazines. Each magazine, in turn, contained 13 small graphite crucibles with an annular cavity that held from 34 to 80 fuel particles. GA samples were placed in eight of the 13 crucibles. Low-enriched UO_2 was placed in the other five crucibles in each magazine to ensure a more uniform power generation and temperature over the life of the experiment. Two of the magazines in each capsule were designed for positions operating at 1200°C particle surface temperature and a fast fluence of 3.9 to 7.6 x 10^{25} n/m^2 $(E > 29\ fJ)_{HTGR}$. The other two magazines in each capsule were in positions to operate at 1500°C particle surface temperature and 7.0 to 9.7 x 10^{25} n/m^2 $(E > 29\ fJ)_{HTGR}$. GA samples occupied the bottom two magazines (16 positions) in capsule HT-31 and all 4 magazines (32 positions) in capsule HT-33.

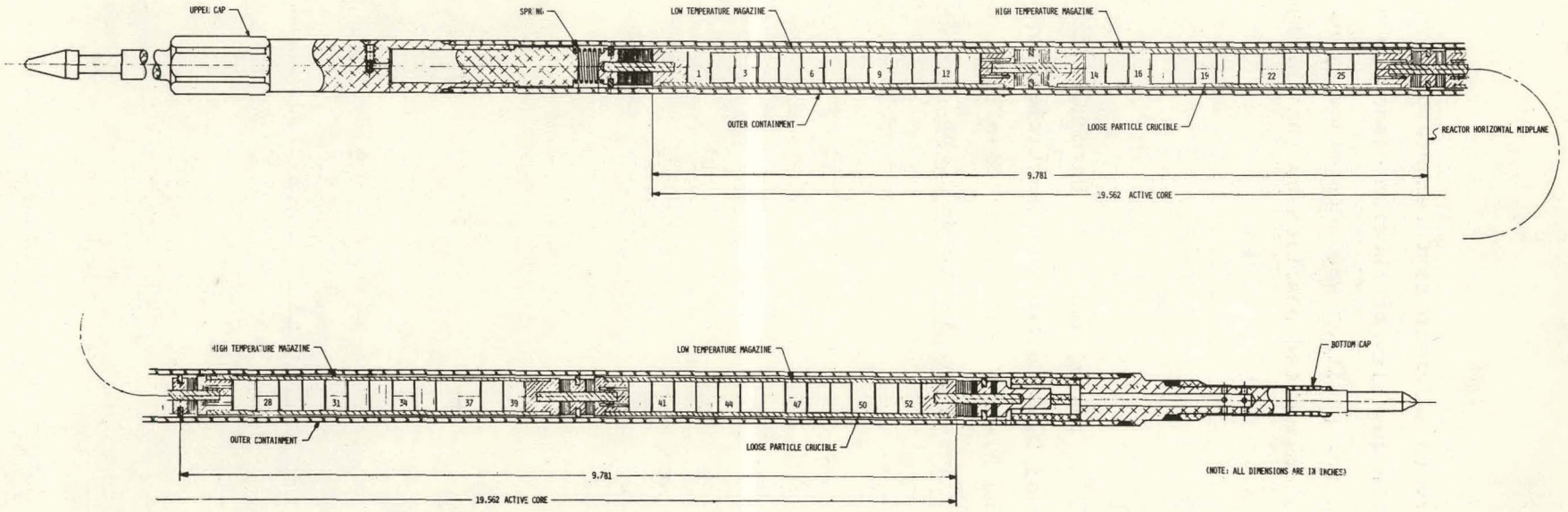

Fig. 2-3. Schematic showing the HT capsule design

The power necessary to maintain test temperatures in each crucible was used to determine the quantity of thorium needed in each position. The number of particles per position was determined by dividing the required weight of thorium for a designated position by the thorium weight per particle.

REFERENCE

2-1. Kovacs, W. J., C. A. Young, and D. P. Harmon, "Preirradiation Report of TRISO and BISO Coated ThO_2 Particles for Irradiation in Capsules HT-31 and HT-33," ERDA Report GA-A13923, General Atomic Company, November 1976, pp. 3-3 to 3-34, pp. 4-2 to 4-27.

3. IRRADIATION PARAMETERS

3.1. CAPSULE OPERATING HISTORY

Capsule HT-31 was inserted into HFIR target position G-5 on March 14, 1976, and removed on June 16, 1976, after 2146.56 hours at 100-MW reactor power (4 cycles). Capsule HT-33 was inserted into HFIR target position G-5 on June 17, 1976, and removed on October 21, 1976, after 5 cycles and 2759 hours at 100-MW reactor power. The irradiation proceeded without incident for both capsules. The HFIR operating history for the cycles encompassing the periods of capsule irradiation is given in Table 3-1.

3.2. NEUTRON FLUX

The fast neutron flux and fluence levels $(E > 29\ fJ)_{HTGR}$ were calculated by workers at ORNL and are reported in Ref. 3-1. The values for fast fluence were revised and reported by private communication from K. R. Thoms at ORNL to C. A. Young at GA. These revised values are used in this report and are given in Tables 3-2 through 3-4.

3.3. HEAVY METAL BURNUP

Capsules HT-31 and HT-33 were the first GA HFIR target capsules to have burnup measured by chemical analysis and calculated by a new computer code (HIFR, named for the high-flux isotope reactor) developed for the HT capsule series at GA. Earlier HT capsule burnup values were only calculated at ORNL using the CACA-2 code (Ref. 3-2). Three fertile fuel particle samples were selected for chemical analysis: one sample each from the high and low neutron flux regions in HT-33 and one sample from a mid-flux region in HT-31.

TABLE 3-1
OPERATIONAL HISTORY OF CAPSULES HT-31 AND HT-33

Capsule	HFIR Cycle	Dates		Irradiation Time[a] During Cycle		Irradiation Time[a] Accumulated	
		Begin	End	Hours	Days	Hours	Days
				[b]		[b]	
HT-31	130	3/14/76	4/6/76	557.76	23.24	557.76	23.24
	131	4/7/76	4/30/76	552.48	23.02	1110.24	46.26
	132	5/1/76	5/22/76	489.60	20.40	1599.84	66.66
	133	5/23/76	6/16/76	546.72	22.78	2146.56	89.44
				[c]		[c]	
HT-33	134	6/17/76	7/9/76	534	22.25	534	22.25
	135	7/10/76	8/1/76	547	22.79	1081	45.04
	136	8/2/76	8/25/76	540	22.50	1621	67.54
	137	9/2/76	9/25/76	564	22.75	2185	90.29
	138	9/27/76	10/21/76	574	23.92	2759	114.21

[a] Irradiation time at 100-MW reactor power.

[b] Ref. 3-1, p. 248.

[c] Ref. 3-1, p. 264.

TABLE 3-2
IRRADIATION CONDITIONS FOR TRISO HT-31 PARTICLES

Particle Batch Retrieval Number	Sample Position	Number of Particles Tested	Time Averaged Temp.(a) (°C)	Fast Fluence ($E > 29$ fJ)$_{HTGR}$ (10^{25} n/m^2)	Burnup (% FIMA)		Percent Difference
					ORNL	GA	
6252-05-0160-006	27	51	1530	8.1	8.6	9.2	-7.2
6252-08-0161-002	29	80	1520	8.1	8.4	9.0	-7.3
6252-10-0161-002	30	79	1430	8.0	8.3	8.8	-6.5
6252-09-0161-002	32	78	1420	7.8	8.1	8.6	-6.2
6252-07-0261-002	33	78	1410	7.8	8.0	8.4	-5.4
6252-07-0161-002	35	80	1400	7.6	7.7	8.1	-5.2
6252-06-0261-002	36	77	1390	7.5	7.6	7.9	-3.7
6252-06-0161-002	38	78	1410	7.3	7.3	7.5	-2.9
6252-10-0161-001	40	53	1250	6.5	6.2	6.1	2.3
6252-09-0161-001	42	53	1220	6.1	5.8	5.6	2.9
6252-05-0160-005	43	34	1250	5.9	5.5	5.4	2.2
6252-07-0261-001	45	53	1190	5.4	5.1	4.9	3.5
6252-07-0161-001	46	54	1180	5.2	4.9	4.7	4.5
6252-06-0261-001	48	52	1160	4.8	4.4	4.2	4.1
6252-06-0161-001	49	53	1150	4.5	4.2	4.0	5.5
6252-08-0161-001	51	54	1150	4.0	3.8	3.5	7.9

(a) Maximum particle surface temperature.

TABLE 3-3
IRRADIATION CONDITIONS FOR TRISO HT-33 PARTICLES

Particle Batch Retrieval Number	Sample Position	Number of Particles Tested	Time Averaged Temp.(a) (°C)	Fast Fluence $(E > 29\ fJ)_{HTGR}$ $(10^{25}\ n/m^2)$	Burnup (% FIMA)		Percent Difference
					ORNL	GA	
6252-08-0161-004	27	80	1420	11.7	12.5	13.2	-5.6
6252-10-0161-004	29	79	1470	11.5	12.3	12.9	-4.9
6252-05-0160-008	30	51	1510	11.4	12.1	12.7	-5.0
6252-06-0261-004	32	77	1460	11.2	11.9	12.4	-4.2
6252-06-0161-004	33	78	1450	11.1	11.7	12.2	-4.3
6252-07-0261-004	35	78	1440	10.9	11.4	11.7	-2.6
6252-07-0161-004	36	80	1430	10.7	11.3	11.5	-1.8
6252-09-0161-004	38	78	1450	10.5	10.9	11.0	-0.9
6252-09-0161-003	40	53	1210	9.3	9.3	9.0	3.2
6252-07-0261-003	42	53	1250	8.7	8.7	8.4	3.4
6252-07-0161-003	43	54	1230	8.4	8.4	8.0	4.8
6252-05-0160-007	45	34	1260	7.8	7.8	7.4	5.1
6252-06-0261-003	46	52	1220	7.5	7.5	7.1	5.3
6252-06-0161-003	48	53	1200	6.8	6.9	6.4	7.2
6252-08-0161-003	49	54	1180	6.5	6.6	6.0	9.1
6252-10-0161-003	51	53	1190	5.7	5.9	5.4	8.5

(a) Maximum particle surface temperature.

TABLE 3-4
IRRADIATION CONDITIONS FOR BISO HT-33 PARTICLES

Particle Batch Retrieval Number	Sample Position	Number of Particles Tested	Time Averaged Temp.(a) (°C)	Fast Fluence $(E > 29\ fJ)_{HTGR}$ $(10^{25}\ n/m^2)$	Burnup (% FIMA)		Burnup Percent Difference
					ORNL	GA	
6542-39-0161-001	2	38	1240	5.7	5.9	5.4	8.5
6542-40-0161-001	4	41	1220	6.5	6.6	6.0	9.1
6542-40-0261-001	5	41	1230	6.8	6.9	6.4	7.2
6542-40-0260-001	7	41	1250	7.5	7.5	7.1	5.3
6542-27-0161-001	8	40	1270	7.8	7.8	7.4	5.1
6542-29-0261-001	10	39	1290	8.4	8.4	8.0	4.8
6542-41-0161-001	11	40	1300	8.7	8.7	8.4	3.4
6542-41-0160-001	13	40	1260	9.3	9.3	9.0	3.2
6542-29-0261-002	15	55	1490	10.5	10.9	11.0	-0.9
6542-27-0161-002	17	57	1470	10.7	11.3	11.5	-1.8
6542-41-0161-002	18	56	1480	10.9	11.4	11.7	-2.6
6542-41-0160-002	20	56	1490	11.1	11.7	12.2	-4.3
6542-39-0161-002	21	54	1500	11.2	11.9	12.4	-4.2
6542-40-0161-002	23	58	1500	11.4	12.1	12.7	-5.0
6542-40-0261-002	24	58	1510	11.5	12.3	12.9	-4.9
6542-40-0260-002	26	58	1460	11.7	12.5	13.2	-5.6

(a) Maximum particle surface temperature.

The chemical analysis was done in accordance with General Atomic Procedure ACD-RC-001, "Atomic Percent Fission in Fissile and Fertile Fuel Particles." Using the heavy metal loading and the results of the chemical analysis, the FIMAs for each of the three batches were calculated using the following equation:

$$F_3 = \frac{F}{Th_I} \times 100 = \frac{F}{(Th_R + U_R + F)} \times 100 = \% \text{ FIMA} \quad ,$$

where F_3 = heavy element atom percent fission from U-233 (Th-232),
Th_I = atoms thorium initial per total sample,
Th_R = atoms thorium remaining per total sample,
U_R = atoms uranium remaining per total sample,
F = atoms fission per total sample.

The FIMAs for each batch are compared as follows:

	Calculated FIMA	Measured FIMA
HT-31-38	7.4%	7.6%
HT-33-51	5.1%	5.4%
HT-33-27	11.4%	12.2%

The heavy metal burnup in the HT capsules was calculated by the computer code HIFR. As shown in Table 3-5, the burnup values calculated with the HIFR code were in good agreement with the measured values. The HIFR code value for batch HT-33-27 did not agree as well with the mass spectrometry values as did the other two batches. It did agree within 8%, however, which is within the error of the measurement.

Figure 3-1 shows FIMA values calculated by ORNL (CACA-2 code) and by GA (HIFR code) and the measured values for the three capsule samples analyzed. The burnup values calculated by ORNL and by GA with their percentage differences are given in Tables 3-2 through 3-4. The values calculated by the two different computer codes differ less than ±10% for all

TABLE 3-5
CALCULATED AND MEASURED BURNUP (% FIMA)

Position HT-31-38	
Mass spectrometry	7.6
HIFR	7.51
Position HT-33-51	
Mass spectrometry	5.4
HIFR	5.38
Position HT-33-27	
Mass spectrometry	12.2
HIFR	13.25

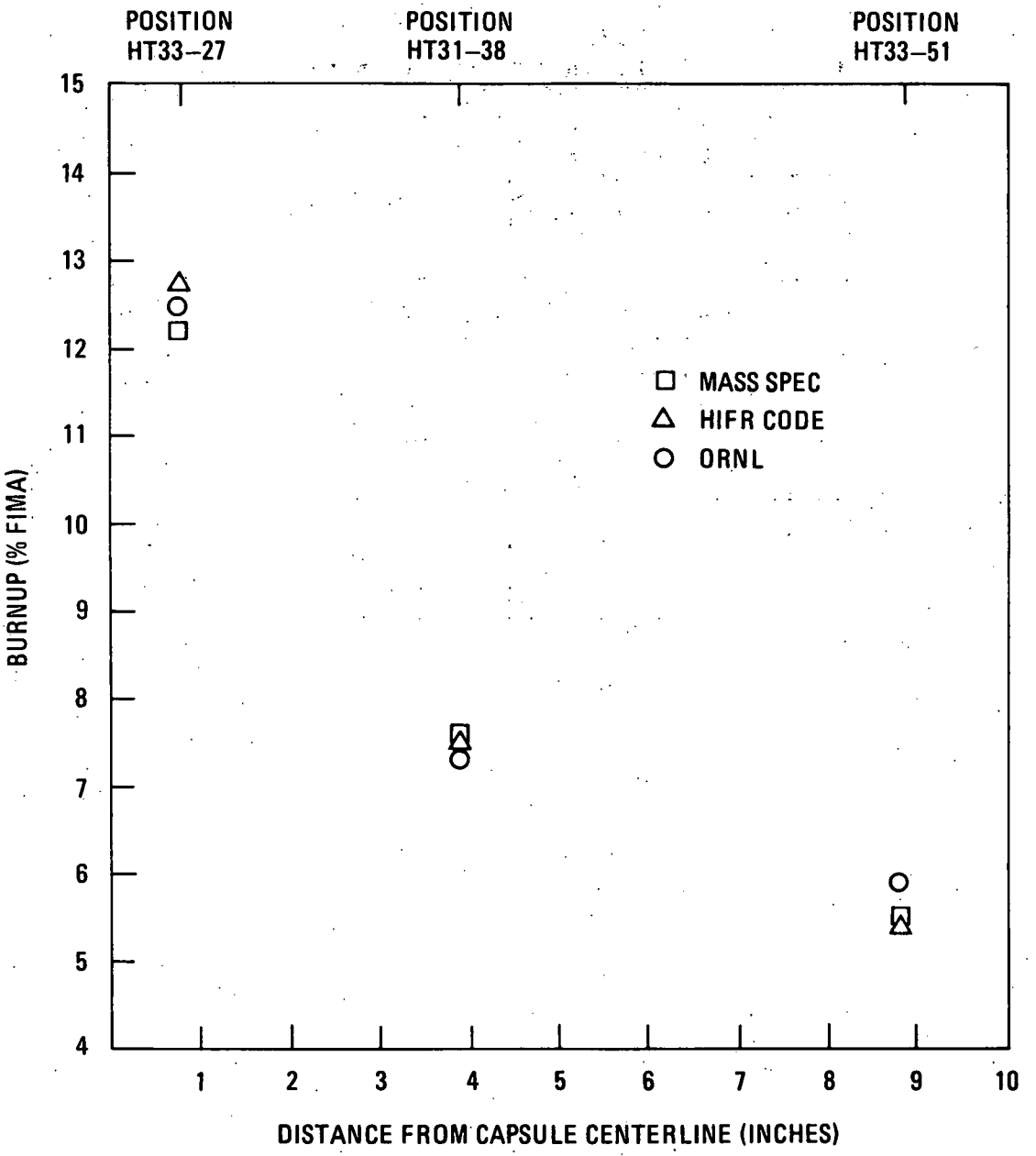

Fig. 3-1. Calculated and measured burnup values for capsules HT-31 and HT-33

the samples in both HT capsules. The burnup values calculated by GA using the new HIFR computer code have been used in this report.

3.4. THERMAL ANALYSIS

There are no provisions for direct temperature monitoring in the HT capsules. A detailed thermal analysis of each capsule was performed by ORNL with the HTCAP computer code (Ref. 3-3). The total heat generation within each capsule was calculated, and a modified one-dimensional heat transfer analysis was performed. The maximum particle surface operating temperatures were calculated at 1-day intervals for each HFIR irradiation cycle. Figures 3-2 and 3-3 show the calculated irradiation temperature and power generated per particle for representative particle samples from a low-temperature magazine in HT-33 and a high-temperature magazine in HT-31, respectively. The calculated irradiation temperature and power generated per particle for each sample are given in Refs. 3-4 and 3-5. The time-averaged temperature for each fuel sample is reported in Tables 3-2 through 3-4.

REFERENCES

3-1. "Gas Cooled Reactor Programs HTGR Base-Technology Program Progress Report July 1, 1975 - December 31, 1976," ERDA Report ORNL-5274, Oak Ridge National Laboratory, November 1977, pp. 240-250.

3-2. Allen, E. J., "CACA-2: Revised Version of CACA - A Heavy Isotope and Fission Product Concentration Calculation Code for Experimental Irradiation Capsules," ERDA Report ORNL-TM-5266, Oak Ridge National Laboratory, February 1976.

3-3. Kania, M. J., "HTCAP - A Fortran IV Program for Calculating Coated Particle Operating Temperatures in HFIR Target Irradiation Experiments," ERDA Report ORNL-TM-5332, Oak Ridge National Laboratory, May 1976.

3-4. "Irradiation Performance of HTGR Fuel in HFIR Capsule HT-31," DOE Report ORNL-5510, Oak Ridge National Laboratory, May 1979, pp. 13-16.

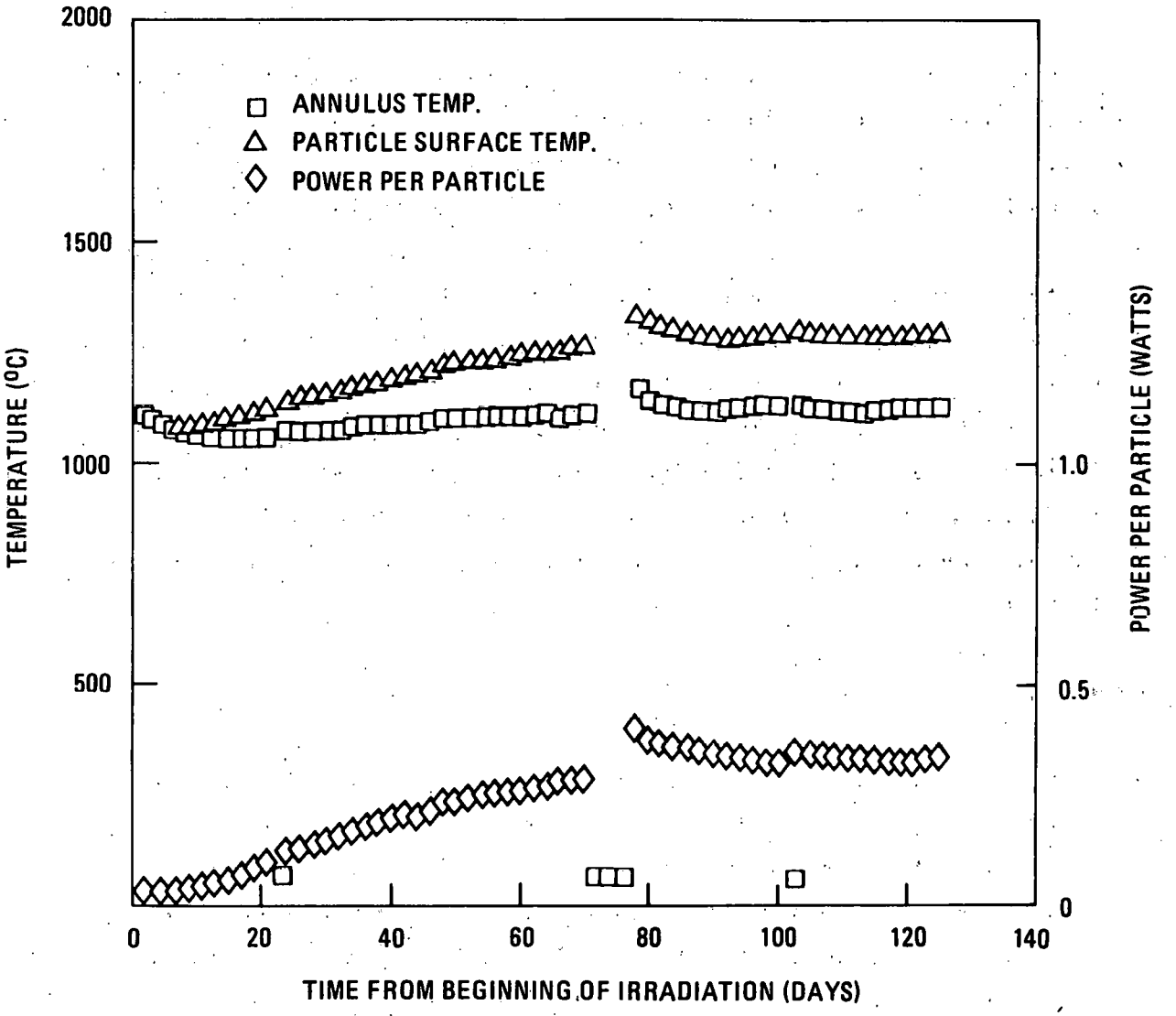

Fig. 3-2. Temperature of HT-33 particle holder 36, sample 6252-06-0261-003, 812.0-μm particle diameter

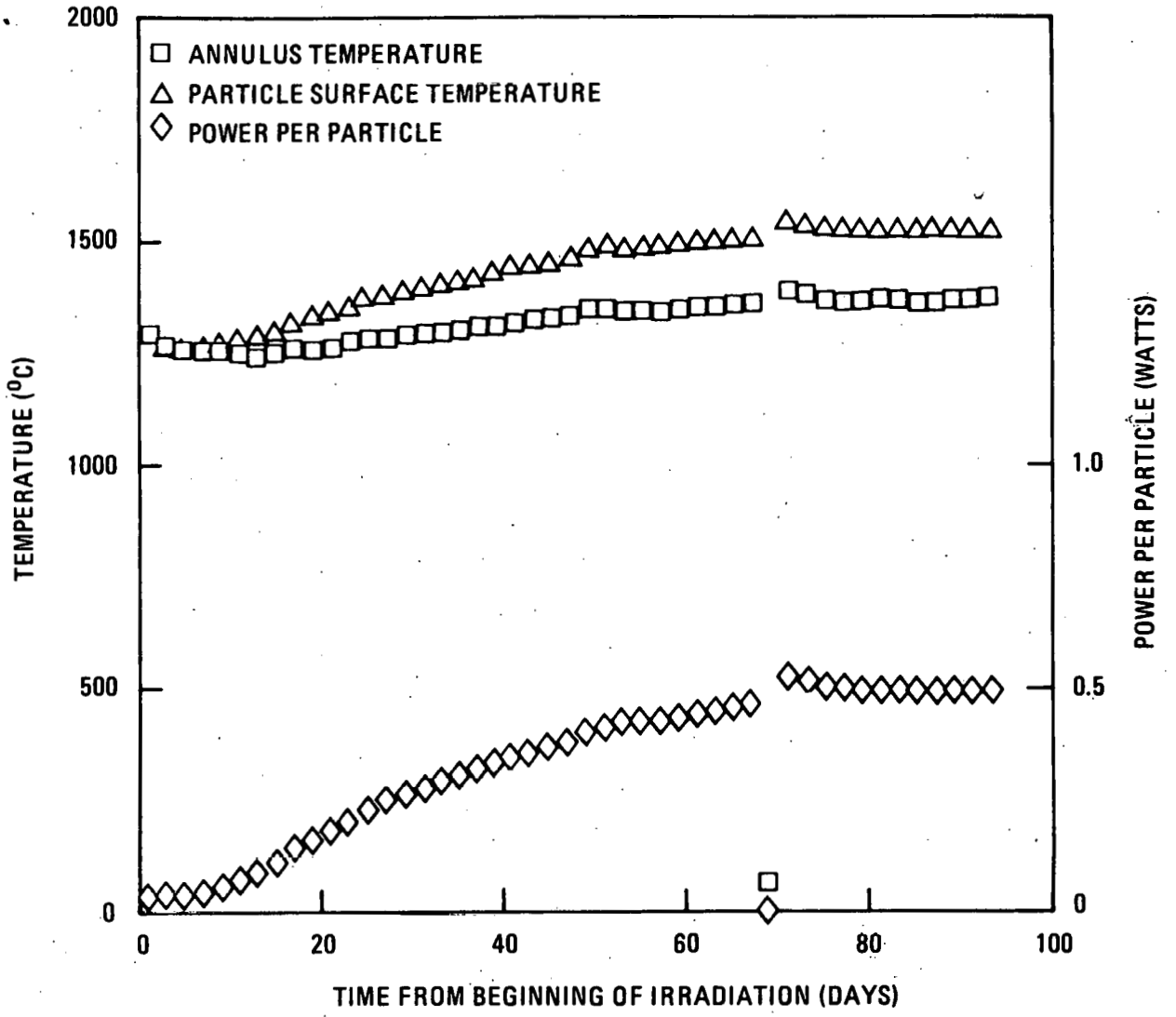

Fig. 3-3. Temperature of HT-31 particle holder 32, sample 6252-09-0161-002, 819.0-μm particle diameter

3-5. "Performance of HTGR Fuel in HFIR Capsule HT-33," DOE Report ORNL-5539, Oak Ridge National Laboratory, June 1979, pp. 15-22.

4. RESULTS OF POSTIRRADIATION EXAMINATIONS

Disassembly of the capsules and unloading of the fuel particles from their graphite crucibles were completed at ORNL (Ref. 4-1). After removal, the fuel specimens were shipped to GA for additional postirradiation characterization. The samples were reexamined visually; particle density, metallography, gamma spectroscopy, and fission gas release measurements were made; and wet chemistry analysis for burnup was performed on selected samples.

4.1. VISUAL EXAMINATION

The visual examination conducted at GA was performed using an in-cell stereomicroscope with a magnification of 4X or 20X. Coating failure levels observed in the particle samples during this examination are reported in Tables 4-1 and 4-2. All TRISO samples irradiated in the lower temperature positions (design particle surface temperature of 1200°C) to a fluence of 4.0 to 9.1 x 10^{25} n/m^2 $(E > 29\ fJ)_{HTGR}$ had zero total coating failure and low OPyC coating failure. Zero total coating failure was expected and was consistent with the TRISO particle design predictions discussed in Section 5.1.2. There was less low-temperature OPyC failure in HT-33, which was the higher-exposure test. Very high total coating failure was exhibited in all the particle samples from the high-temperature (1500°C design particle surface temperature) magazines in both capsules (see Table 4-1). Some of the samples from the same parent batches had low failure in one capsule but high failure in the other. Lower failure was usually observed in the samples located at the ends of the high-temperature magazine where the temperatures were lower.

As shown in Table 4-2, all the BISO samples that had an OPyC BAF_o of ≤1.04 exhibited zero failure in the low-temperature magazine (design

TABLE 4-1
PARTICLE DESCRIPTION AND VISUAL FAILURE OF TRISO ThO_2 SAMPLES FROM CAPSULES HT-31 AND HT-33

Particle Batch Retrieval Number	Kernel Diameter (μm)	Coater Size (mm)	BAF_o[a]	Capsule Position[b]	Time Averaged Temperature (°C)	Burnup (% FIMA)	Fast Fluence ($E > 29$ fJ)$_{HTGR}$ (10^{25} n/m^2)	Number of Particles Tested	Number of Particles Examined	Number of OPyC Failures	Percent OPyC Failures	Number of Total Coating Failures	Percent Total Coating Failures	Predicted Pressure Vessel Failures
HT-31 1200°C Design Particle Surface Temperature (900°C Graphite Crucible Temperature)														
6252-10-0161-001	447	240	1.052	40	1250	6.1	6.5	53	53	1	1.9	0	0	0[g]
6252-09-0161-001	447	240	1.036	42	1220	5.6	6.1	53	53	1	1.9	0	0	0[g]
6252-05-0160-005	511	127	1.026	43	1250	5.4	5.9	34	35[c]	0	0	0	0	0[g]
6252-07-0261-001	447	240	1.041	45	1190	4.9	5.4	53	53	1	1.9	0	0	0[g]
6252-07-0161-001	448	240	1.042	46	1180	4.7	5.2	54	54	2	3.7	0	0	0[g]
6252-06-0261-001	448	240	1.038	48	1160	4.2	4.8	52	52	0	0	0	0	0[g]
6252-06-0161-001	449	240	1.033	49	1150	4.0	4.5	53	53	0	0	0	0	0[g]
6252-08-0161-001	447	240	1.045	51	1150	3.5	4.0	54	50[c]	0	0	0	0	0[g]
HT-31 1500°C Design Particle Surface Temperature (1250°C Graphite Crucible Temperature)														
6252-05-0160-006	509	127	1.026	27	1530	9.2	8.1	51	51[d]	(e)	(e)	49	96.1	(f)
6252-08-0161-002	447	240	1.045	29	1520	9.0	8.1	80	80[d]	(e)	(e)	64	80	(f)
6252-10-0161-002	446	240	1.052	30	1430	8.8	8.0	79	79[d]	(e)	(e)	42	53.2	(f)
6252-09-0161-002	447	240	1.036	32	1420	8.6	7.8	78	78[d]	(e)	(e)	74	94.9	(f)
6252-07-0261-002	446	240	1.041	33	1410	8.4	7.8	78	78[d]	(e)	(e)	30	38.5	(f)
6252-07-0161-002	448	240	1.042	35	1400	8.1	7.6	80	80[d]	(e)	(e)	42	52.5	(f)
6252-06-0261-002	448	240	1.038	36	1390	7.9	7.5	77	77[d]	(e)	(e)	9	11.7	(f)
6252-06-0161-002	448	240	1.033	38	1410	7.5	7.3	78	78	0	0	0	0	(f)
HT-33 1500°C Design Particle Surface Temperature (1250°C Graphite Crucible Temperature)														
6252-08-0161-004	448	240	1.045	27	1420	13.2	11.7	80	80	(e)	(e)	22	27.5	(f)
6252-10-0161-004	445	240	1.052	29	1470	12.9	11.5	79	79	(e)	(e)	78	98.7	(f)
6252-05-0160-008	510	127	1.026	30	1510	12.7	11.4	51	51	(e)	(e)	51	100	(f)
6252-06-0261-004	449	240	1.038	32	1460	12.4	11.2	77	77	(e)	(e)	77	100	(f)
6252-06-0161-004	450	240	1.033	33	1450	12.2	11.1	78	78	(e)	(e)	78	100	(f)
6252-07-0261-004	447	240	1.041	35	1440	11.7	10.9	78	78	(e)	(e)	78	100	(f)
6252-07-0161-004	447	240	1.042	36	1430	11.5	10.7	80	80	(e)	(e)	79	98.8	(f)
6252-09-0161-004	447	240	1.036	38	1450	11.0	10.5	78	78	(e)	(e)	40	51.3	(f)
HT-33 1200°C Design Particle Surface Temperature (900°C Graphite Crucible Temperature)														
6252-09-0161-003	448	240	1.036	40	1210	9.0	9.3	53	53	0	0	0	0	0[g]
6252-07-0261-003	446	240	1.041	42	1250	8.4	8.7	53	53	0	0	0	0	0[g]
6252-07-0161-003	448	240	1.042	43	1230	8.0	8.4	54	54	0	0	0	0	0[g]
6252-05-0160-007	509	127	1.026	45	1260	7.4	7.8	34	34	0	0	0	0	0[g]
6252-06-0261-003	448	240	1.038	46	1220	7.1	7.5	52	52	2	3.9	0	0	0[g]
6252-06-0161-003	448	240	1.033	48	1200	6.4	6.8	53	53	0	0	0	0	0[g]
6252-08-0161-003	447	240	1.045	49	1180	6.0	6.5	54	54	0	0	0	0	0[g]
6252-10-0161-003	447	240	1.052	51	1190	5.4	5.7	53	53	0	0	0	0	0[g]

[a] Measured with a Seibersdorf optical anisotropy unit using a 24-μm circle.

[b] The number designates the axial position in the capsule; the numbers increase consecutively towards the bottom of the capsule (relative to the reactor core).

[c] Sample size different from original size.

[d] The total number of particles could not be counted due to high failure; value given is the design number of particles for the sample.

[e] OPyC coating failure without total coating failure was not observed.

[f] No pressure vessel failure predictions were done at 1500°C because failure at such high temperatures is caused by SiC degradation in addition to internal pressure.

[g] TRISO particle performance predictions described in Ref. 4-2 and based on an apparent failure stress of -4.9 MPa (-3400 psi).

TABLE 4-2
PARTICLE DESCRIPTION AND VISUAL FAILURE OF BISO ThO_2 SAMPLES FROM CAPSULE HT-33

Particle Batch Retrieval Number	Heat Treatment	Kernel Diameter (μm)	Coater Size (mm)	OPyC Diluent Gas	BAF_o[a]	Capsule Position[b]	Time Averaged Temperature (°C)	Burnup (% FIMA)	Fast Fluence ($E > 29$ fJ)$_{HTGR}$ (10^{25} n/m^2)	Number of Particles Tested	Number of Particles Examined	Total Coating Failures	Percent Coating Failures
1200°C Design Particle Surface Temperature (900°C Graphite Crucible Temperature)													
6542-39-0161-001	Yes	508	240	N_2	1.079	2	1240	5.4	5.7	38	38	3	7.9
6542-40-0161-001	Yes	500	240	H_2	1.043	4	1220	6.0	6.5	41	41	0	0
6542-40-0261-001	Yes	500	240	H_2	1.038	5	1230	6.4	6.8	41	41	0	0
6542-40-0260-001	No	503	240	H_2	1.038	7	1250	7.1	7.5	41	41	0	0
6542-27-0161-001	Yes	500	127	Ar	1.041	8	1270	7.4	7.8	40	40	0	0
6542-29-0261-001	Yes	504	240	N_2	1.081	10	1290	8.0	8.4	39	39	23	59
6542-41-0161-001	Yes	503	240	N_2	1.081	11	1300	8.4	8.7	40	40	14	35
6542-41-0160-001	No	507	240	N_2	1.060	13	1260	9.0	9.3	40	40	12	30
1500°C Design Particle Surface Temperature (1250°C Graphite Crucible Temperature)													
6542-29-0261-002	Yes	503	240	N_2	1.081	15	1490	11.0	10.5	55	55	49	89.1
6542-27-0161-002	Yes	503	127	Ar	1.041	17	1470	11.5	10.7	57	57	0	0
6542-41-0161-002	Yes	503	240	N_2	1.081	18	1480	11.7	10.9	56	56	53	94.6
6542-41-0160-002	No	505	240	N_2	1.060	20	1490	12.2	11.1	56	56	Lost	
6542-39-0161-002	Yes	508	240	N_2	1.079	21	1500	12.4	11.2	54	54	50	92.6
6542-40-0161-002	Yes	502	240	H_2	1.043	23	1500	12.7	11.4	58	58	53	91.4
6542-40-0261-002	Yes	501	240	H_2	1.038	24	1510	12.9	11.5	58	56[c]	0	0
6542-40-0260-002	No	500	240	H_2	1.038	26	1460	13.2	11.7	58	58	10	17.2

[a] Measured with a Seibersdorf optical anisotropy unit using a 24- m circle.

[b] The number designates the axial position in the capsule; the numbers increase consecutively towards the bottom of the capsule (relative to the reactor core).

[c] Sample size different from original size.

particle surface temperature 1200°C). These samples included the two large coater batches made using H_2 dilution and the one reference 127-mm coater batch. In the high-temperature magazine (1500°C design particle surface temperature), the same batches exhibited failure of up to 17%, except for one large coater batch (6542-40-0161-002) which had a visual OPyC coating failure level of 91%. All of the BISO samples with ≥1.06 BAF_o values in the OPyC had high failure in both the high- and low-temperature magazines.

As discussed in Ref. 4-3, it was expected that heat-treatment-induced changes in the OPyC would cause higher particle failure levels, especially in the heat-treated sample from parent batch 6542-41-015. As shown in Table 4-2, the coating failure levels of the 12 BISO samples that were heat treated do not differ significantly from the three samples examined that were not heat treated.

4.2. METALLOGRAPHY

Five TRISO and two BISO particle samples from capsules HT-31 and HT-33 were initially examined metallographically to evaluate the irradiation induced changes in the particles. Nine to 15 particles from each sample were mounted and, after grinding, the specimens were reimpregnated with mounting compound to reduce kernel pullout during polishing. The polished specimens were examined under bright field illumination and polarized light with a Leitz metallograph.

4.2.1. High-Temperature TRISO

High-temperature irradiation TRISO samples 6252-07-0261-002, 6542-06-0161-002, and 6252-08-0161-004 in HT-31 and HT-33 all revealed a high degree of buffer densification and pyrocarbon anisotropy. In some particles, the SiC layer exhibited a fine porosity that increased toward the inner surface of the coating, as shown in Figs. 4-1 and 4-2. The kernel microstructure consisted of a continuous gray phase with large pores and a small, white, apparently metallic phase scattered throughout. No grain

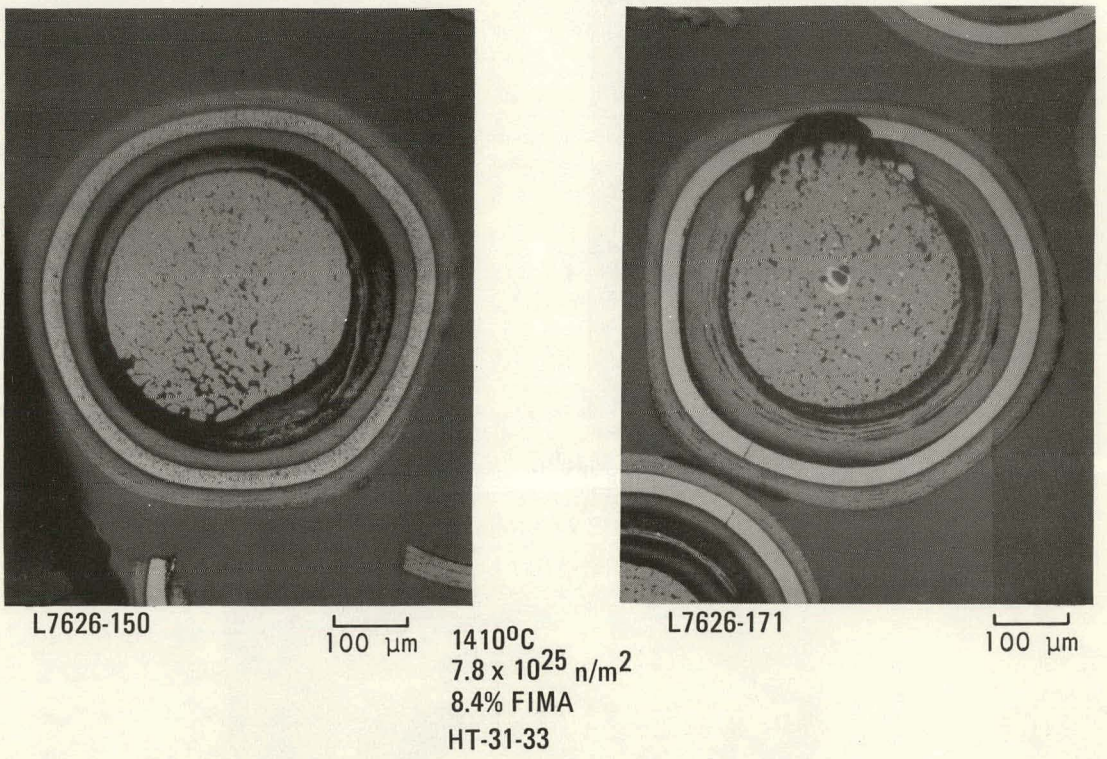

Fig. 4-1. Bright field photomicrographs of ThO_2 TRISO particles from batch 6252-07-0261-002

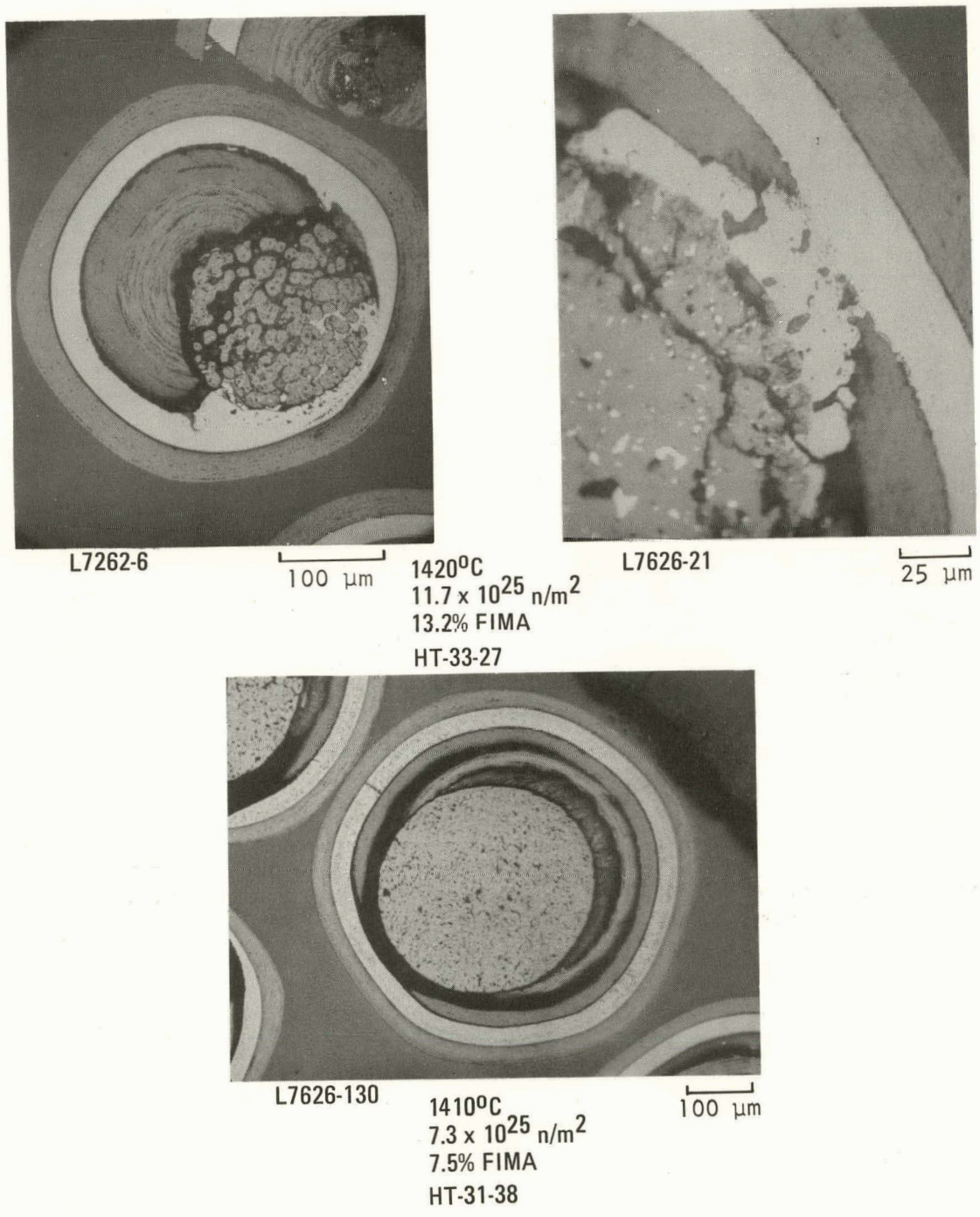

Fig. 4-2. Bright field photomicrographs of ThO_2 TRISO particles from batches 6252-08-0161-004 (HT-33-27) and 6252-06-0161-002 (HT-31-38)

boundaries were discernible in the kernel. The shape of the kernel was usually oblong and sometimes broken up into globules at the periphery. Kernel migration and SiC attack were seen in most cases. In some cases, a large concentration of a white phase was located near the advancing side of the kernel. Kernel migration coefficients were calculated and the results are shown in Table 4-3. The distance the kernels traveled was measured on the polished sections of two specimens from capsule HT-31. Kernel migration is discussed in detail in Section 5.1.2.1.

4.2.2. High-Temperature BISO

From the high-temperature magazine in HT-33, BISO sample 6542-40-0261-002 exhibited highly anisotropic buffer and OPyC coatings; however, no OPyC failure was observed. In all of the particles there was a gap between the kernel and the buffer (see Fig. 4-3). The circumference of the kernel was rough. Two out of 13 of the kernels had cracks or voids and all of the kernels exhibited fine porosity and a small dispersed white phase. No kernel migration was observed in the BISO ThO_2 particles.

4.2.3. Low-Temperature BISO

As shown in Fig. 4-3, the BISO low-temperature irradiation sample, 6542-40-0260-001 (HT-33-7), was in excellent condition after irradiation. The metallographic examination showed a relatively low level of buffer and OPyC anisotropy under polarized light. No metallic phase in the kernel and no kernel migration were observed. There were no visible coating failures. Although some of the particles were severely faceted, the R/B measurement results were low, showing that the short-lived fission gases had been retained by the particles.

4.2.4. Low-Temperature TRISO

TRISO samples 6252-07-0261-003 and 6252-09-0161-003 from the HT-33 low-temperature magazine positions 42 and 40 appeared to be in good condition under metallographic examination as shown in Figs. 4-4 and 4-5. The

TABLE 4-3
CALCULATED KERNEL MIGRATION COEFFICIENTS FOR TRISO ThO_2 PARTICLES IRRADIATED IN CAPSULE HT-31

	Sample 33	Sample 38
Fast fluence[(a)] $\left[10^{25}\ n/m^2\ (E > 29\ fJ)_{HTGR}\right]$	7.8	7.3
Burnup[(a)] (% FIMA)	8.4	7.5
Irradiation time (s)	7.73×10^6	7.73×10^6
Amoeba equivalent temperature[(b)] (°C)	1470	1435
Thermal gradient[(a)] (K/m)	5.75×10^4	5.99×10^4
Kernel migration distance[(c)] (μm)		
Individual measurement	37	24
	38	25
	39	26
	50	41
	61	42
	71	45
	78	59
	--	62
	--	73
	--	82
Average kernel migration distance (μm)	53	48
Kernel migration coefficient (m^2-K/s)		
Measured in-pile[(d)]	3.6×10^{-10}	3.0×10^{-10}
Predicted out-of-pile[(e)]	5.2×10^{-10}	3.4×10^{-10}

(a) Calculated value.

(b) The constant temperature that would result in the migration distance predicted using the variation in the temperature with time.

(c) Measured on particles in metallographic polished section.

(d) Equation used: $KMC = \frac{\Delta x}{\Delta t} T^2 \left(\frac{\Delta T}{\Delta X}\right)^{-1}$.

(e) Ref. 4-4.

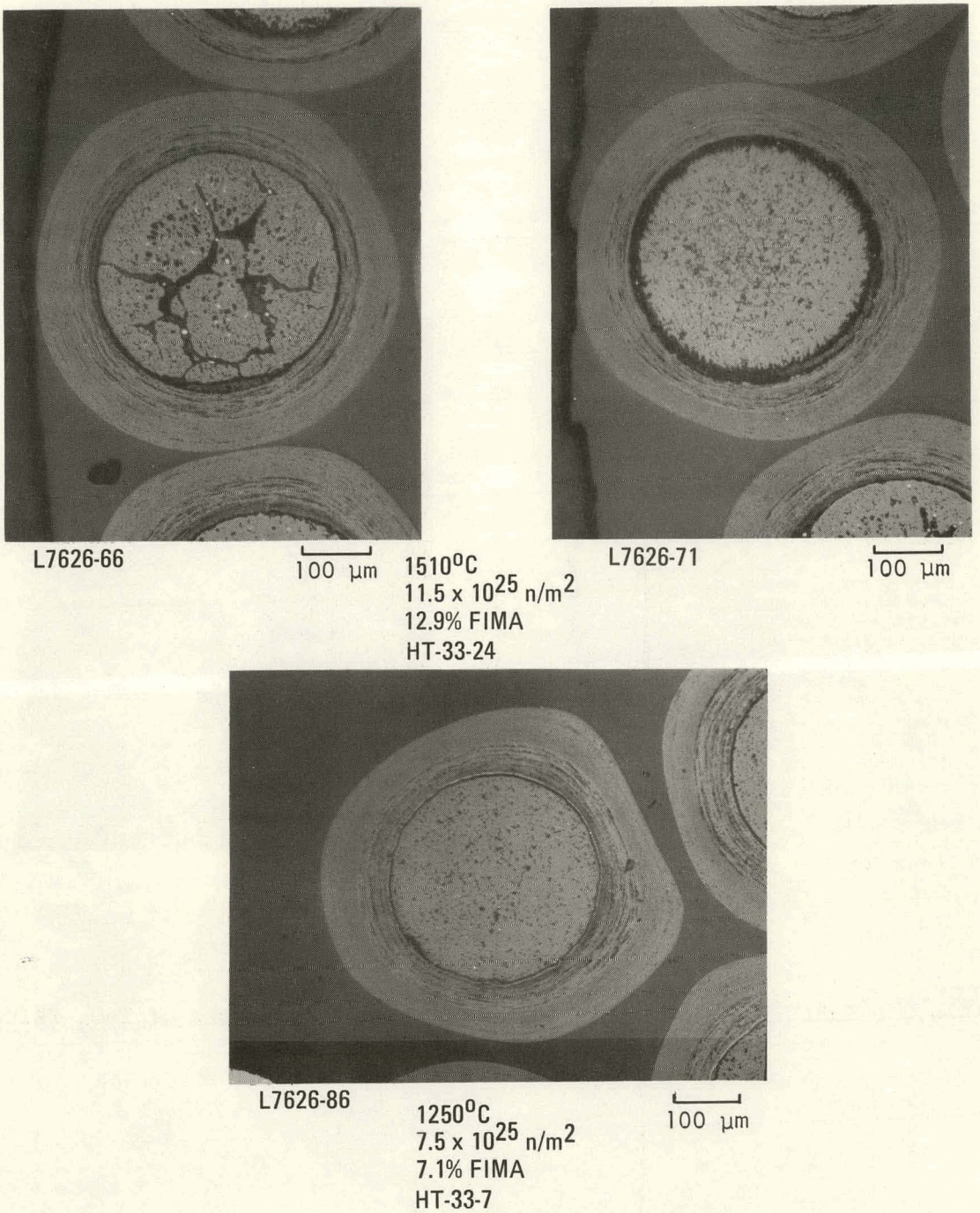

Fig. 4-3. Bright field photomicrographs of ThO_2 BISO particles from batches 6542-40-0261-002 (HT-33-24) and 6542-40-0260-001 (HT-33-7)

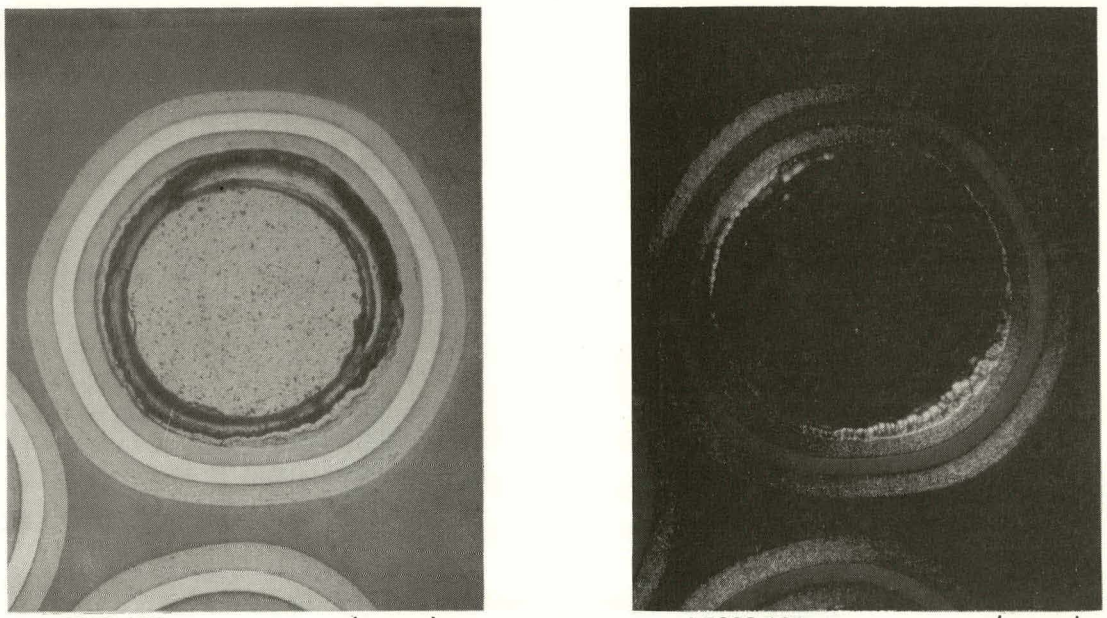

Fig. 4-4. Bright field and polarized light photomicrographs of ThO_2 TRISO particles from batch 6252-07-0261-003

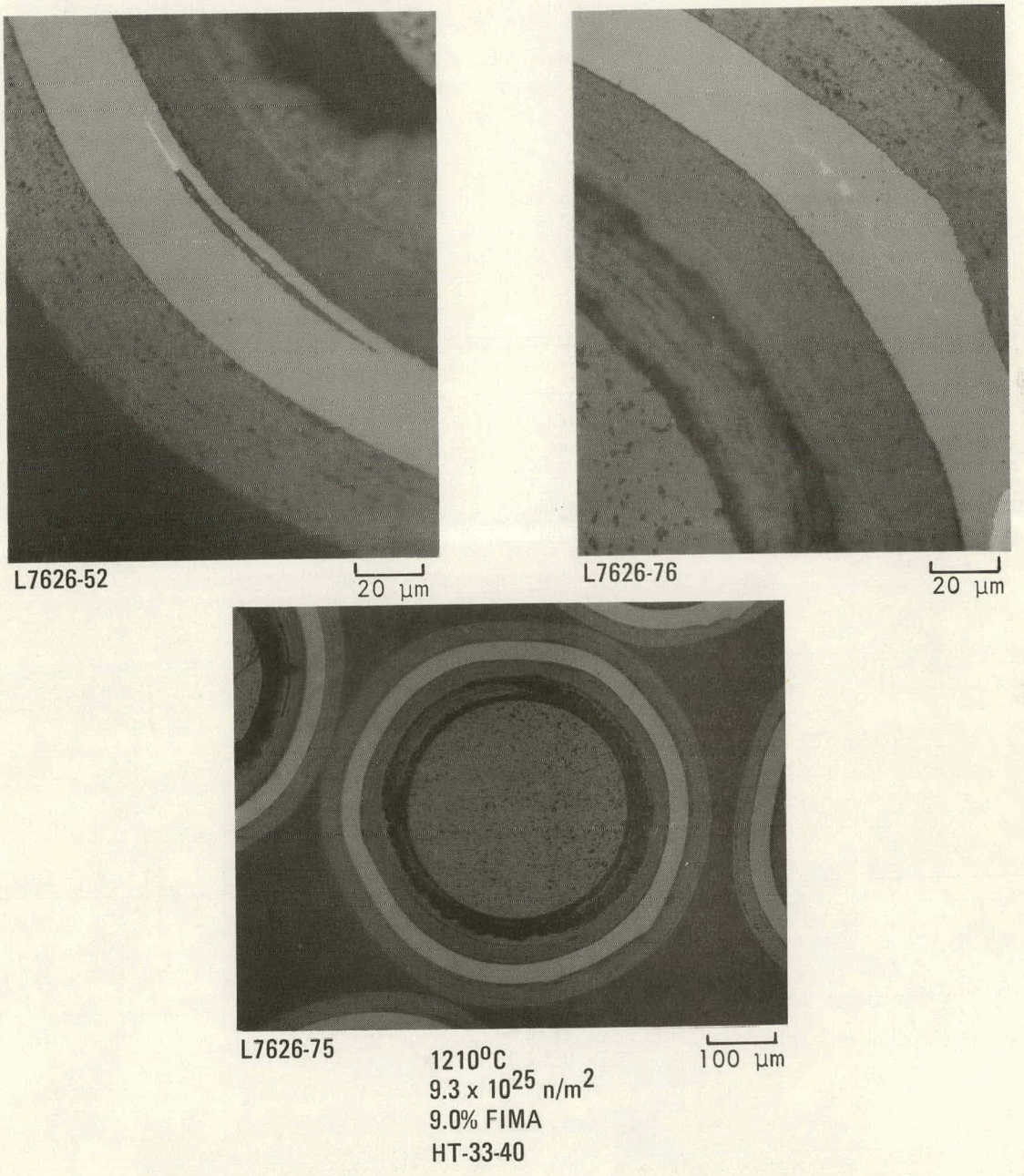

Fig. 4-5. Bright-field photomicrographs of ThO_2 TRISO particles from batch 6252-09-0161-003 (Sheet 1 of 2)

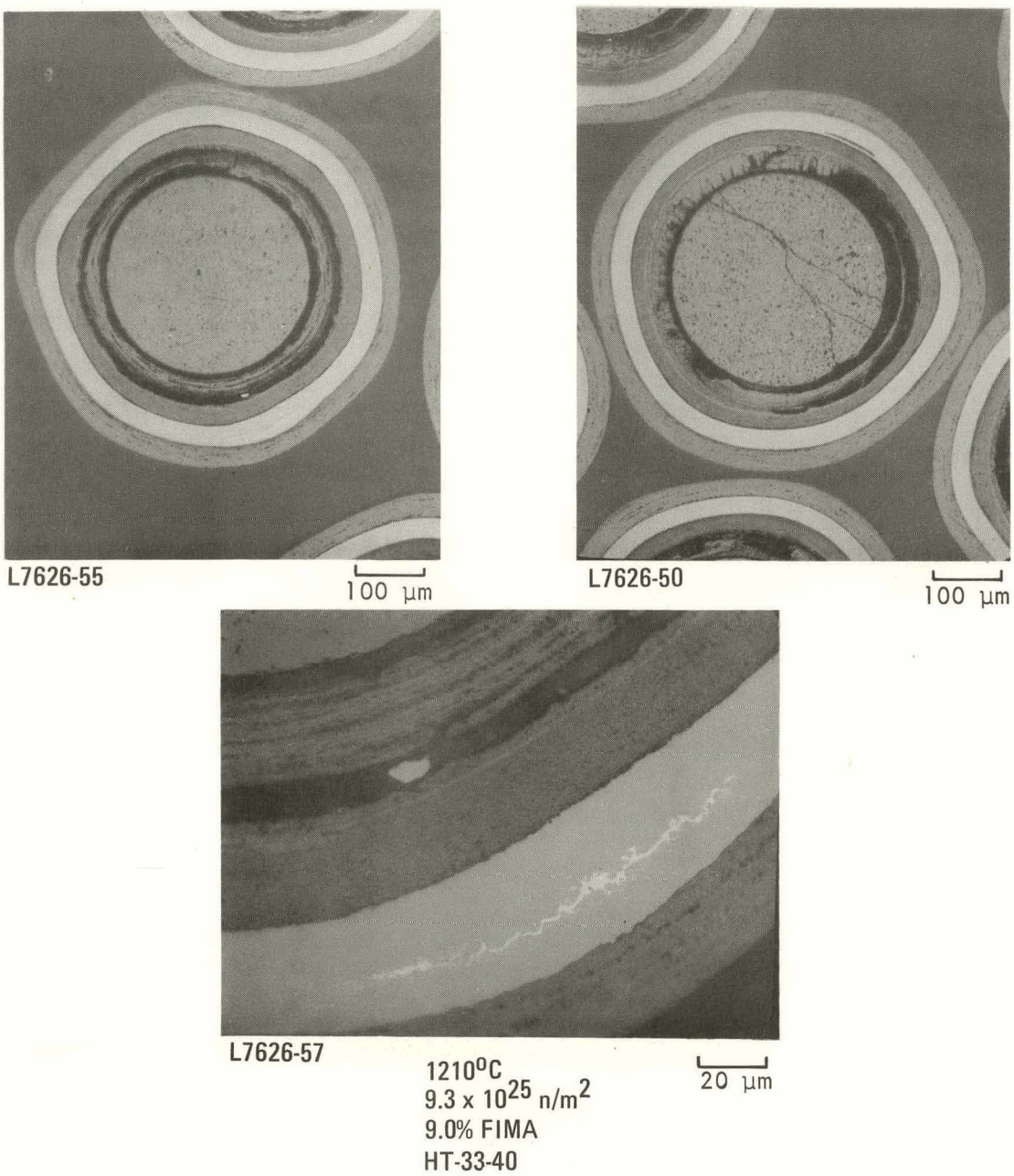

Fig. 4-5. Bright-field photomicrographs of ThO_2 TRISO particles from batch 6252-09-0161-003 (Sheet 2 of 2)

pyrocarbon coatings were slightly anisotropic under polarized light. No degradation or corrosion of the SiC was observed. The kernel microstructure was uniform with fine porosity and a scattered metallic phase. No kernel migration was observed in either sample. In sample 6252-09-0161-003, an apparently metallic white phase was discovered in the SiC coatings in six out of 15 of the particles mounted. This phase was not seen in the other TRISO sample irradiated at low temperature (6252-07-0261-003). The white phase occurred in the central region of the SiC coating, often in lenticular flaws. The phase was never observed at the SiC-IPyC or SiC-OPyC interfaces. In all cases, the SiC layer appeared thicker wherever a white phase was seen, as shown in Fig. 4-5. The mount was reground and polished three times to ensure that the white phase observed was not a polishing artifact. After the fourth polish, the white phase had been observed in 10 out of the 15 particles. This white phase is discussed more fully in Section 5.1.3.

4.3. FISSION GAS RELEASE

The retention of short-lived fission gases by TRISO and BISO ThO_2 particles from capsules HT-31 and HT-33 was evaluated by using the GA TRIGA reactor, the linear accelerator, and thorium hydrolysis. The objective of the measurements was to compare the particle coating failure fractions calculated from the R/B measurements with those determined by other postirradiation examination methods. The barriers to release of short-lived fission gases are the coatings of the fuel particles. Short-lived fission gas release is a determination of total coating failure.

Particle fuel failure levels for each specimen were determined from fission gas release data obtained from the whole sample irradiated in each position. The postirradiation fission gas released during TRIGA activation comes from two sources: (1) heavy metal contamination on the particle surface, and (2) failed fuel particles as shown by the following equations:

$$R/B_{EOL} = R/B_{\text{failed fuel}} + R/B_{BOL} \qquad (4\text{-}1)$$

$$R/B_{EOL} = R/B_{failed\ fuel} + R/B_{C(Th)} \quad , \tag{4-2}$$

$$R/B_{C} = (Th_{C})\ (r/b_{C}) \quad , \tag{4-3}$$

where R/B_{EOL} = measured postirradiation fission gas release (TRIGA),
$R/B_{failed\ fuel}$ = fission gas release from failed fuel particles,
R/B_{BOL} = measured preirradiation fission gas release (LINAC),
$R/B_{C(Th)}$ = fission gas release from thorium (U-233) contamination,
Th_{C} = thorium contamination measured by hydrolysis,
r/b_{C} = fractional release from contamination (0.30).

Trace amounts of thorium contamination on the fuel particle surface are unavoidable during fabrication. Contamination during irradiation and postirradiation handling is assumed to be zero. Therefore, the difference between fission gas release (1) determined before irradiation or (2) calculated from measured thorium contamination and the measured postirradiation fission gas release (R/B_{EOL}) is assumed to be the fission gas released from fuel particles that failed during irradiation ($R/B_{failed\ fuel}$). The thorium contamination contribution due to the postirradiation fission gas release can be calculated from thorium hydrolysis values or measured directly by the photofission of thorium in the linear accelerator (LINAC). As shown in Table 4-4, 12 of the 18 samples evaluated for short-lived fission gas retention were measured for thorium contamination by LINAC activation. Thorium hydrolysis values were used to calculate the contamination contribution for the other six samples.

The direct measurement of fission gas release by LINAC activation is a more accurate determination of thorium surface contamination but because a large amount of sample is required, it was not always used. The photofission of Th-232 uses a high intensity beam of photons generated in a linear accelerator to bombard the fuel sample. The linear accelerator facility consists of a three-section 75-MeV L-band electron linear accelerator with the beam energy set at 30 MeV. The 30-MeV electron beam

TABLE 4-4
TRIGA FISSION GAS RELEASE DATA AND FAILURE LEVELS FOR PARTICLES IN HT-31 AND HT-33

Particle Batch Retrieval Number	Capsule Position	Coater Size (mm)	Fast Fluence ($E > 29$ fJ)$_{HTGR}$ (10^{25} n/m^2)	Time Averaged Temperature (°C)	Burnup (% FIMA)	EOL Equivalent Fissile Loading[a] (mg U-235)	Fission Gas Release R/B Kr-85m at 1100°C		ThO_2 Contamination[d] (g Th/g Th)	$R/B_{failed\ fuel}$ (e)(f)	r/b_f[g]	In-Service Particle Failure[h] (%)	Number of Particles in Sample	Apparent Number of Failed Particles
							BOL[b]	EOL[c]						
6252-06-0161-002	31-38	240	7.3	1410	7.5	2.88	4.6×10^{-6}	5.5×10^{-3}	8.3×10^{-6}	5.5×10^{-3}[e]	0.0123	45	78	35
6252-10-0161-001	31-40	240	6.5	1250	6.1	1.83	ND	2.0×10^{-5}	2.0×10^{-6}	1.9×10^{-5}[f]	0.0103	0.20	53	0
6252-09-0161-001	31-42	240	6.1	1220	5.6	1.80	ND	7.0×10^{-5}	1.0×10^{-6}	7.0×10^{-5}[f]	0.0101	0.70	53	0
6252-05-0160-005	31-43	127	5.9	1250	5.4	1.77	ND	2.5×10^{-5}	2.0×10^{-6}	2.4×10^{-5}[f]	0.0098	0.20	34	0
6252-07-0261-001	31-45	240	5.4	1190	4.9	1.72	1.2×10^{-5}	3.6×10^{-5}	0.8×10^{-6}	2.4×10^{-5}[e]	0.0092	0.26	53	0
6252-07-0161-001	31-46	240	5.2	1180	4.7	1.70	1.6×10^{-5}	1.3×10^{-4}	9.2×10^{-6}	1.1×10^{-4}[f]	0.0088	1.30	54	0-1
6252-09-0161-003	33-40	240	9.3	1210	9.0	1.77	ND	1.3×10^{-5}	1.0×10^{-6}	1.3×10^{-5}[f]	0.0146	0.10	53	0
6252-07-0161-003	33-43	240	8.4	1230	8.0	1.71	1.6×10^{-5}	2.3×10^{-5}	9.2×10^{-6}	7.0×10^{-6}[e]	0.0132	0.05	54	0
6252-06-0261-003	33-46	240	7.5	1220	7.1	1.65	ND	8.4×10^{-5}	0.8×10^{-6}	8.4×10^{-5}[f]	0.0121	0.70	52	0
6252-06-0161-003	33-48	240	6.8	1200	6.4	1.61	4.6×10^{-6}	1.3×10^{-5}	8.3×10^{-6}	1.2×10^{-5}[e]	0.0114	0.07	53	0
6252-08-0161-003	33-49	240	6.5	1180	6.0	1.57	ND	1.1×10^{-4}	1.0×10^{-6}	1.1×10^{-4}[f]	0.0106	1.00	54	0-1
6542-39-0161-001	33-2	240	5.7	1240	5.4	1.60	6.2×10^{-6}	6.2×10^{-4}	8.7×10^{-5}	6.1×10^{-4}[e]	0.0098	6.20	38	2
6542-40-0161-001	33-4	240	6.5	1220	6.0	1.64	$<1.4 \times 10^{-6}$	1.7×10^{-5}	7.6×10^{-6}	1.6×10^{-5}[e]	0.0106	0.20	41	0
6542-40-0261-001	33-5	240	6.8	1230	6.4	1.68	$<1.4 \times 10^{-6}$	1.0×10^{-4}	2.1×10^{-7}	9.9×10^{-5}[e]	0.0114	0.90	41	0
6542-40-0260-001	33-7	240	7.5	1250	7.1	1.72	3.6×10^{-6}	1.0×10^{-5}	2.1×10^{-7}	6.4×10^{-6}[e]	0.0121	0.10	41	0
6542-27-0161-001	33-8	127	7.8	1270	7.4	1.73	3.4×10^{-6}	2.3×10^{-4}	1.4×10^{-5}	2.3×10^{-4}[e]	0.0126	1.80	40	0-1
6542-27-0161-002	33-17	127	10.7	1470	11.5	2.78	3.4×10^{-6}	2.0×10^{-5}	1.4×10^{-5}	1.7×10^{-5}[e]	0.0177	0.10	57	0
6542-40-0261-002	33-24	240	11.5	1510	12.9	2.82	$<1.4 \times 10^{-6}$	6.9×10^{-6}	2.1×10^{-7}	5.5×10^{-6}[e]	0.0195	0.03	58	0

[a] EOL fissile loading is the weight of U-235 that would produce the equivalent Kr-85m yield of all fissionable material calculated to be in the same sample.

[b] R/B Kr-85m determined by the photofission of Th-232 in the LINAC.

[c] R/B Kr-85m determined by uranium fission in a TRIGA reactor.

[d] Determined by hydrolysis test on parent batch, and indicates total amount of exposed heavy metal.

[e] $R/B_{failed\ fuel} = R/B_{EOL} - R/B_{BOL}$.

[f] $R/B_{failed\ fuel} = R/B_{EOL} - (Th_C)(0.30)$.

[g] $r/b_f = 0.0013 + 0.00186\ (\%\ FIMA)^{0.9}$ for ThO_2 fuel (Ref. 4-6).

[h] $F = [R/B_{failed\ fuel}/(r/b_f)] \times 100$.

strikes a tantalum target, producing a 15-MeV average energy bremsstrahlung beam which causes the fissioning of the Th-232. Approximately 10^{10} fissions are induced in a 30-g sample after 1 hour of irradiation at room temperature. After irradiation the fission gases are swept into a liquid-nitrogen-cooled charcoal collection trap. The sample is then placed in the King furnace in the TRIGA reactor and annealed at 1100°C for 30 minutes to simulate the temperature conditions during in-core irradiation.

The fission gases released during annealing are collected in the trap and gamma counted with the fission gases released during LINAC irradiation. The gamma counting and R/B calculations were done by using the Sigma-II computer-analyzer system. A thorium stearate standard, known to be 100% releasing for fission gases with half-lives >30 s, is irradiated with the particle samples. The fractional R/B values are calculated by comparing the release of the gaseous radionuclides from the fuel with the release from the standard irradiated and gamma counted under the same conditions.

End-of-life fission gas release values were obtained by irradiating the fuel sample in a graphite tube furnace designed to fit into a fuel element position in a TRIGA reactor core. The samples were irradiated to produce about 10^{14} fissions by adjusting the reactor power level. During irradiation, the fission gases released were swept from the furnace with helium into a liquid-nitrogen-cooled charcoal collection trap. After the 30-minute irradiation period, the reactor is shut down and gas is collected for an additional 15 minutes. Then the collection trap containing the released fission gases was gamma counted using a lithium-drifted germanium detector. The gamma counting and R/B calculations were done by using the Sigma II computer-analyzer and the FISSIN computer code. The fractional R/B values, for xenon and krypton release, are calculated by comparing the release of the gaseous radionuclides from the fuel with the release from a powdered sample of uranium stearate, irradiated and gamma counted under the same conditions. Uranium stearate has been shown to be 100% releasing for gaseous nuclides with half-lives greater than 30 seconds (Ref. 4-5). The adjusted EOL fissile fuel loadings for each specimen were

determined by expressing the sum of the weight of all remaining fissionable material in terms of U-235, producing the equivalent Kr-85m yield.

The results of the preirradiation and postirradiation release measurements in terms of R/B for Kr-85m are reported in Table 4-4. The Kr-85m was selected as the reference isotope because it has a short half-life (4.4 hours) and its gamma-ray energy peak can easily be resolved. A reference temperature of 1100°C was used for analysis of fuel failure levels.

The in-service particle failure level was calculated for each sample using the following equation:

$$F = \frac{R/B_{\text{failed fuel}}}{r/b_f} \quad , \tag{4-4}$$

where F = in-service fuel failure level,

r/b_f = mean fractional release of Kr-85m at 1100°C from failed fuel particles.

The fuel failure level values obtained are given in Table 4-4. The most recent data on r/b_f (Refs. 4-6 and 4-7) give the following equation as a revised estimate of the burnup dependence for failed ThO_2 fuel:

$$r/b_f = 0.0013 + 0.0018\ (\%\ \text{FIMA})^{0.9} \quad . \tag{4-5}$$

Values of r/b_f determined using this equation are given in Table 4-4.

Of the 18 TRISO and BISO samples tested, three had a 1% particle failure level, one had a 6% level, and one TRISO sample had an in-service failure level of 45% (see Table 4-4). The other 13 samples showed a zero percent failure level. Failure mechanisms are discussed in greater detail in Section 5.1.2.

4.4. GAMMA-RAY SPECTROMETRY

Gamma-ray spectrometry was used to determine metallic fission product inventories in 27 HT-31 and HT-33 fuel particle samples. The loss of metallic fission products by intact BISO particles is caused by diffusion through the PyC layers. TRISO particles, however, retain their metallic fission products as long as the SiC layer remains intact. Thus the loss of metallic fission products gives a measure of SiC failure in the TRISO particles. Gamma counting was done using a lithium-drifted germanium (Ge-Li) gamma spectrometer coupled to a 4096-channel Sigma II computer analyzer. Single channel analyzers were used to print out relative profiles of individual isotopes. The samples were counted in the low-level hot cell using a 107-cm-long collimator.

Twelve particles that were judged to be intact by visual examination were chosen from each sample for gamma counting. Because of the very high total coating failure in samples from the high-temperature magazines, only 4 of the 27 samples chosen for gamma counting were high-temperature samples. Two particles were scanned at a time and six scans were run on each 12-particle sample. The two particles were loaded into plastic sample vials, which were positioned in front of the 1.27 cm by 1.27 cm collimator using a Nuclear Chicago automatic sample changer.

A quantitative fission product isotope inventory was determined from the multichannel scans using the following equation:

$$DPM = \frac{CPM}{(CE)(AI)} \quad , \tag{4-6}$$

where DPM = disintegrations per minute of each isotope,
CPM = counts per minute of each isotope measured by the detector,
CE = counting efficiency of the particular counting geometry,
AI = absolute intensity of the various isotopes.

Fuel sample 6252-08-0161-003 (HT33-49) was used as the internal peak standard. A counting efficiency versus peak energy calibration curve was constructed using the measured isotope CPM, the known values of the absolute intensities, and Eq. 4-6. A quantitative value for each isotope was calculated using this calibration curve and the measured CPM. A theoretical DPM of each isotope was calculated using the FISSPROD computer program. These values are reported for Ce-144, Cs-137, and Zr-95 in Tables 4-5 through 4-7. The differences between the two inventories are systematic with the measured isotope value generally higher than the predicted value. The differences are most likely due to uncertainties in the input data for the FISSPROD program and counting and calibration errors.

A qualitative evaluation of the metallic fission product retention of each particle batch was made by comparing the measured and calculated Cs/Zr ratios. The Zr-95 isotope was chosen as the reference isotope because it is retained by ThO_2 kernels and was easily detected. The measured and calculated Cs-137/Zr-95 ratios are reported in Tables 4-5 through 4-7 and plotted as a function of burnup in Figs. 4-6 through 4-8. The data showed that the particle samples could be divided into two populations consisting of particles with either high Cs/Zr ratios or low Cs/Zr ratios.

The lower limit for the high Cs/Zr ratio population was based on a 95% confidence that no more than 1% of the particles, which are assumed to be retentive of their Cs inventory, have a Cs/Zr ratio of less than their indicated limit. Confidence in the limit will be improved as the amount of empirical data increases. The measured and theoretical ratios are in agreement within 7% for particles that are considered intact.

For comparison Figs. 4-6 through 4-8 also show the fractional cesium release expected from bare ThO_2 kernels irradiated under the same conditions as the BISO particle samples. The bare kernel fractional release is the predicted upper limit of cesium release for these particle samples. The fractional release was calculated using the following equation:

TABLE 4-5
FISSION PRODUCT INVENTORY OF TRISO PARTICLES IRRADIATED IN HT-31

Sample Number	Capsule Position	Zr-95 (dpm)		Cs-137 (dpm)		Ce-144 (dpm)		Cs/Zr			
										Measured	
		Theoretical	Measured	Theoretical	Measured	Theoretical	Measured	Theoretical	Measured	Mean	Standard Deviation
6252-06-0161-002	31-33	5.02×10^{10}	5.3325×10^{10}	4.43×10^{8}	4.7818×10^{8}	1.14×10^{10}	1.1063×10^{10}	0.0088	0.0090	0.0063	0.0019
			5.5750×10^{10}		2.6841×10^{8}		1.1931×10^{10}		0.0048		
			5.2627×10^{10}		3.0733×10^{8}		1.1063×10^{10}		0.0059		
			5.3929×10^{10}		2.2330×10^{8}		1.2726×10^{10}		0.0041		
			5.3620×10^{10}		3.0337×10^{8}		1.2654×10^{10}		0.0057		
			5.2792×10^{10}		4.3194×10^{8}		1.0991×10^{10}		0.0082		
6252-10-0161-001	31-40	4.08×10^{10}	4.3931×10^{10}	3.58×10^{8}	4.0149×10^{8}	9.14×10^{9}	9.6891×10^{9}	0.0088	0.0091	0.0092	0.0001
			4.3128×10^{10}		4.0374×10^{8}		9.5445×10^{9}		0.0094		
			4.3043×10^{10}		3.8570×10^{8}		9.3275×10^{9}		0.0090		
			4.4479×10^{10}		4.1051×10^{8}		8.9660×10^{9}		0.0092		
			4.3995×10^{10}		4.0149×10^{8}		9.1106×10^{9}		0.0091		
			4.6435×10^{10}		4.2179×10^{8}		1.0484×10^{10}		0.0091		
6252-09-0161-001	31-42	3.80×10^{10}	4.2593×10^{10}	3.34×10^{8}	3.6427×10^{8}	8.49×10^{9}	8.3876×10^{9}	0.0088	0.0086	0.0087	0.0007
			4.3087×10^{10}		3.1691×10^{8}		1.0195×10^{10}		0.0074		
			4.1139×10^{10}		3.7668×10^{8}		8.8937×10^{9}		0.0092		
			4.0319×10^{10}		3.7442×10^{8}		9.5445×10^{9}		0.0093		
			4.1003×10^{10}		3.6037×10^{8}		8.5322×10^{9}		0.0088		
			4.2057×10^{10}		3.5976×10^{8}		8.6045×10^{9}		0.0086		
6252-05-0160-005	31-43	5.45×10^{10}	6.0333×10^{10}	4.78×10^{8}	5.4021×10^{8}	1.21×10^{10}	1.3521×10^{10}	0.0088	0.0090	0.0090	0.0002
			5.7780×10^{10}		5.2329×10^{8}		1.1569×10^{10}		0.0091		
			5.5241×10^{10}		4.7818×10^{8}		1.3449×10^{10}		0.0087		
			5.9404×10^{10}		5.2893×10^{8}		1.2581×10^{10}		0.0089		
			5.4740×10^{10}		5.0299×10^{8}		1.2654×10^{10}		0.0092		
			5.8853×10^{10}		5.2329×10^{8}		1.2798×10^{10}		0.0089		
6252-07-0261-001	31-45	3.35×10^{10}	3.5380×10^{10}	2.94×10^{8}	3.3608×10^{8}	7.43×10^{9}	7.3030×10^{9}	0.0088	0.0095	0.0091	0.0002
			3.6989×10^{10}		3.2593×10^{8}		8.5322×10^{9}		0.0088		
			3.7651×10^{10}		3.4059×10^{8}		8.0983×10^{9}		0.0090		
			3.6838×10^{10}		3.3382×10^{8}		7.0137×10^{9}		0.0091		
			3.8410×10^{10}		3.3157×10^{8}		8.2430×10^{9}		0.0090		
			3.5803×10^{10}		3.2480×10^{8}		6.6522×10^{9}		0.0091		
6252-07-0161-001	31-46	3.22×10^{10}	3.5034×10^{10}	2.82×10^{8}	3.0337×10^{8}	7.13×10^{9}	8.5322×10^{9}	0.0088	0.0087	0.0089	0.0002
			3.4959×10^{10}		3.1691×10^{8}		7.5199×10^{9}		0.0091		
			3.3732×10^{10}		3.0224×10^{8}		7.7368×10^{9}		0.0090		
			3.6667×10^{10}		3.2254×10^{8}		7.6645×10^{9}		0.0088		
			3.4306×10^{10}		3.1465×10^{8}		7.3030×10^{9}		0.0092		
			3.5363×10^{10}		3.0901×10^{8}		8.0260×10^{9}		0.0087		
6252-06-0261-003	31-48	2.93×10^{10}	3.0426×10^{10}	2.56×10^{8}	2.6728×10^{8}	6.45×10^{9}	6.0738×10^{9}	0.0087	0.0088	0.0087	0.0005
			3.0372×10^{10}		2.7292×10^{8}		5.9291×10^{9}		0.0090		
			3.4766×10^{10}		3.0112×10^{8}		6.7245×10^{9}		0.0087		
			2.9747×10^{10}		2.8194×10^{8}		5.8568×10^{9}		0.0095		
			3.4657×10^{10}		2.7518×10^{8}		6.1461×10^{9}		0.0079		
			3.2731×10^{10}		2.7856×10^{8}		6.5071×10^{9}		0.0085		
6252-06-0161-001	31-49	2.77×10^{10}	3.03×10^{10}	2.42×10^{8}	2.70×10^{8}	6.09×10^{9}	5.86×10^{9}	0.0087	0.0089	0.0090	0.0002
			3.07×10^{10}		2.79×10^{8}		6.15×10^{9}		0.0091		
			3.07×10^{10}		2.74×10^{8}		5.91×10^{9}		0.0089		
			3.01×10^{10}		2.73×10^{8}		6.07×10^{9}		0.0091		
			2.84×10^{10}		2.62×10^{8}		6.22×10^{9}		0.0092		
			3.78×10^{10}		2.82×10^{8}		7.95×10^{9}		0.0086		
6252-08-0161-001	31-51	2.43×10^{10}	2.64×10^{10}	2.12×10^{8}	2.29×10^{8}	5.31×10^{9}	5.86×10^{9}	0.0087	0.0087	0.0091	0.0003
			2.70×10^{10}		2.54×10^{8}		7.09×10^{9}		0.0094		
			2.75×10^{10}		2.44×10^{8}		6.72×10^{9}		0.0089		
			2.69×10^{10}		2.48×10^{8}		4.05×10^{9}		0.0092		
			2.51×10^{10}		2.35×10^{8}		5.35×10^{9}		0.0094		
			2.77×10^{10}		2.57×10^{8}		5.06×10^{9}		0.0093		

TABLE 4-6
FISSION PRODUCT INVENTORY OF TRISO PARTICLES IRRADIATED IN HT-33

Sample Number	Capsule Position	Zr-95 (dpm)		Cs-137 (dpm)		Ce-144 (dpm)		Cs/Zr			
										Measured	
		Theoretical	Measured	Theoretical	Measured	Theoretical	Measured	Theoretical	Measured	Mean	Standard Deviation
6252-08-0161-004	33-27	7.70×10^{10}	7.85×10^{10}	7.81×10^{8}	6.71×10^{8}	1.96×10^{10}	2.00×10^{10}	0.0101	0.0085	0.0040	0.0029
			8.30×10^{10}		1.55×10^{8}		2.02×10^{10}		0.0019		
			7.44×10^{10}		9.13×10^{7}		1.69×10^{10}		0.0012		
			7.72×10^{10}		4.17×10^{8}		1.99×10^{10}		0.0054		
			7.69×10^{10}		1.31×10^{8}		1.78×10^{10}		0.0017		
			7.43×10^{10}		3.71×10^{8}		1.74×10^{10}		0.0050		
6252-09-0161-003	33-40	5.38×10^{10}	5.63×10^{10}	5.37×10^{8}	5.83×10^{8}	1.33×10^{10}	1.37×10^{10}	0.0100	0.0104	0.0102	0.0002
			5.61×10^{10}		5.72×10^{8}		1.14×10^{10}		0.0102		
			5.68×10^{10}		5.70×10^{8}		1.37×10^{10}		0.0100		
			5.55×10^{10}		5.70×10^{8}		1.39×10^{10}		0.0103		
			5.66×10^{10}		5.70×10^{8}		1.30×10^{10}		0.0101		
			5.49×10^{10}		5.51×10^{8}		1.48×10^{10}		0.0100		
6252-07-0261-003	33-42	4.99×10^{10}	5.41×10^{10}	4.97×10^{8}	5.24×10^{8}	1.23×10^{10}	1.26×10^{10}	0.0100	0.0097	0.0100	0.0002
			5.31×10^{10}		5.15×10^{8}		1.27×10^{10}		0.0097		
			5.24×10^{10}		5.40×10^{8}		1.25×10^{10}		0.0103		
			5.19×10^{10}		5.21×10^{8}		1.11×10^{10}		0.0100		
			5.17×10^{10}		5.15×10^{8}		1.14×10^{10}		0.0100		
			5.19×10^{10}		5.27×10^{8}		1.37×10^{10}		0.0102		
6252-07-0161-003	33-43	4.87×10^{10}	5.08×10^{10}	4.84×10^{8}	5.01×10^{8}	1.19×10^{10}	1.20×10^{10}	0.0099	0.0099	0.0100	0.0001
			5.29×10^{10}		5.32×10^{8}		1.37×10^{10}		0.0101		
			5.20×10^{10}		5.13×10^{8}		1.17×10^{10}		0.0099		
			5.07×10^{10}		5.02×10^{8}		1.21×10^{10}		0.0099		
			5.40×10^{10}		5.39×10^{8}		1.19×10^{10}		0.0100		
			5.26×10^{10}		5.33×10^{8}		1.24×10^{10}		0.0101		
6252-05-0160-007	33-45	6.56×10^{10}	7.10×10^{10}	6.51×10^{8}	7.06×10^{8}	1.60×10^{10}	1.62×10^{10}	0.0099	0.0099	0.0100	0.0002
			6.76×10^{10}		6.90×10^{8}		1.59×10^{10}		0.0102		
			6.99×10^{10}		6.87×10^{8}		1.65×10^{10}		0.0098		
			7.04×10^{10}		6.99×10^{8}		1.48×10^{10}		0.0099		
6252-06-0261-003	33-46	4.31×10^{10}	4.68×10^{10}	4.26×10^{8}	4.74×10^{8}	1.05×10^{10}	1.16×10^{10}	0.0099	0.0101	0.0099	0.0007
			4.57×10^{10}		3.89×10^{8}		1.16×10^{10}		0.0085		
			4.69×10^{10}		4.68×10^{8}		1.14×10^{10}		0.0100		
			4.59×10^{10}		4.60×10^{8}		1.04×10^{10}		0.0100		
			4.52×10^{10}		4.69×10^{8}		1.08×10^{10}		0.0104		
			4.57×10^{10}		4.67×10^{8}		1.01×10^{10}		0.0102		
6252-06-0161-003	33-48	3.94×10^{10}	4.30×10^{10}	3.88×10^{8}	4.38×10^{8}	9.52×10^{9}	1.09×10^{10}	0.0098	0.0102	0.0100	0.0003
			4.25×10^{10}		4.09×10^{8}		9.69×10^{9}		0.0096		
			6.20×10^{10}		6.11×10^{8}		1.58×10^{10}		0.0099		
			4.11×10^{10}		4.13×10^{8}		8.89×10^{9}		0.0101		
			4.12×10^{10}		4.22×10^{8}		8.89×10^{9}		0.0102		
			4.44×10^{10}		4.29×10^{8}		1.03×10^{10}		0.0097		
6252-08-0161-003	33-49	3.73×10^{10}	4.03×10^{10}	3.67×10^{8}	3.99×10^{8}	8.99×10^{9}	9.04×10^{9}	0.0098	0.0099	0.0100	0.0002
			3.88×10^{10}		3.97×10^{8}		9.04×10^{9}		0.0102		
			3.93×10^{10}		3.94×10^{8}		8.97×10^{9}		0.0100		
			3.84×10^{10}		3.92×10^{8}		8.32×10^{9}		0.0102		
			3.89×10^{10}		3.80×10^{8}		9.54×10^{9}		0.0098		
			3.88×10^{10}		3.81×10^{8}		8.32×10^{9}		0.0098		
6252-10-0161-003	33-51	3.33×10^{10}	3.56×10^{10}	3.27×10^{8}	3.69×10^{8}	7.98×10^{9}	9.18×10^{9}	0.0098	0.0104	0.0099	0.0003
			3.64×10^{10}		3.56×10^{8}		8.24×10^{9}		0.0098		
			3.75×10^{10}		3.63×10^{8}		9.26×10^{9}		0.0097		
			3.72×10^{10}		3.63×10^{0}		8.82×10^{9}		0.0098		
			3.55×10^{10}		3.54×10^{8}		8.53×10^{9}		0.0100		
			3.58×10^{10}		3.38×10^{8}		8.10×10^{9}		0.0094		

TABLE 4-7
FISSION PRODUCT INVENTORY OF BISO PARTICLES IRRADIATED IN HT-33

Sample Number	Capsule Position	Zr-95 (dpm)		Cs-137 (dpm)		Ce-144 (dpm)		Cs/Zr			
										Measured	
		Theoretical	Measured	Theoretical	Measured	Theoretical	Measured	Theoretical	Measured	Mean	Standard Deviation
6542-39-0161-001	33-2	4.80×10^{10}	5.19×10^{10}	4.70×10^{8}	5.20×10^{8}	1.15×10^{10}	1.24×10^{10}	0.0098	0.0100	0.0100	0.0002
			5.04×10^{10}		5.02×10^{8}		1.09×10^{10}		0.0100		
			5.07×10^{10}		5.13×10^{8}		1.14×10^{10}		0.0101		
			5.01×10^{10}		4.86×10^{8}		1.08×10^{10}		0.0097		
			5.08×10^{10}		5.22×10^{8}		1.21×10^{10}		0.0103		
			4.98×10^{10}		5.00×10^{8}		1.06×10^{10}		0.0100		
6542-40-0161-001	33-4	5.09×10^{10}	5.00×10^{10}	5.03×10^{8}	4.96×10^{8}	1.23×10^{10}	1.22×10^{10}	0.0099	0.0099	0.0098	0.0002
			5.30×10^{10}		5.29×10^{8}		1.21×10^{10}		0.0100		
			5.27×10^{10}		5.17×10^{8}		1.19×10^{10}		0.0098		
			5.39×10^{10}		5.04×10^{8}		1.19×10^{10}		0.0094		
			5.45×10^{10}		5.49×10^{8}		1.25×10^{10}		0.0101		
			5.40×10^{10}		5.28×10^{8}		1.38×10^{10}		0.0098		
6542-40-0261-001	33-5	5.41×10^{10}	5.68×10^{10}	5.34×10^{8}	5.76×10^{8}	1.31×10^{10}	1.29×10^{10}	0.0099	0.0101	0.0099	0.0002
			5.64×10^{10}		5.62×10^{8}		1.21×10^{10}		0.0100		
			5.43×10^{10}		5.15×10^{8}		1.30×10^{10}		0.0095		
			5.64×10^{10}		5.72×10^{8}		1.34×10^{34}		0.0101		
			5.67×10^{10}		5.48×10^{8}		1.24×10^{10}		0.0097		
			5.71×10^{10}		5.68×10^{8}		1.41×10^{10}		0.0099		
6542-40-0261-001	33-7	6.02×10^{10}	6.16×10^{10}	5.97×10^{8}	5.86×10^{8}	1.47×10^{10}	1.52×10^{10}	0.0099	0.0095	0.0097	0.0004
			5.93×10^{10}		5.72×10^{8}		1.35×10^{10}		0.0096		
			5.86×10^{10}		5.98×10^{8}		1.34×10^{10}		0.0102		
			6.15×10^{10}		5.61×10^{8}		1.39×10^{10}		0.0091		
			5.74×10^{10}		5.68×10^{8}		1.33×10^{10}		0.0099		
			6.14×10^{10}		5.92×10^{8}		1.55×10^{10}		0.0096		
6542-27-0161-001	33-8	6.24×10^{10}	6.07×10^{10}	6.19×10^{8}	6.18×10^{8}	1.52×10^{10}	1.56×10^{10}	0.0099	0.0102	0.0099	0.0002
			6.40×10^{10}		6.15×10^{8}		1.58×10^{10}		0.0096		
			6.53×10^{10}		6.48×10^{8}		1.44×10^{10}		0.0099		
			6.55×10^{10}		6.36×10^{8}		1.48×10^{10}		0.0097		
			6.65×10^{10}		6.62×10^{8}		1.47×10^{10}		0.0100		
			6.59×10^{10}		6.64×10^{8}		1.45×10^{10}		0.0101		
6542-40-0161-001	33-11	6.99×10^{10}	7.48×10^{10}	6.96×10^{8}	6.64×10^{8}	1.72×10^{10}	1.83×10^{10}	0.0100	0.0089	0.0086	0.0012
			7.56×10^{10}		4.59×10^{8}		1.60×10^{10}		0.0061		
			7.20×10^{10}		6.64×10^{8}		1.68×10^{10}		0.0092		
			7.12×10^{10}		6.54×10^{8}		1.76×10^{10}		0.0092		
			7.15×10^{10}		6.35×10^{8}		1.70×10^{10}		0.0089		
			7.40×10^{10}		6.74×10^{8}		1.54×10^{10}		0.0091		
6542-41-0160-001	33-13	7.66×10^{10}	7.78×10^{10}	7.64×10^{8}	3.51×10^{8}	1.89×10^{10}	1.60×10^{10}	0.0100	0.0045	0.0074	0.0018
			7.82×10^{10}		6.35×10^{8}		1.87×10^{10}		0.0081		
			7.44×10^{10}		6.99×10^{8}		1.74×10^{10}		0.0094		
			8.23×10^{10}		6.57×10^{8}		1.85×10^{10}		0.0080		
			7.71×10^{10}		6.39×10^{8}		1.74×10^{10}		0.0083		
			7.63×10^{10}		4.64×10^{8}		1.83×10^{10}		0.0061		
6542-27-0161-002	33-17	9.50×10^{10}	1.01×10^{11}	9.56×10^{8}	4.57×10^{8}	2.39×10^{10}	2.32×10^{10}	0.0101	0.0045	0.0033	0.0009
			9.70×10^{10}		2.79×10^{8}		2.28×10^{10}		0.0029		
			9.49×10^{10}		2.28×10^{8}		2.18×10^{10}		0.0024		
			9.61×10^{10}		4.06×10^{8}		2.22×10^{10}		0.0042		
			9.69×10^{10}		2.31×10^{8}		2.35×10^{10}		0.0024		
			9.43×10^{10}		2.94×10^{8}		2.23×10^{10}		0.0031		
6542-40-0261-002	33-24	1.04×10^{11}	1.09×10^{11}	1.05×10^{9}	2.29×10^{8}	2.64×10^{10}	2.59×10^{10}	0.0101	0.0021	0.0024	0.0003
			1.05×10^{11}		2.40×10^{8}		2.28×10^{10}		0.0023		
			1.02×10^{11}		2.46×10^{8}		2.44×10^{10}		0.0024		
			9.92×10^{10}		2.09×10^{8}		2.39×10^{10}		0.0021		
			1.08×10^{11}		2.90×10^{8}		2.57×10^{10}		0.0027		
			1.03×10^{11}		2.86×10^{8}		2.42×10^{10}		0.0028		

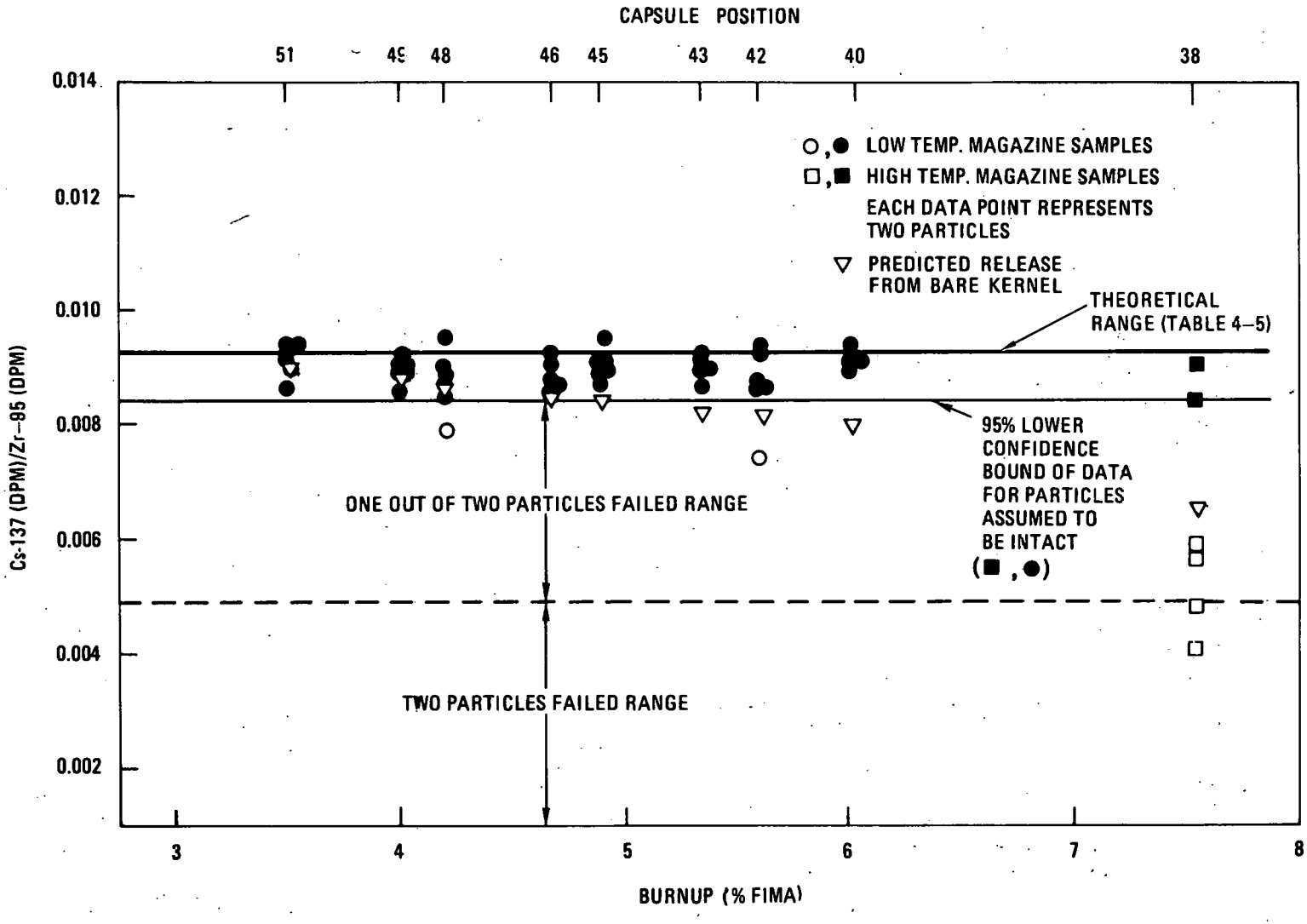

Fig. 4-6. Cs-137/Zr-95 ratio for TRISO ThO_2 samples from HT-31

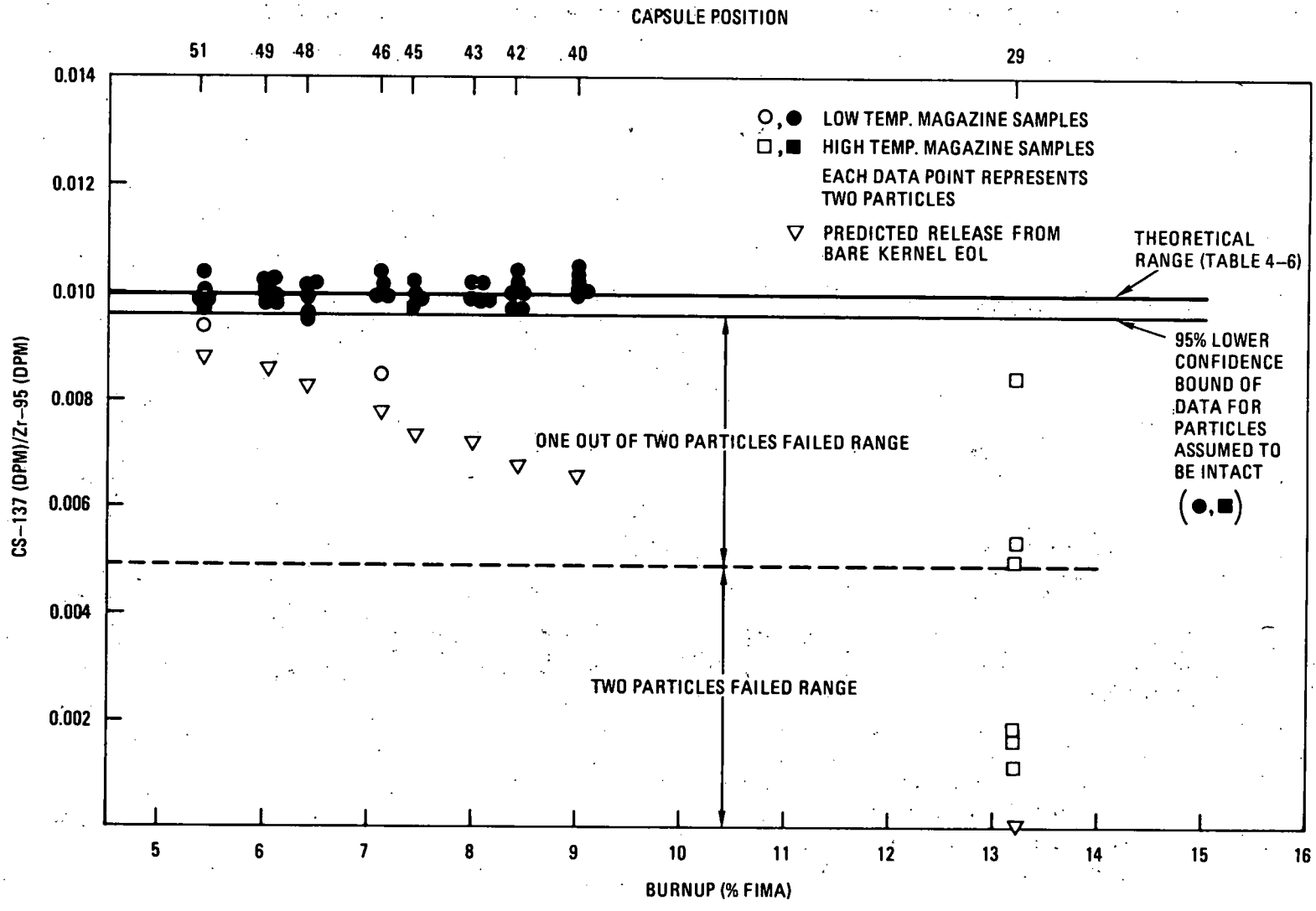

Fig. 4-7. Cs-137/Zr-95 ratio for TRISO ThO_2 samples from HT-33

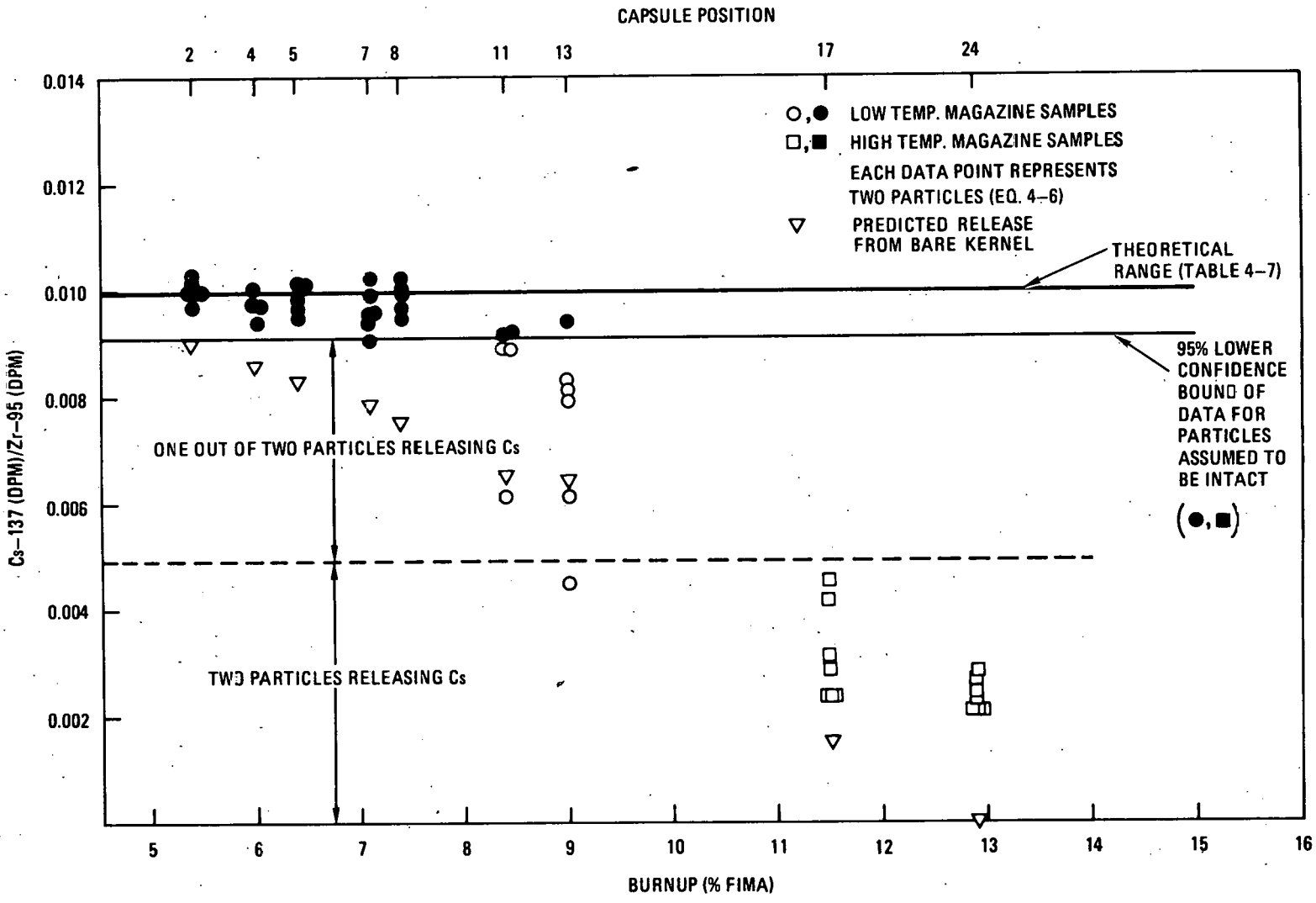

Fig. 4-8. Cs-137/Zr-95 ratio for BISO ThO_2 samples from HT-33

$$f = 2.95 \times 10^{-5} F^2 \sqrt{t}\, e^{-4680/T} \text{ (Ref. 4-8)} \quad , \tag{4-7}$$

where f = fractional release from a bare ThO_2 kernel,

F = burnup in % FIMA,

t = time (s),

T = temperature (K).

Equation 4-7 is based on an analysis of in-pile cesium release data as a function of burnup (Ref. 4-9). From this analysis the reduced diffusion coefficient was found to be

$$D' \text{ (1/s)} = 8 \times 10^{-12} (F/2.5)^4 \quad , \tag{4-8}$$

where F is the burnup in % FIMA and the equation applies to 1390 K. The temperature dependence was found to be given by $\exp[0.936\ (10^4/T - 7.19)]$. Combining the latter with Eq. 4-8 leads to the expression

$$D' \text{ (1/s)} = 1.71 \times 10^{-10} F^4 e^{-9360/T} \quad . \tag{4-9}$$

The fractional release is related to the reduced diffusion coefficient (Ref. 4-10) by the expression

$$f \cong 4 \sqrt{D't/\pi} \quad , \tag{4-10}$$

which, when combined with Eq. 4-9, yields Eq. 4-7.

Less than 2% of the TRISO coated particles from the low-temperature magazines in both HT-31 and HT-33 exhibited cesium loss, as shown in Figs. 4-6 and 4-7. The high-temperature magazine samples show about 60% and 75% SiC failure as determined from cesium release.

As shown in Fig. 4-8, the BISO low-temperature samples retained their cesium inventory to a burnup of 7.5% FIMA; however, at burnup values of

8.4% and 9% FIMA, 50% to 60% of the particles exhibited cesium loss. The particles in the high-temperature BISO samples released a large fraction of their cesium. Cesium release is discussed further in Section 5.1.2.

4.5. PARTICLE DENSITY MEASUREMENTS

Postirradiation particle density measurements were made on four BISO samples from HT-33. A liquid gradient technique described in Ref. 4-11 was used to measure the density of the coated particles before and after irradiation. The results of these measurements and the percent density change are reported in Table 4-8. Assuming the mass of the particles remained constant during irradiation, the postirradiation particle diameter was calculated using the following equation:

$$D_f = D_o \left(\frac{\rho_o}{\rho_f} \right)^{1/3} \tag{4-11}$$

where D_f = postirradiation particle diameter,
D_o = preirradiation particle diameter,
ρ_o = preirradiation particle density,
ρ_f = postirradiation particle density.

The change in diameter was calculated and is given in Table 4-8. This is discussed in further detail in Section 5.1.4.2.

REFERENCES

4-1. "Gas Cooled Reactor Programs HTGR Base Technology Program Progress Report July 1, 1975-December 31, 1976," ERDA Report ORNL-5274, Oak Ridge National Laboratory, November 1977.

4-2. Wessman, G. L., General Atomic Company, "Response to NRC Lead Item I For ThO_2 Review," private communication to W. Gammill, April 9, 1979.

TABLE 4-8
IRRADIATION-INDUCED DENSIFICATION OF BISO ThO_2 PARTICLES

Sample Retrieval Number	Capsule Position	Average Temperature (°C)	Fast Fluence ($E > 29$ fJ)$_{HTGR}$ (10^{25} n/m^2)	Burnup (% FIMA)	Preirradiation Density[a] (Mg/m^3)	Standard Deviation	Postirradiation Density[a] (Mg/m^3)	Standard Deviation	Percent Change[b]	Standard Deviation (%)	Particle Diameter (μm)		ΔD/D
											Preirradiation[c]	Postirradiation[d]	
6542-27-0161-001	8	1270	7.8	7.4	3.45	0.018	3.97	0.005	15.1	0.62	823	788	-0.043
6542-27-0161-002	17	1470	10.7	11.5	3.45	0.018	3.68	0.099	6.7	2.92	829	812	-0.021
6542-40-0261-001	5	1230	6.8	6.4	3.39	0.028	4.08	0.007	20.4	1.02	832	783	-0.059
6542-40-0261-002	24	1510	11.5	12.9	3.39	0.028	3.77	0.012	11.2	0.98	828	799	-0.035

[a] Measured by a liquid gradient technique.

[b] Percent change = $\left[(\rho_{post} - \rho_{pre})/\rho_{pre}\right] \times 100$.

[c] Measured or calculated on test sample.

[d] Calculated from $D_{final} = D_o\left(\frac{\rho_o}{\rho_f}\right)^{1/3}$ conservation of mass.

4-3. Kovacs, W. J., C. A. Young, and D. P. Harmon, "Preirradiation Report of TRISO and BISO Coated ThO_2 Particles for Irradiation in Capsules HT-31 and HT-33," ERDA Report GA-A13923, General Atomic Company, November 1977.

4-4. Smith, C. L., "Migration of ThO_2 Kernels Under the Influence of a Temperature Gradient," General Atomic Report GA-A14058, November 1976.

4-5. Wahl, A. C., "Nuclear-Charge Distribution in Fission: Cumulative Yields of Short-Live and Krypton and Xenon Isotopes from Thermal-Neutron Fission of U-235," J. Inorg. Nucl. Chem. 6, 263 (1958).

4-6. "HTGR Generic Technology Program Fuels and Core Development Quarterly Progress Report for the Period Ending August 31, 1978," ERDA Report GA-A15093, General Atomic Company, September 1977.

4-7. "Fuel Design Data Manual," Issue C, General Atomic unpublished data.

4-8. Myers, B., General Atomic Company, private communication.

4-9. "HTGR Fuel Development Department Technical Status Report for the Quarter Ending September 30, 1979," General Atomic Company, unpublished data, October 31, 1979.

4-10. Olander, D. R., "Fundamental Aspects of Nuclear Reactor Fuel Elements," ERDA Report TID-26711-P1, April 1976, p. 301.

4-11. "Particle Density Measurements," General Atomic Company, unpublished data.

5. DISCUSSION

5.1. PARTICLE IRRADIATION PERFORMANCE

5.1.1. Comparison of Particles from 240-mm-Diameter and 127-mm-Diameter Coaters

One of the primary objectives of the irradiation tests of capsules HT-31 and HT-33 was to evaluate the irradiation performance of TRISO and BISO fuel particles fabricated in the 240-mm-diameter pilot plant coater as part of the processing scale-up from the 127-mm coater. TRISO and BISO batches 6252-05-0160 and 6542-27-0161 were coated in the 127-mm coater and used as a reference for the coater size comparison. As was shown in Tables 4-1 through 4-7, there was no correlation of fuel performance with coater size. Therefore, particles from the 240-mm-diameter production coater should perform as well as particles coated in the 127-mm-diameter laboratory coater.

5.1.2. Comparison of TRISO and BISO ThO_2 Fuel

The results of the postirradiation visual, fission gas release, and gamma ray spectrometry examinations show that the BISO ThO_2 and TRISO ThO_2 particles in capsule HT-33 showed no significant fission product release or failure up to a burnup level of 7.5% FIMA (see Figs. 5-1 through 5-3) at particle surface temperatures of approximately 1200°C. As shown in Figs. 5-1 through 5-3, TRISO and BISO samples from the high-temperature magazines in both capsules show high visual failure fractions except for TRISO sample HT-31-38 and BISO samples HT-33-17 and HT-33-24. The TRISO sample appeared to be intact under visual examination, but the fission gas release results showed a 45% total coating failure. The results of the gamma scan showed that 6 of the 12 particles of this sample that were

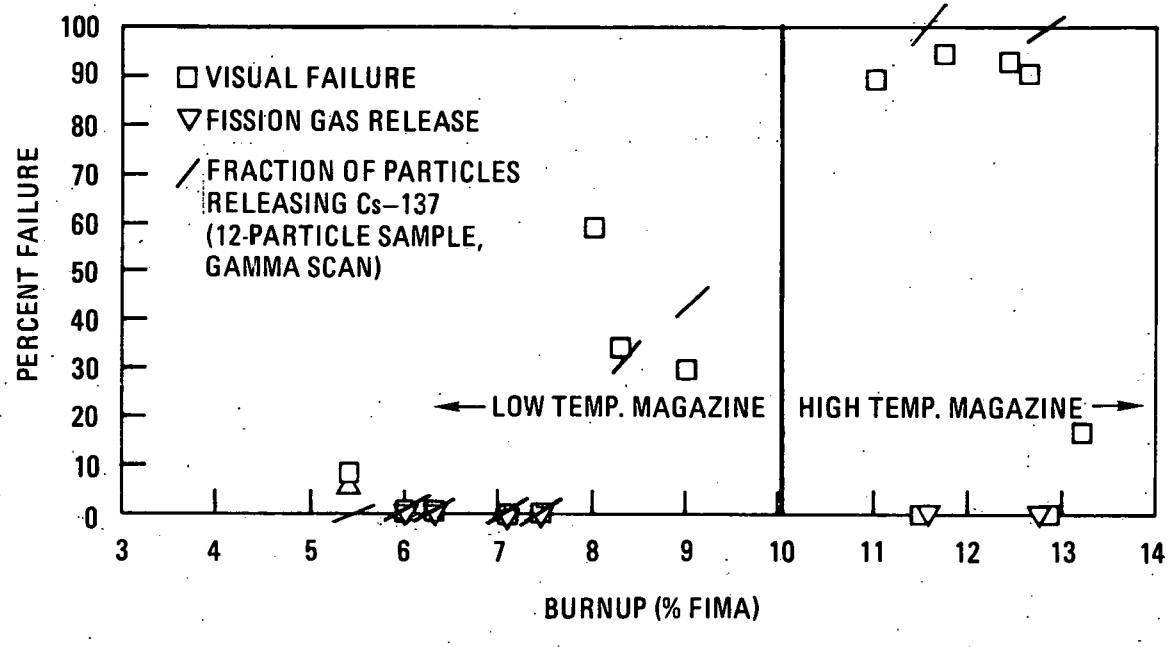

Fig. 5-1. Failure levels versus burnup for BISO samples from HT-33

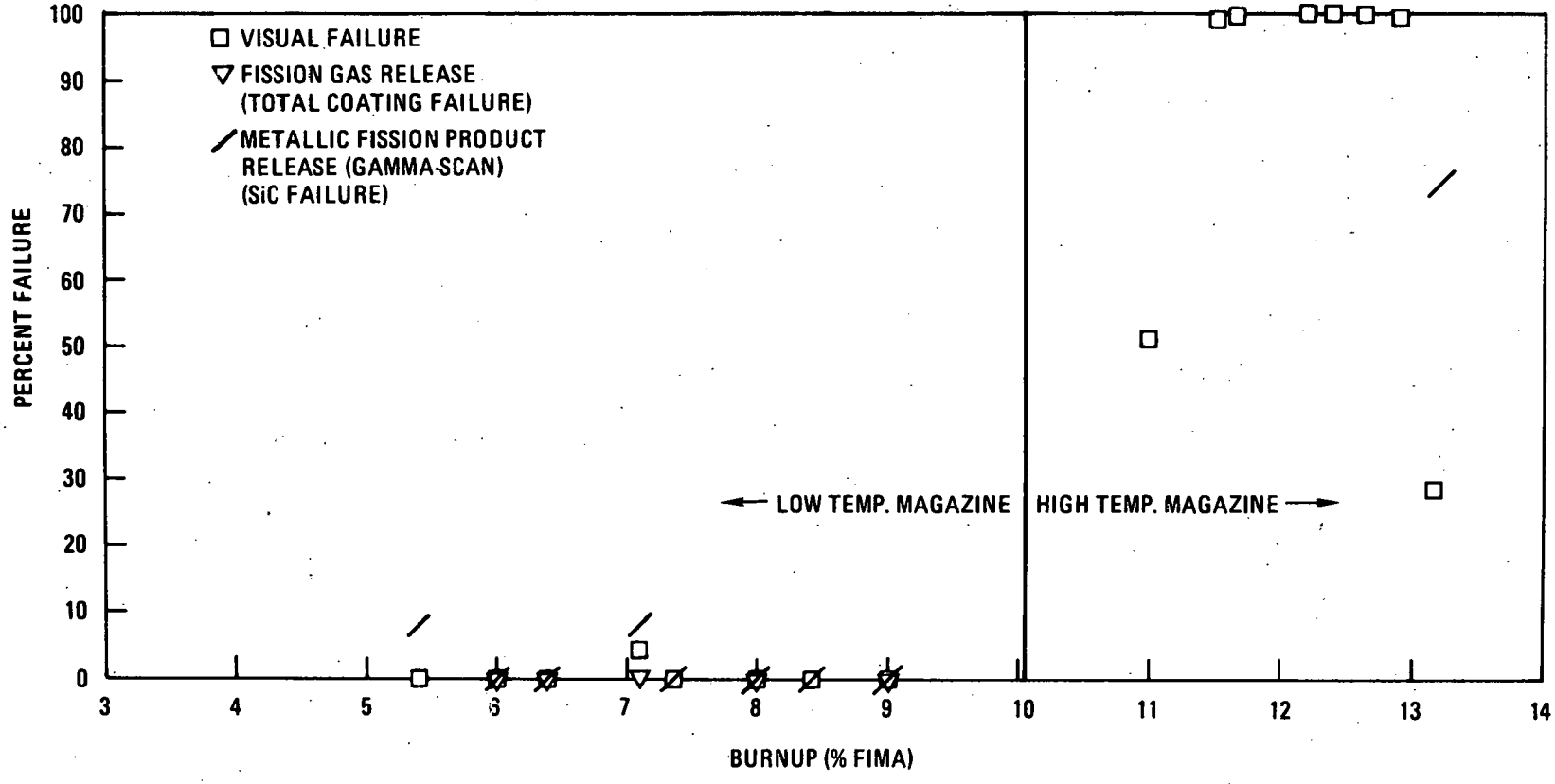

Fig. 5-2. Failure levels versus burnup for TRISO samples from HT-33

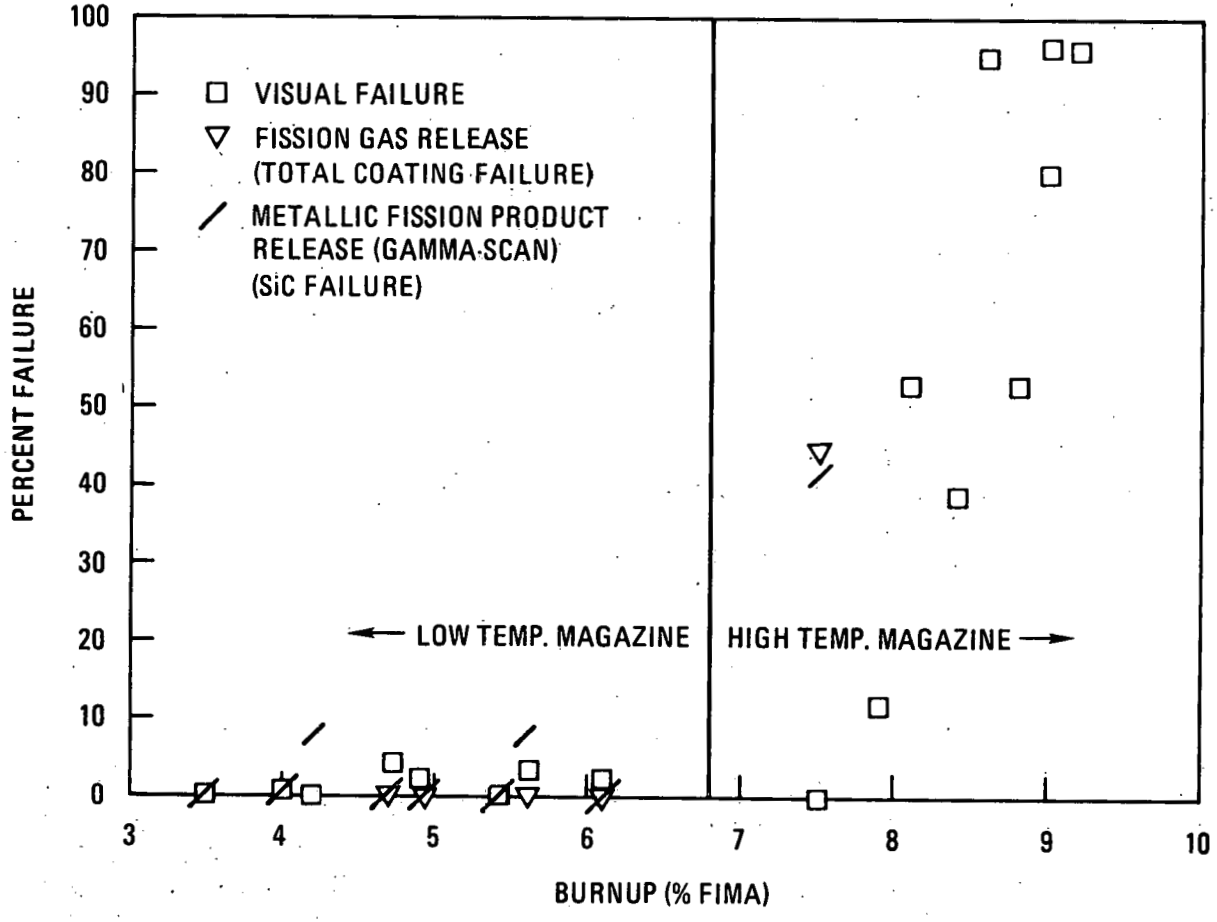

Fig. 5-3. Failure levels versus burnup for TRISO samples from HT-31

gamma counted showed some cesium loss, indicating SiC failure. Metallography of HT-31-38 revealed a large amount of kernel migration and SiC degradation, which supports the fission product release results. Thus, although the particles appeared intact under visual inspection, the fission gas release data suggest a total coating failure level of about 50%. The BISO samples HT-33-17 and HT-33-24 also appeared to be intact under visual inspection, and the short-lived fission gas results (Fig. 5-1) show the particle samples to be retentive of their Kr-85m inventory. Thus, the BISO particle coatings of these two samples did not fail during irradiation. However, all 12 of the particles in each sample that were gamma scanned released most of their cesium inventory. Since the coatings were known to be intact from the fission gas release results, the cesium loss was by diffusion through the BISO coatings. These results show that under high-temperature, high-burnup irradiation conditions, the BISO particles will exhibit diffusional release of cesium even though they do not fail and that the TRISO particles will experience high total coating failure levels.

Comparison of the TRISO and BISO particle irradiation performance at 1200°C and burnups between 7.5% and 9% FIMA is more difficult than for the lower or higher burnup samples. As shown in Fig. 5-2, under these conditions the TRISO samples do not show fission product release or appear failed under visual examination. The three BISO samples, however, under visual inspection show total coating failure fractions of about 28% to 60%, as shown in Fig. 5-1. No fission gas release measurements were done; therefore, the total coating failure fraction cannot be verified. Gamma counting was done on two of the three samples. Twelve particles that appeared intact after visual examination were selected from each sample for gamma counting; 40% and 50% of the particles in the two samples gamma counted showed cesium loss. Whether the cesium release occurred by a diffusional process through intact PyC or escaped through cracked PyC coatings cannot be determined with the data available. From the visual examination and fission product data, however, the irradiation performance of the TRISO particles is excellent at 1200°C and from 7.5% to 9% FIMA, while the BISO particles show significant total coating failure under visual examination.

Another objective of the HT-31 and HT-33 capsule experiment was confirmation of the reference TRISO coated (450-μm ThO_2 kernel) particle design under peak HTGR exposure conditions. There was no discernible difference between the irradiation performance of the TRISO coatings of the 450-μm kernel particles and the 500-μm kernel particles. As shown in Table 4-1, the TRISO particle pressure vessel performance is consistent with the pressure vessel performance predicted by stress modeling. No pressure vessel failure predictions were done at 1500°C because failure at such high temperatures is caused by SiC degradation in addition to partial pressure. A detailed description of the calculational procedure for this model is given in Ref. 5-1.

5.1.2.1. Kernel Migration in TRISO ThO_2. As shown in Figs. 4-1 and 4-2, ThO_2 kernel migration was observed in the high-temperature TRISO particles. Kernel migration coefficients (KMCs) were calculated and the results are shown in Table 4-3. The distance the kernels traveled was measured on the polished sections of the two specimens from HT-31. This is a crude measurement because the particles are randomly sectioned and there is no way to determine the sectioned plane of each particle relative to the true thermal gradient direction. The thermal gradient and the amoeba equivalent temperature were nevertheless estimated from the calculated graphite annulus and peak particle surface temperatures.

The temperatures and thermal gradients of the unbonded particles have large uncertainties and the in-pile data are not corrected for the incubation period. As shown in Fig. 5-4, the calculated in-pile KMCs of TRISO ThO_2 particles are in agreement (within a factor of 1.5) with the out-of-pile KMC values for BISO ThO_2 particles (Ref. 5-2) and help to confirm out-of-pile postirradiation thermal gradient heating experiments.

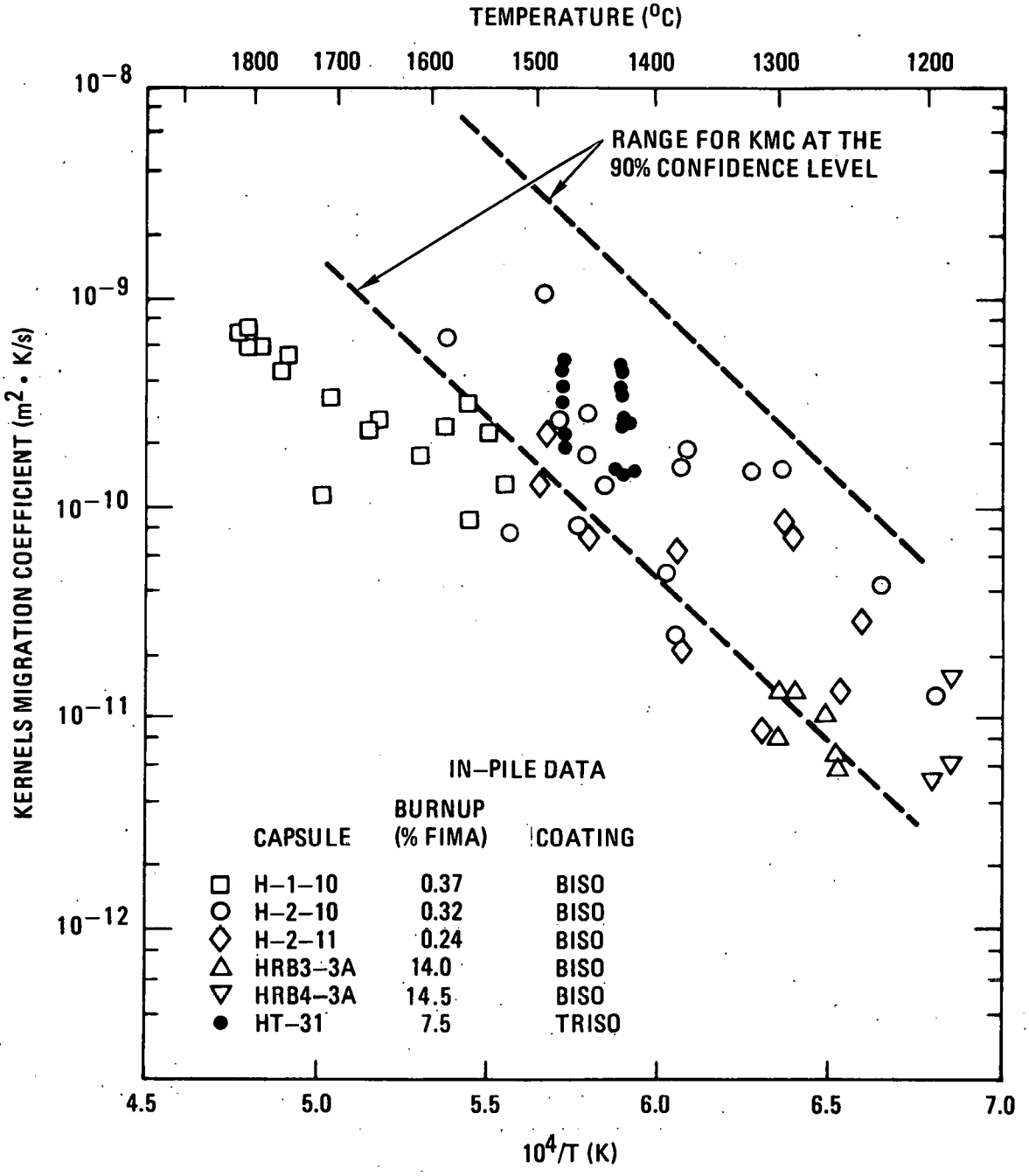

Fig. 5-4. Comparison of in-pile and out-of-pile ThO_2 KMC data (Ref. 5-2)

5.1.3. Free Silicon in TRISO ThO_2 Particles

The white phase observed in sample 6252-09-0161-003, and discussed in Section 4.2, was analyzed by microprobe and found to be elemental silicon. No other elements were found in the phase except a small amount of carbon (<13%). Six samples in each capsule were fabricated with the same SiC substrate (6780-25). The parent batches with the same SiC were 6252-06-010, 6252-09-010, and 6252-10-010. One of the samples (6252-06-0161-002, HT-31-38), which had been irradiated in a high-temperature magazine, was examined metallographically and no white phase was found. Subsequent metallography on the samples from the low-temperature magazines in both capsules revealed the white phase in each sample (see Figs. 5-5 through 5-8). Metallography on the preirradiated batch (6252-09-010) showed lenticular flaws in 24% of the particles (see Fig. 5-8). No white phase of the type seen after irradiation was observed in the unirradiated batch. Subsequent analysis by SEM and EDAX showed no Si-, C-, or O-rich areas in the voids or the SiC layer of unirradiated particles.

Workers at Kernforschungsanlage in the Federal Republic of Germany found a similar white phase in 10% of UC_2 TRISO unbonded particles irradiated in experiment RC-RM1 (Ref. 5-3). These particles were irradiated for 60 full-power days at a temperature of 970° to 1040°C and a fast fluence level of 3.79×10^{25} n/m^2 $(E > 29\ fJ)_{HTGR}$. Microprobe analysis was done on these particles at KFA, showing the composition of the white phase area to be 95 ± 1 wt % Si and 6 ± 1 wt % C. KFA also did microprobe analysis on the unirradiated SiC and could find no Si-rich areas.

An experiment was undertaken at GA to determine if free silicon would accumulate in the SiC flaws induced by heat treatment in the absence of a neutron flux. Six samples of 56 particles each from batch 6252-09-0161 were placed in a graphite holder in a furnace and heated in an Ar atmosphere to simulate the reactor cycles and temperatures experienced by the HT capsule sample 6252-09-0161-003 (HT-33-40). After each cycle the furnace was shut down and one sample was removed for optical and scanning

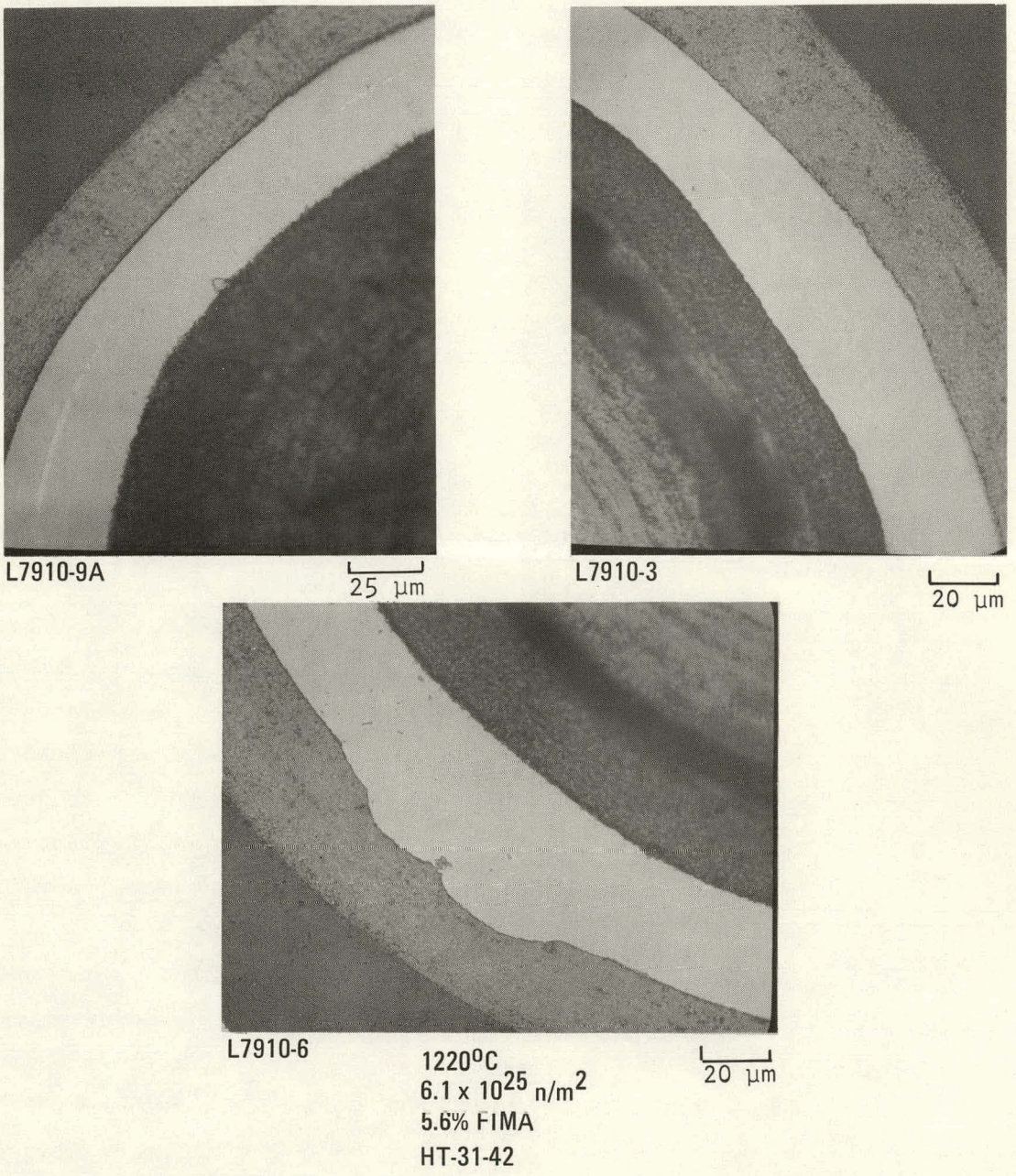

Fig. 5-5. Bright field photomicrographs of ThO_2 TRISO particles from batch 6252-09-0161-001

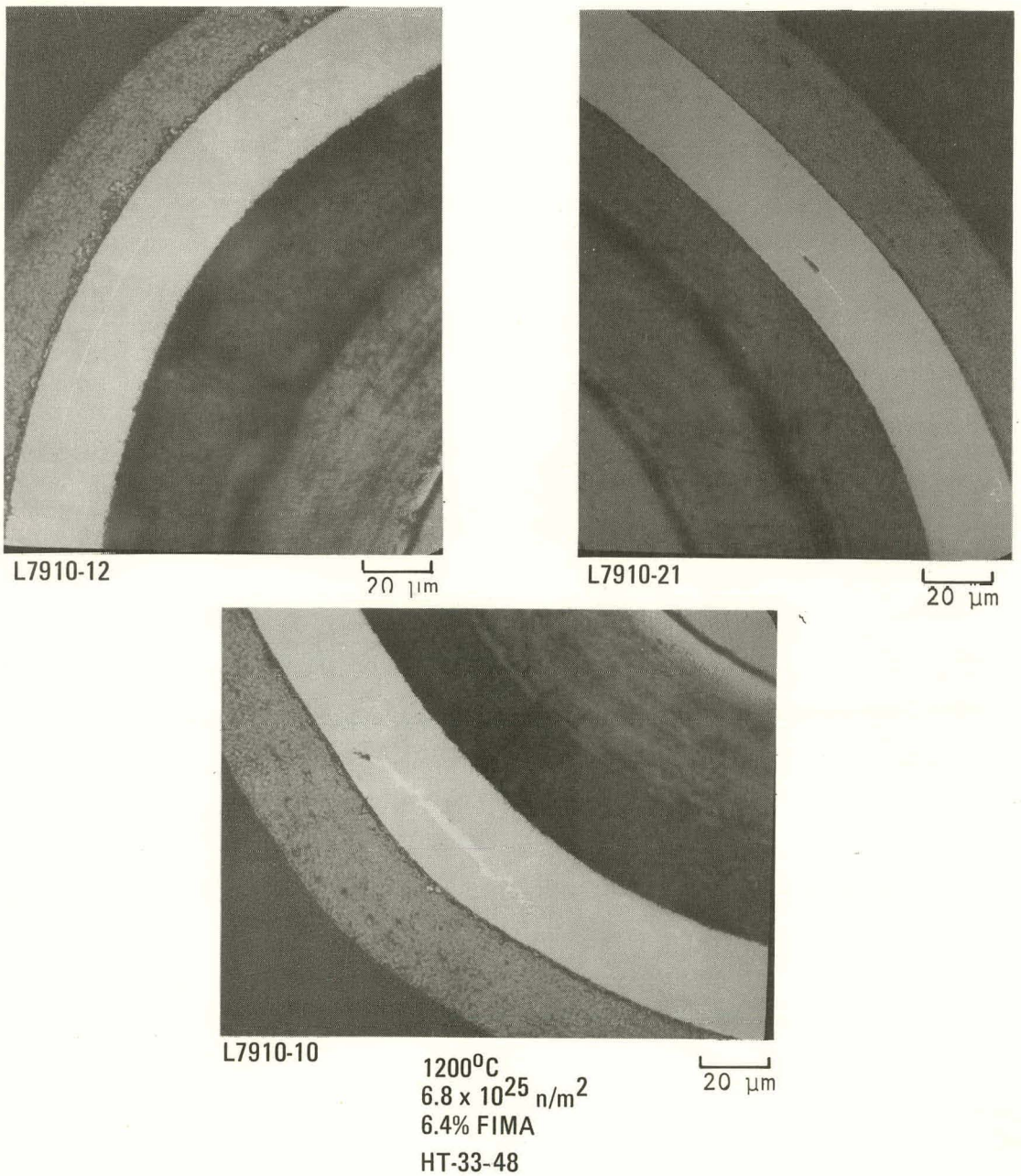

Fig. 5-6. Bright-field photomicrographs of ThO_2 TRISO particles from batch 6252-06-0161-003

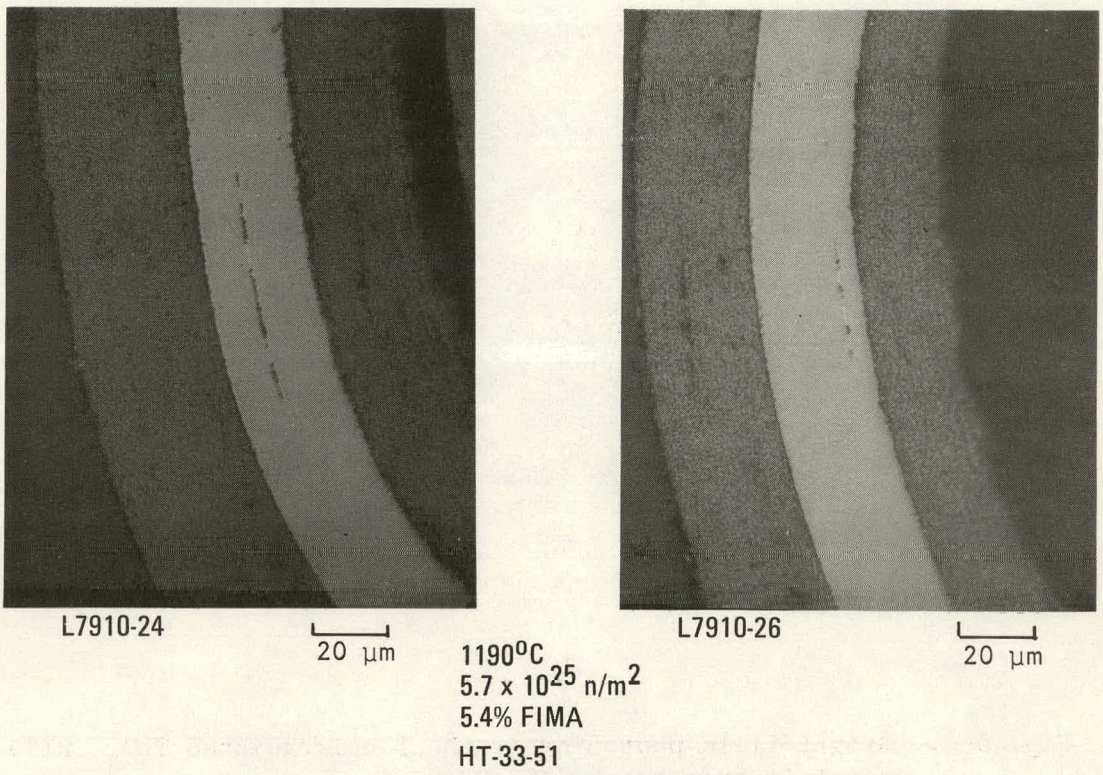

Fig. 5-7. Bright field photomicrographs of ThO_2 TRISO particles from batch 6252-10-0161-003

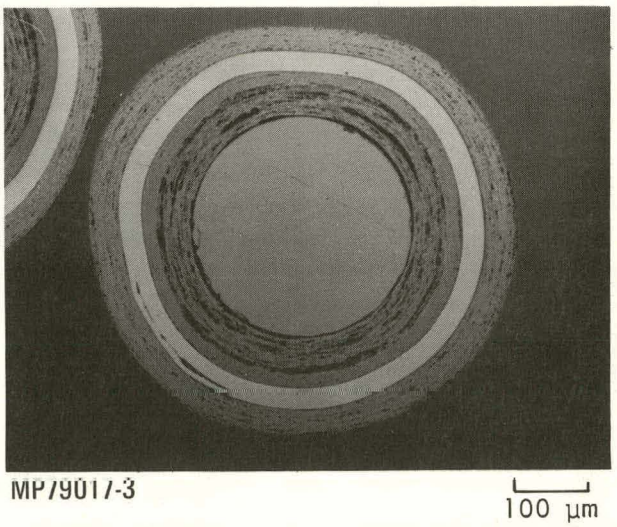

Fig. 5-8. Bright field photomicrograph of unirradiated ThO_2 TRISO particle from batch 6252-09-0161

electron microscopy. Energy dispersive X-ray analysis was done on each flaw and over the SiC layers. Table 5-1 shows the time and temperatures of the five cycles in the experiment. No change in the appearance or composition was detected in any of the samples by any of the analyses. Thus, heating at times and temperatures similar to those the HT capsule samples experienced will not cause free silicon to accumulate in the SiC flaws of particles from sample 6252-09-0161.

From the results obtained at GA and KFA, the only conclusion that could be drawn was that the white phase consisted of elemental silicon. A possible explanation for this phenomenon is that the unirradiated SiC coating contained excess silicon, which accumulated in flaws in the SiC layer during irradiation. However, none of the analysis techniques were able to detect excess silicon in the unirradiated SiC coating or reveal a SiC structure that was indicative of excess silicon.

The particle samples that showed the white phase performed as well during the irradiation testing as did those samples without the phase. These SiC batches all had SiC density values near theoretical. The coatings retained metallic fission products even though enough free Si was in the coating to be seen after irradiation. Apparently there was not enough to provide "free silicon" channels for the diffusion of fission products as discussed in Ref. 5-4.

5.1.4. OPyC Variables

One of the primary objectives of capsules HT-31 and HT-33 was to evaluate the irradiation performance of TRISO and BISO coated ThO_2 particles with an OPyC variable. When the fuel was made, the OPyC variables thought to give the best indication of irradiation performance were (1) coating rate, (2) density, (3) anisotropy, and (4) diluent gas composition for the BISO coatings. Since then it has been thought that microporosity and the ratio of active coating gas flow rate to the total coating gas flow rate would give a more reliable indication of OPyC coating performance than coating rate and anisotropy.

TABLE 5-1
TIME AND TEMPERATURE FOR FIVE EXPERIMENT CYCLES

Cycle	Temperature (°C)	Number of Days
1	1110	11
	1080	10
	1110	3
	RT	2
2	1180	12
	1165	9
	1200	2
	RT	3
3	1215	12
	1230	11
	1245	1
	RT	1
4	1325	11
	1270	11
	1255	3
	RT	2
5	1275	7
	1265	14
	RT	

5.1.4.1. TRISO OPyC Variables. Figures 5-9 and 5-10 show visual failure versus OPyC density for samples in HT-31 and HT-33. The graphs show that failure was more a function of temperature than density variation between 1.70 and 2.0 Mg/m^3. Only one batch (6252-06-0261) had a density (1.70 ± 0.011 Mg/m^3) that was out of specification (1.75-1.80) and outside the critical region (1.72-1.83). This batch had a sample (6252-06-0261-008) that exhibited a 4% visual OPyC failure fraction in HT-33, while all the other samples from the low-temperature magazine in HT-33 showed zero failure. However, in capsule HT-31 this sample exhibited zero visual failure in the low-temperature magazine, while samples with OPyC density values within specification failed as shown in Fig. 5-9. Thus, the specifications for density alone do not ensure good performance.

Figure 5-11 shows OPyC coating failure as a function of anisotropy for TRISO ThO_2 particles irradiated in the low-temperature magazines in capsules HT-31 and HT-33. Anisotropy between 1.026 and 1.052 BAF_o does not affect irradiation performance at particle surface temperatures less than 1260°C (see Table 4-1 for time-averaged temperatures) in TRISO particles.

The TRISO ThO_2 manufacturing specifications for HTGR fuel call for an active coating gas ratio of $\geq$0.25 during coating as a means of assuring that an appropriate microstructure and adequate particle performance are obtained (Ref. 5-5). In capsules HT-31 and HT-33, only one batch (6252-05-010) had a coating gas ratio of <0.25 (see Table 2-1 and Figs. 5-12 and 5-13). The active coating gas ratio for batch 6252-05-010 was 0.16. The failure level of this batch was zero in the low-temperature magazine and 95% in the high-temperature magazine, which was virtually the same behavior as that for other samples (which had coating gas ratios $\geq$0.16) irradiated under the same conditions in either capsule HT-31 or HT-33. Therefore, no dependence of OPyC performance on OPyC active coating gas ratio $\geq$0.16 was observed.

OPyC microporosity is a property affecting the irradiation stability of OPyC layers, especially on TRISO coated particles. Microporosity is a

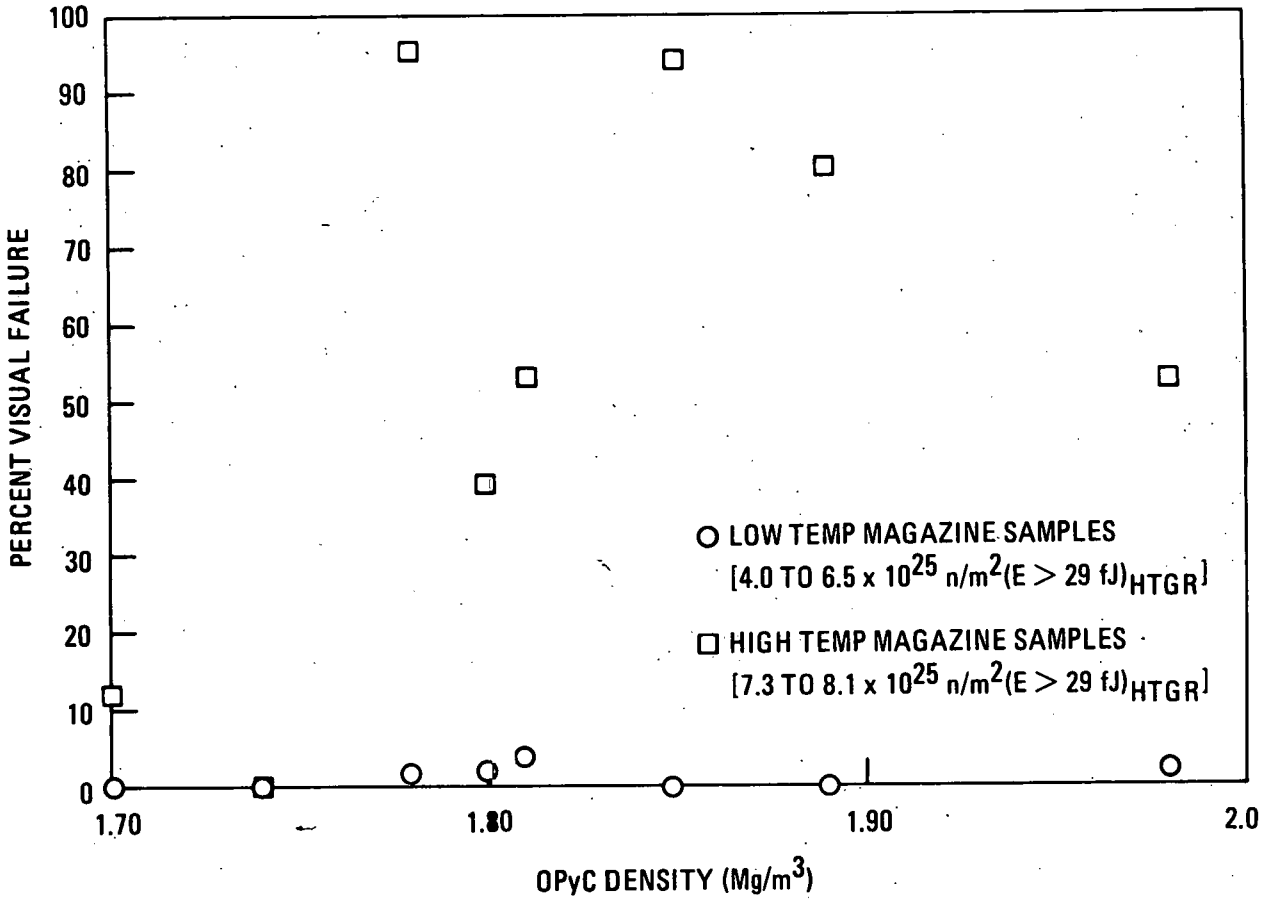

Fig. 5-9. HT-31 TRISO failure versus OPyC density

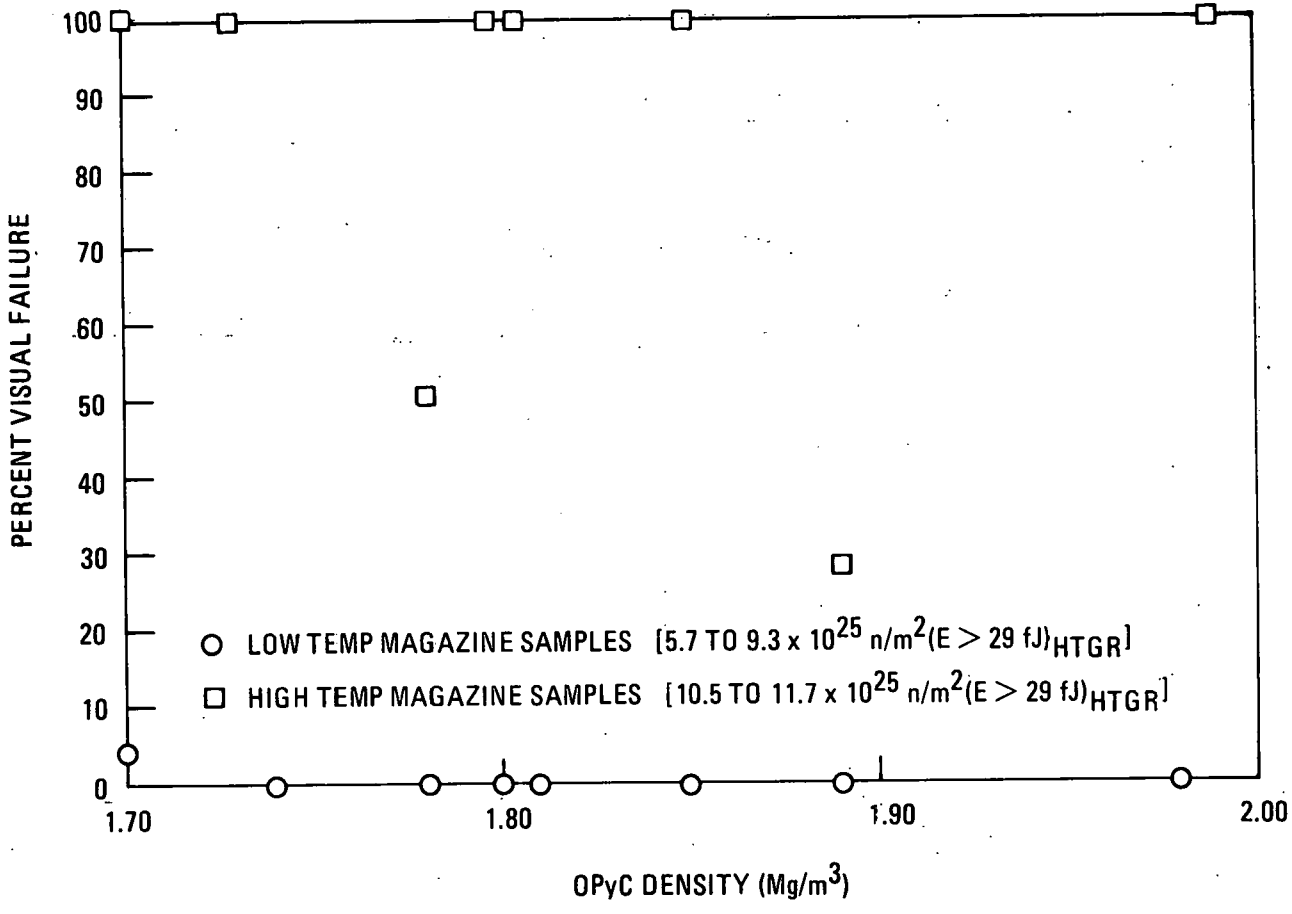

Fig. 5-10. HT-33 TRISO failure versus OPyC density

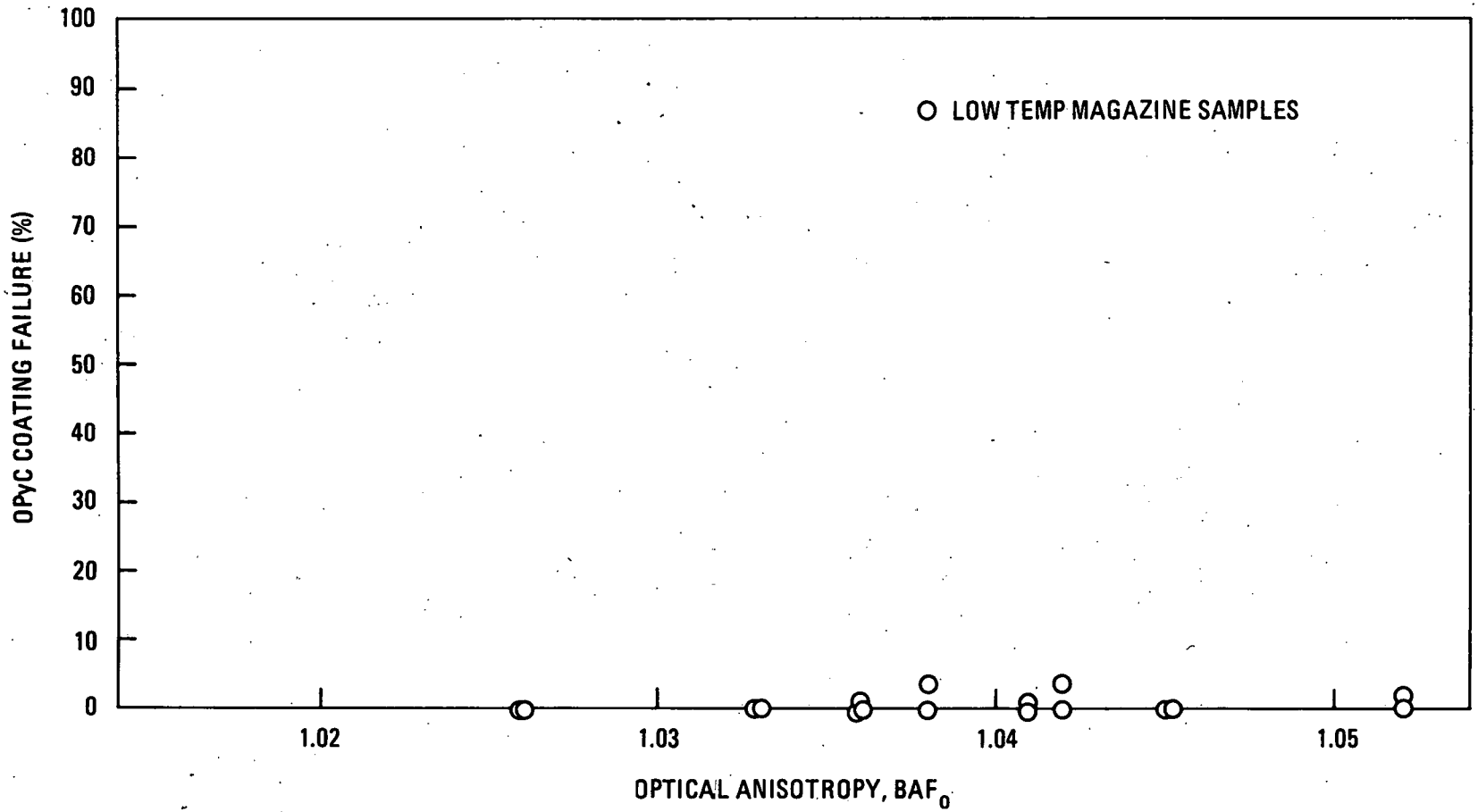

Fig. 5-11. OPyC coating failure versus BAF_o for TRISO ThO_2 particles

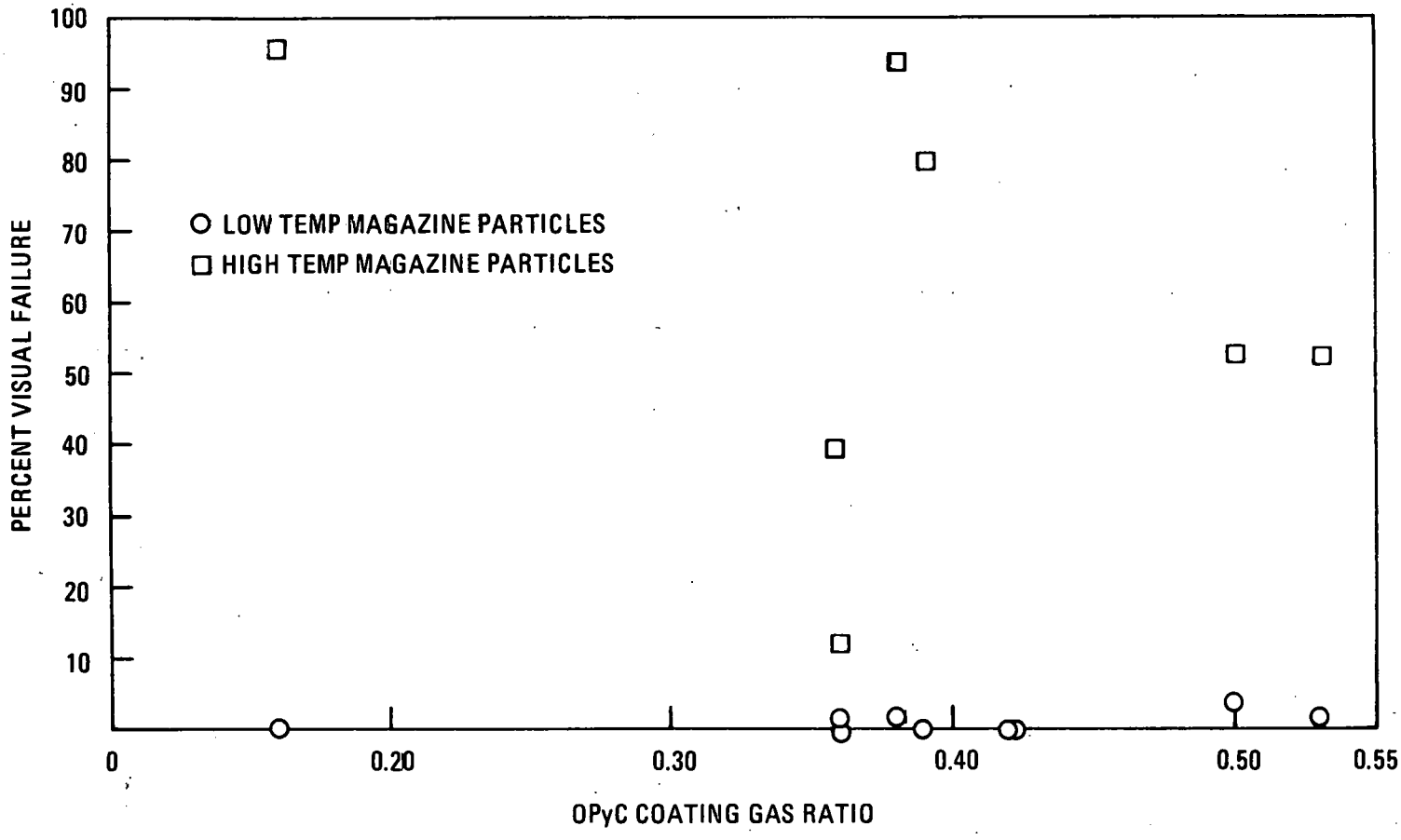

Fig. 5-12. HT-31 TRISO particle failure versus coating gas ratio

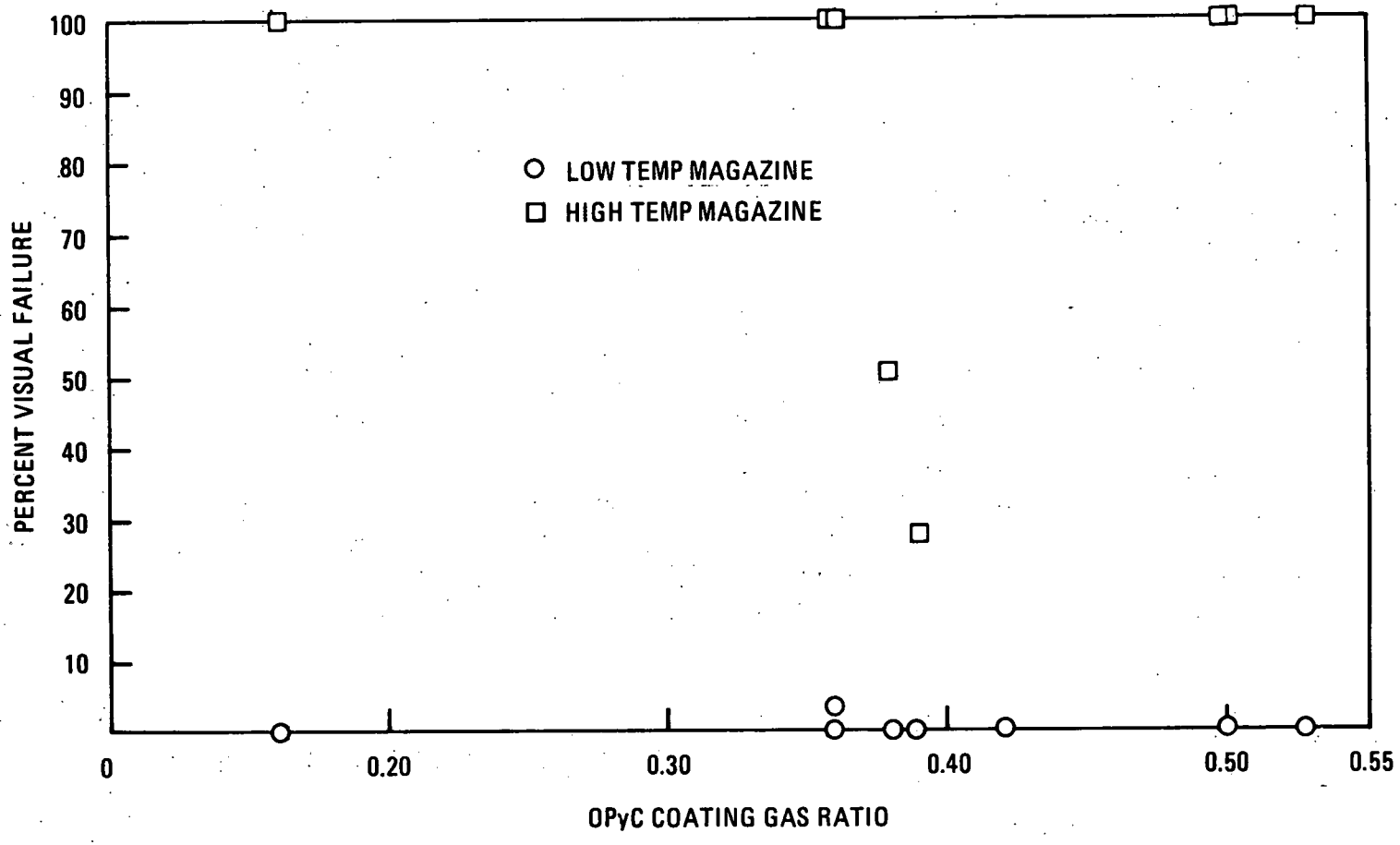

Fig. 5-13. HT-33 TRISO particle failure versus coating gas ratio

measure of the surface-connected porosity and is determined by high-pressure mercury intrusion. Below a value of about 17 ml/kg OPyC, the pyrocarbon tends to fail due to an inability to accommodate strain. When the microporosity of the OPyC is greater than about 33 ml/kg OPyC, a matrix-coating interaction causes OPyC failure in the fuel rods (Ref. 5-5). The samples in HT-31 and HT-33 all had microporosity values greater than 32.9 ml/kg OPyC; however, because the sample was made up of loose particles, matrix-coating interaction was not involved and the failure levels are independent of microporosity. Figures 5-14 and 5-15 show that the failure levels for these samples are independent of microporosity values greater than 33 ml/kg OPyC.

Sample 6252-05-0160 had a microporosity value of 32.9 ml/kg OPyC and an active coating gas ratio of 0.16. The microporosity was higher than was expected from the empirical correlation between microporosity and coating gas ratio given in Fig. 5-16 and Ref. 5-6. Figure 5-16 shows the data given from Ref. 5-6 and the data point provided by sample 6252-05-0160. The reason for the poor correlation is unknown.

As shown in Fig. 5-17, the TRISO particles tested in HT-31 and HT-33 had OPyC coating rates between 4.5 and 8.4 μm/min. The OPyC failure level shows no correlation with coating rate in either the high- or low-temperature magazines.

In capsule HT-31 and HT-33 no correlation between TRISO OPyC performance and the OPyC variables of density, microporosity, active coating gas ratio, coating rate, or anisotropy was shown. The samples from the low-temperature magazines had low failure levels and the high-temperature magazine samples had high failure levels.

5.1.4.2. BISO OPyC Variables. Figure 5-18 is a plot of the percent density change versus fast fluence for BISO coated particles irradiated in capsule HT-33. The density change and the calculated diametral change are given in Table 4-8. For comparison, irradiation data from capsules HT-18 and HT-19 and the predicted density change, based on data presented

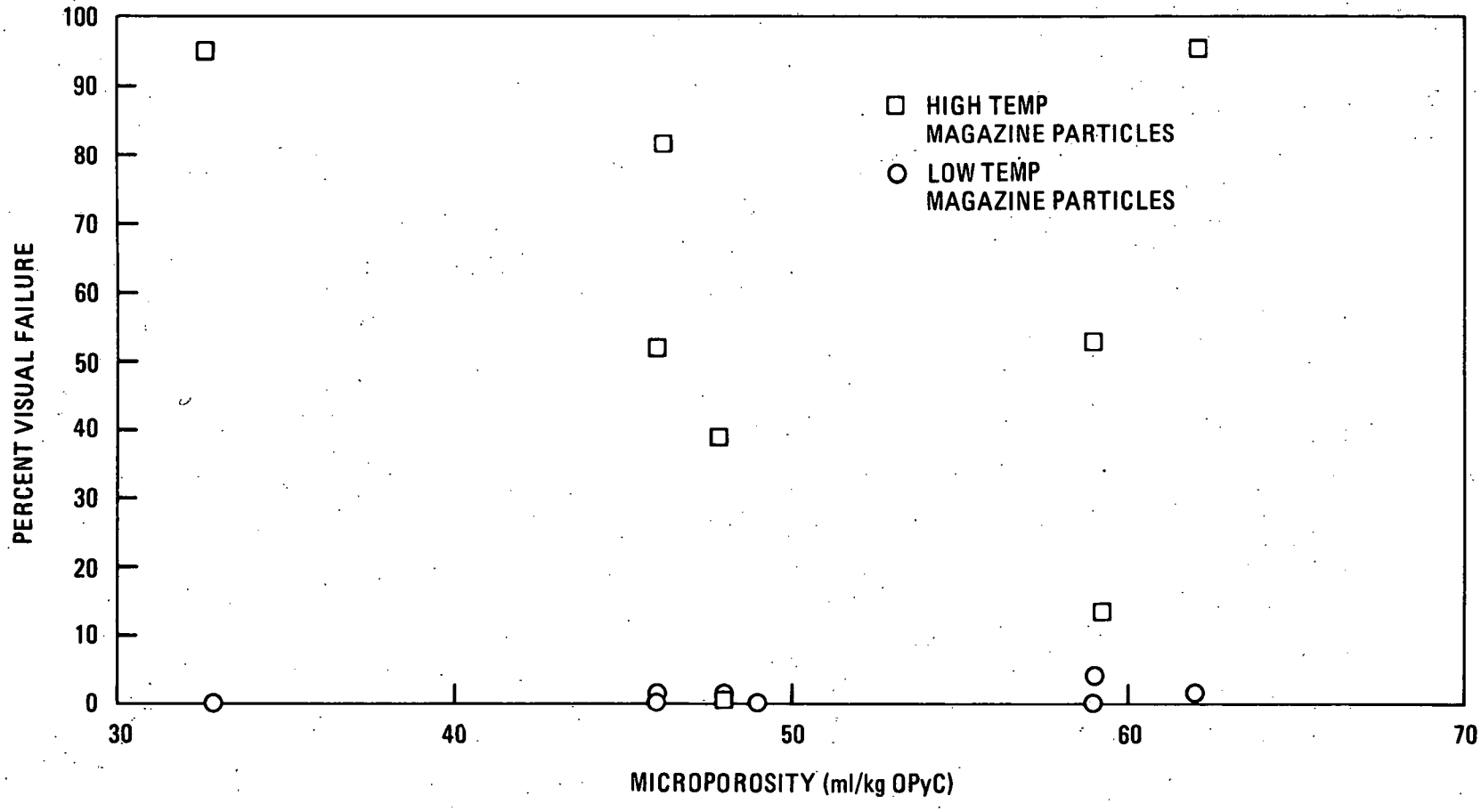

Fig. 5-14. HT-31 TRISO particle failure versus microporosity

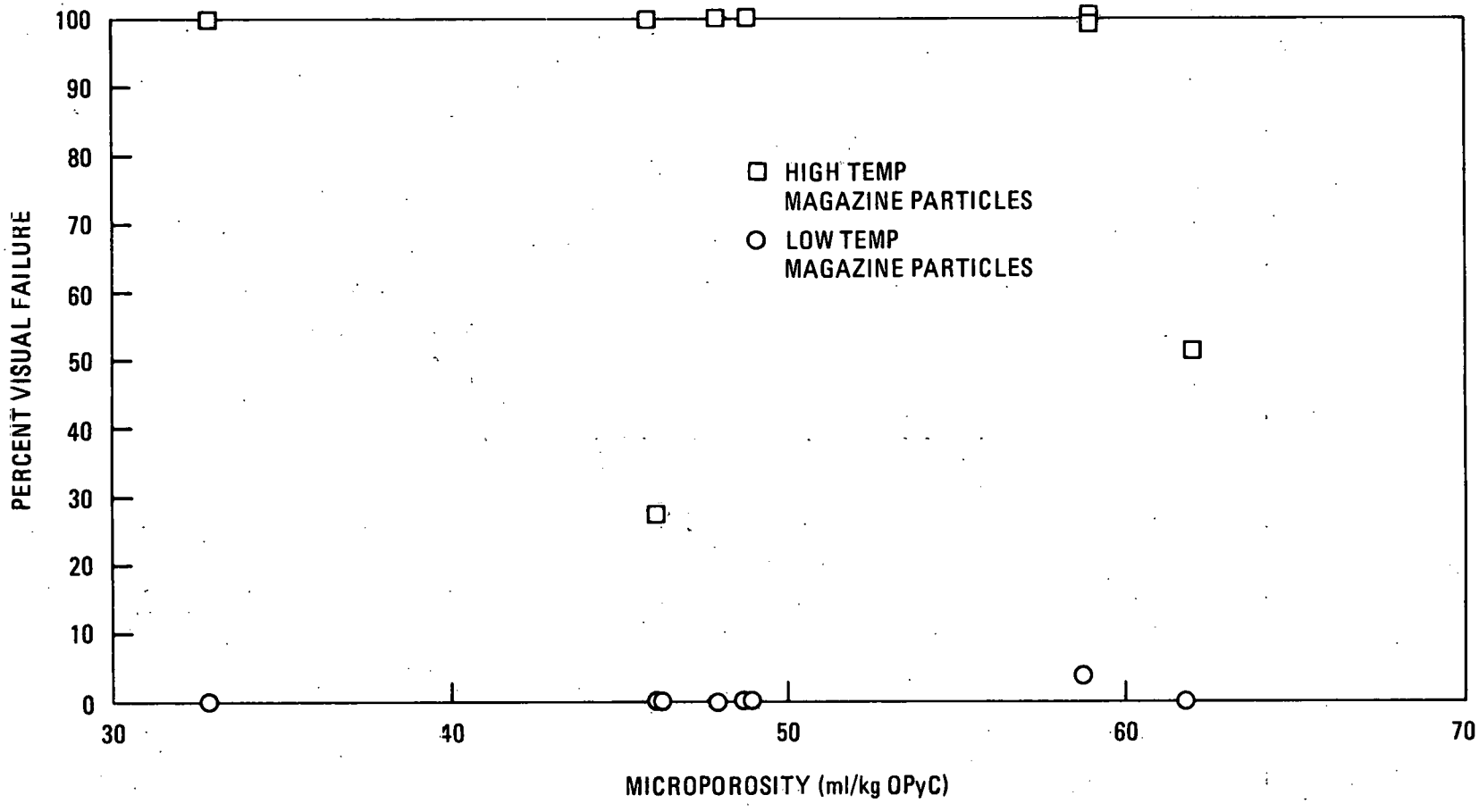

Fig. 5-15. HT-33 TRISO particle failure versus microporosity

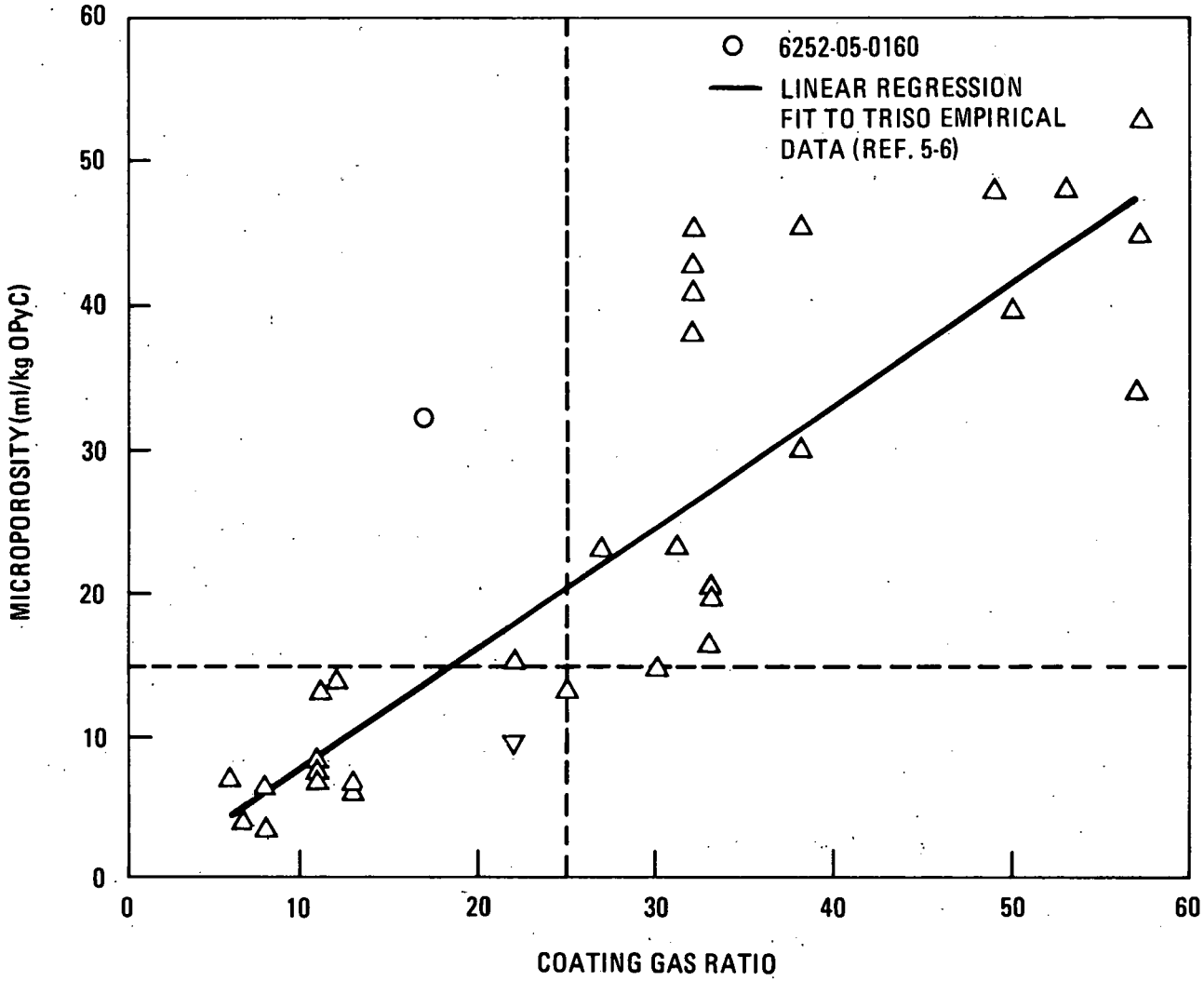

Fig. 5-16. Microporosity versus coating gas ratio

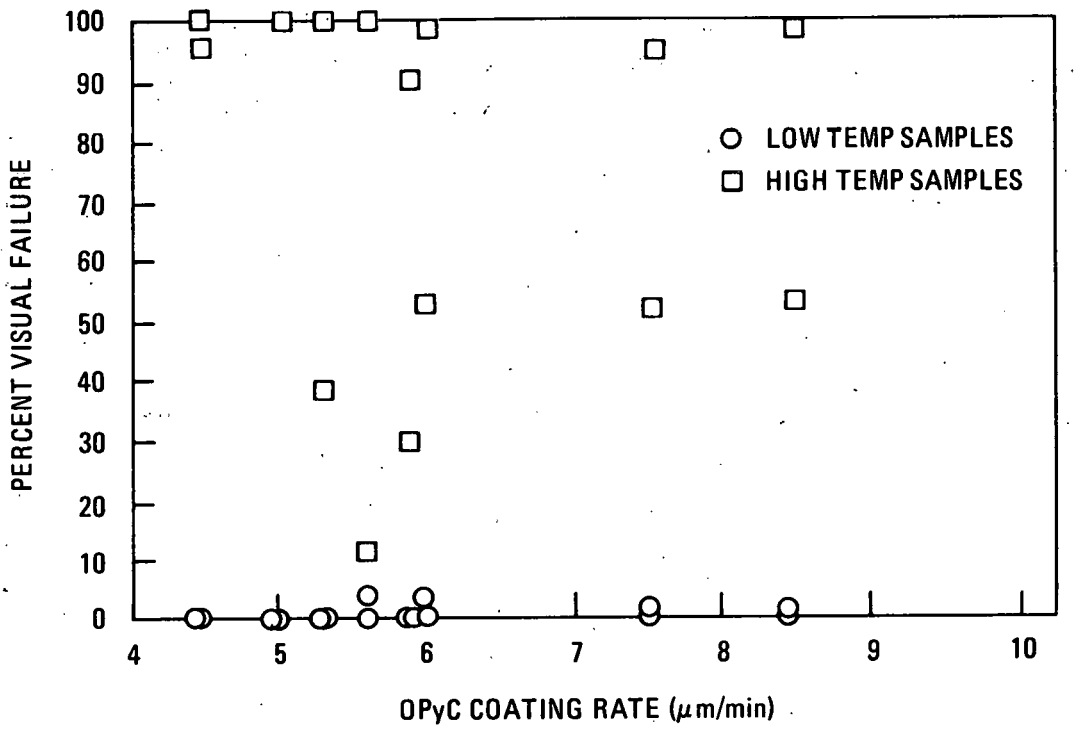

Fig. 5-17. HT-31 and HT-33 TRISO failure versus OPyC coating rate

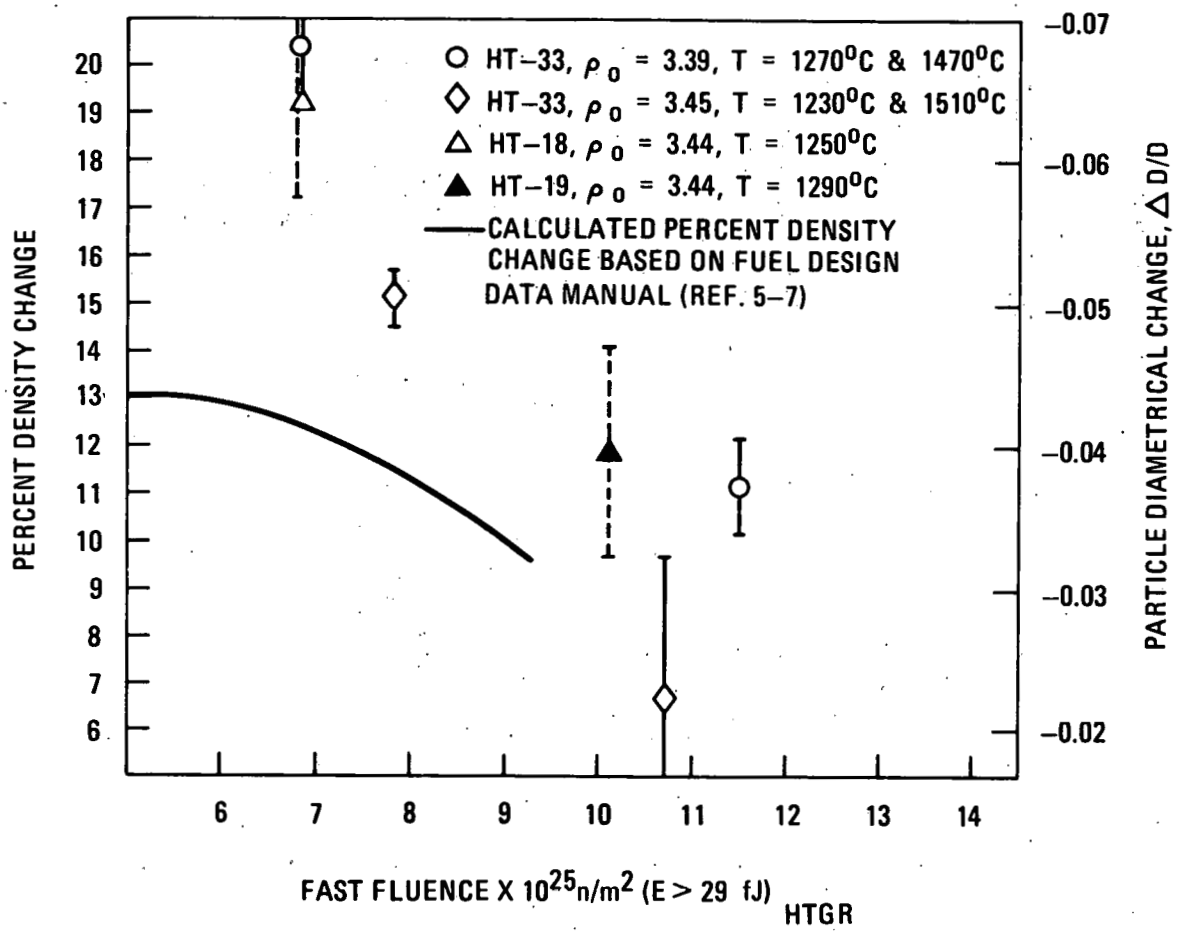

Fig. 5-18. Irradiation-induced density change in BISO samples HT-33, HT-18, and HT-19

in Ref. 5-7, are included in Fig. 5-18. The BISO particles shrink rapidly with the initial irradiation-induced densification of the pyrocarbon and then expand as the fission gas pressure increases with increasing burnup. The experimental data in Fig. 5-18 show a progressive reduction in the density, or increase in particle size, as the fast fluence increases from 6.5 to 11.5 x 10^{25} n/m^2 $(E > 29\ fJ)_{HTGR}$. The model also shows a reduction in density as the fluence increases; however, the predicted value is about 50% of the experimental values. This is attributed to the current BISO particle models, which do not adequately reflect the effects of OPyC anisotropy on particle dimensional change. These data will be useful in the development of an improved BISO model.

Figures 5-19 through 5-22 show BISO failure levels versus active coating gas ratio, density, microporosity, and coating rate. Figure 5-19 shows a high failure level for samples with coating gas ratios >0.40 that were irradiated in the low-temperature magazine. As shown in Fig. 5-20, the samples with densities >1.95 Mg/m^3 have high failure levels in the low-temperature magazine. The samples with the high failure levels have coating gas ratios >0.40 and OPyC densities ≥1.95 Mg/m^3, were fabricated with N_2 as the diluent gas, and have higher BAF_o values than the other samples. Figure 5-21 shows failure level versus microporosity. The failure level of low-temperature samples rises and falls between microporosity values of 17 to 25, but no conclusion can be drawn from this small amount of data. It is known, however, from the results of capsules HT-12 through HT-19 that high-density, high-anisotropy BISO coatings have higher failure rates at low temperatures (Ref. 5-8). Therefore, the high failure observed here was probably caused more by anisotropy of OPyC rather than the effects of microporosity. Figure 5-22 shows BISO failure versus OPyC coating rate. No correlation between coating rate and OPyC failure can be seen for these samples.

5.1.4.3. Heat-Treated BISO Particles. As was shown in Table 4-2, there was no significant difference between failure levels of heat-treated and as-coated BISO particle batches. Because the heat treating caused an increase in the BAF_o value and a decrease in coating thickness in some

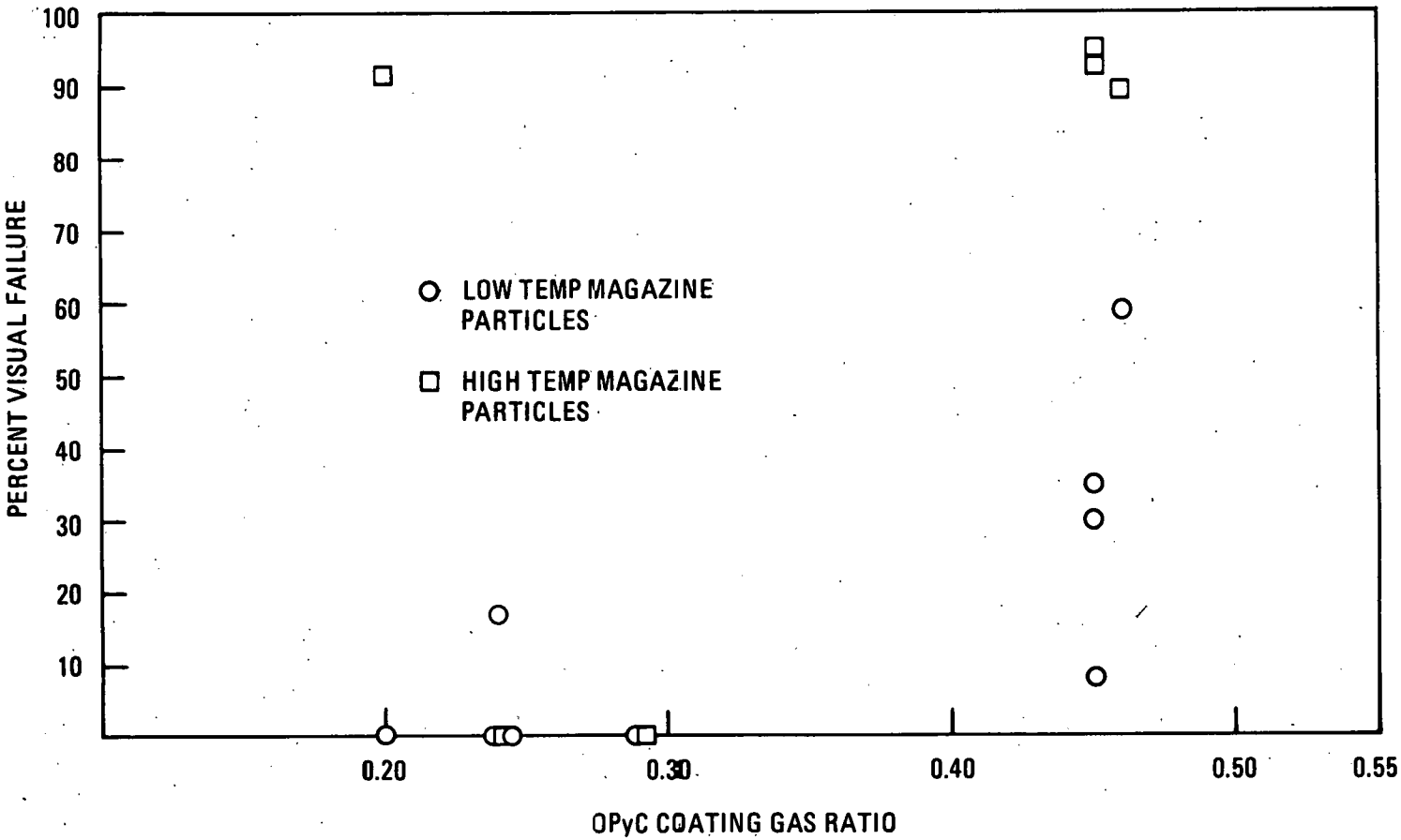

Fig. 5-19. HT-33 TRISO particle failure versus OPyC coating gas ratio

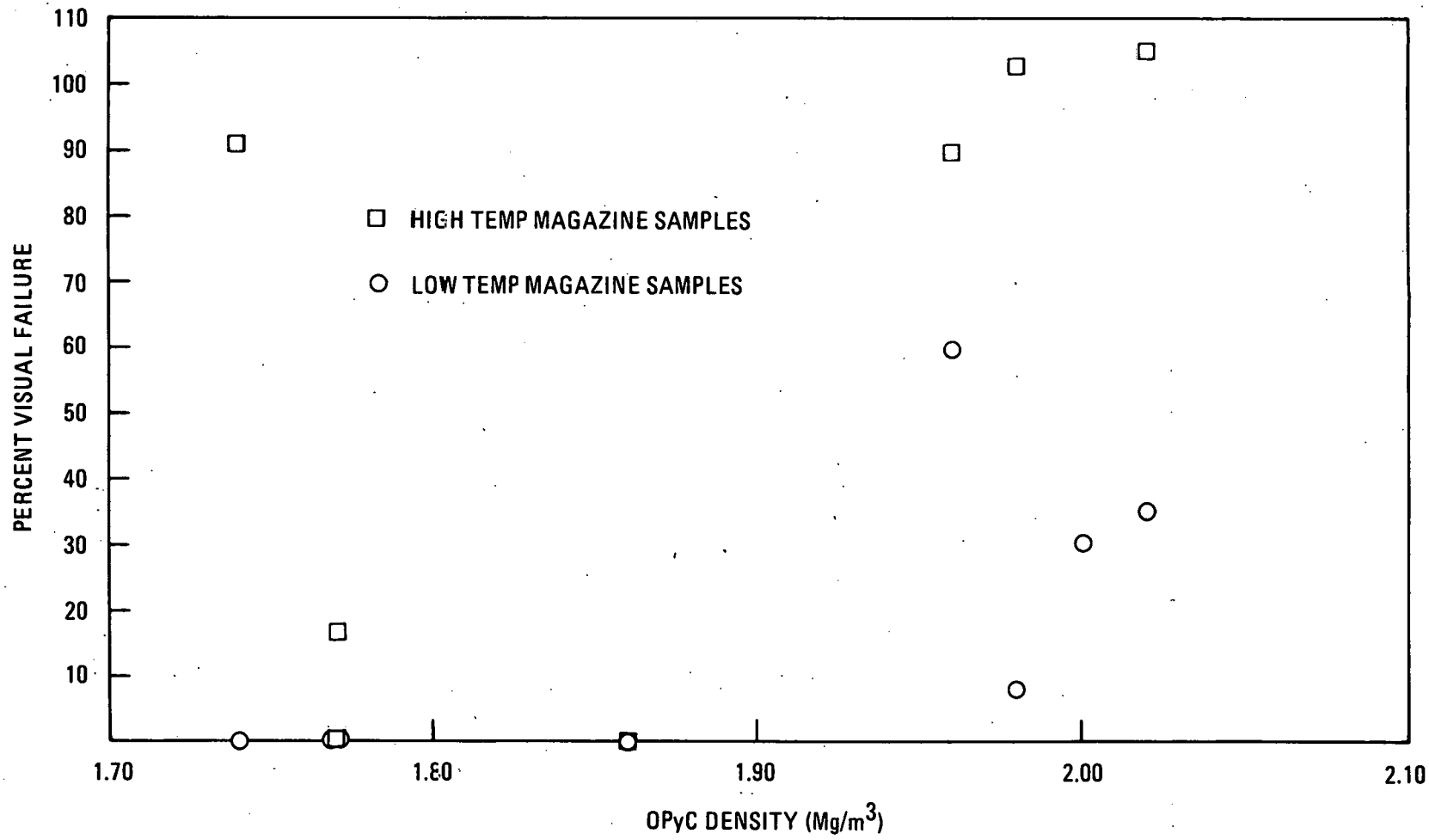

Fig. 5-20. HT-33 BISO particle failure versus OPyC density

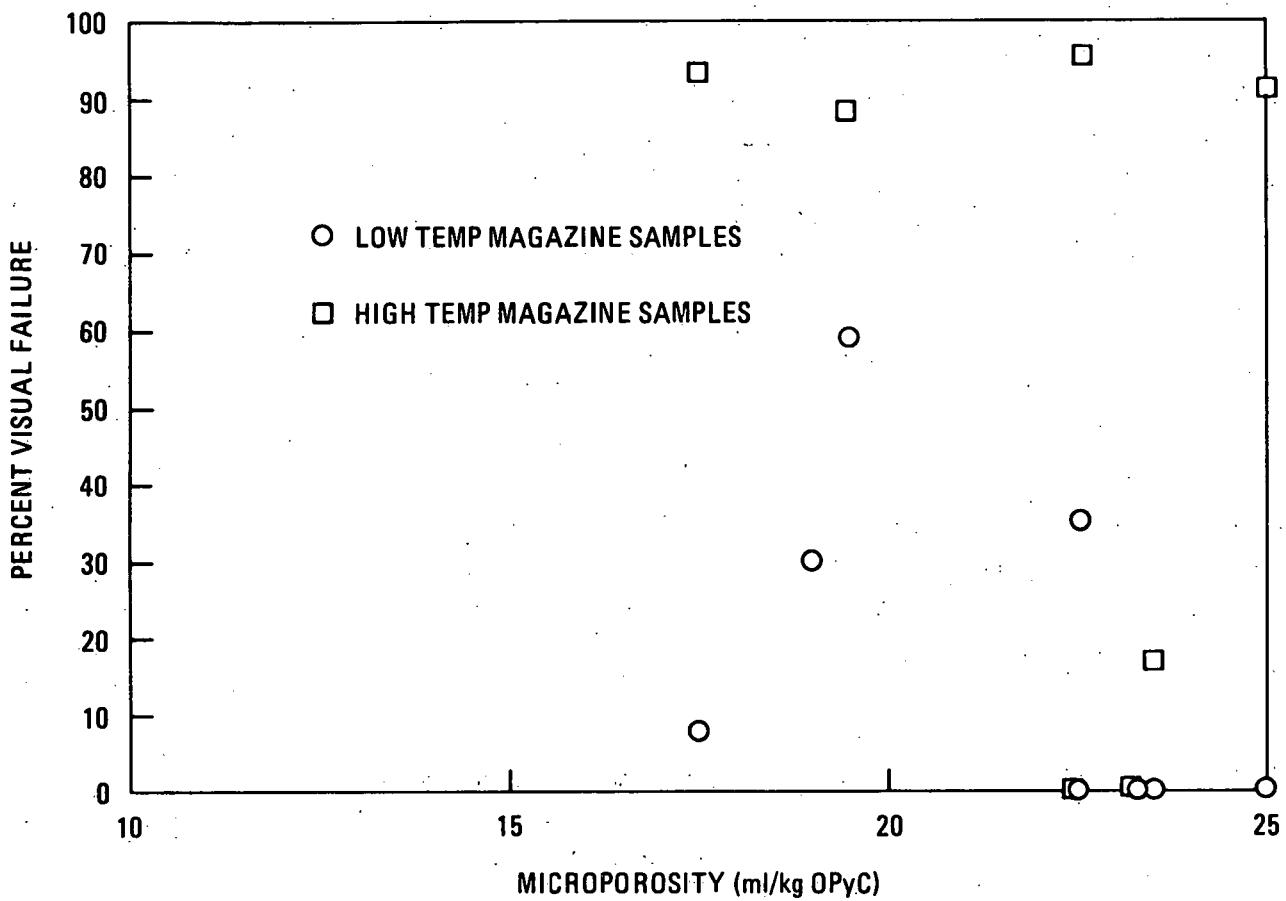

Fig. 5-21. HT-33 BISO particle failure versus microporosity

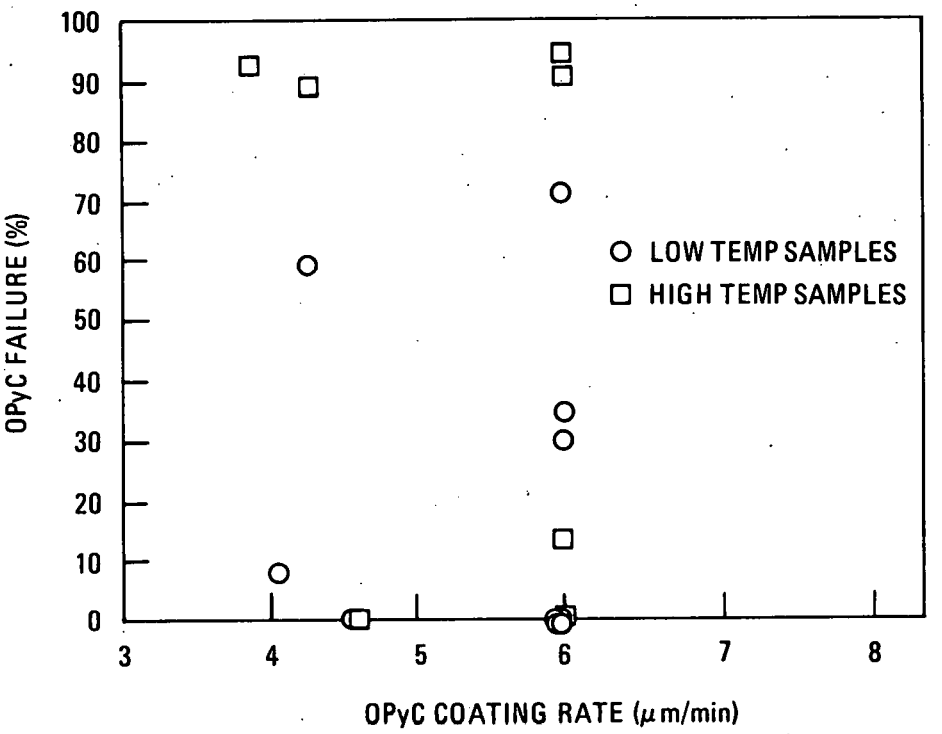

Fig. 5-22. BISO failure versus coating rate

batches, a higher failure level was expected for heat-treated samples from parent batch 6542-41-015. In the low-temperature magazine the samples from parent batch 6542-41-015 were in positions 11 and 13. The sample in position 11 had been heat treated and had a coating failure level of 35%. The sample in position 13 was not heat treated and had a coating failure level of 30%. The heat-treated sample had a 5% higher failure level than the as-coated sample; however, the heat-treated sample was irradiated at a higher temperature. The other comparison samples from positions 5 and 7 both showed zero coating failure. In the high-temperature magazine the as-coated sample from parent batch 6542-41-015 was lost and no comparison could be made. The other comparison samples were in positions 24 and 26. The as-coated sample showed 17.2% failure and the heat-treated sample showed zero failure, which was opposite to the expected failure performance. Figure 5-23 is a plot of BISO coating failure versus anisotropy and shows the failure levels of the heat-treated and as-coated particle samples. The failure levels seem to be more dependent on anisotropy and irradiation temperature than they are on heat treatment or any of the other OPyC variables.

REFERENCES

5-1. Wessman, G. L., General Atomic Company, "Response to NCR Lead Item I for ThO_2 Review," private communication to William Gammil, April 9, 1979.

5-2. Stansfield, O. M., et al., "Performance of ThO_2 in HTGR Fuel Particles," DOE Report GA-A14745, General Atomic Company, March 1978.

5-3. Kania, M. J., KFA, private communication, June 20, 1979.

5-4. Voice, E. H., "Key Parameters for the Evaluation of Silicon Carbide," Internal Document Dragon Project, June 5, 1974.

5-5. "HTGR Fuel Product Specification, Issue B," General Atomic Company, unpublished data.

5-6. Kovacs, W. J., "Technical Support Document, Issue C, HTGR Fuel Product Specification," General Atomic Company, unpublished data.

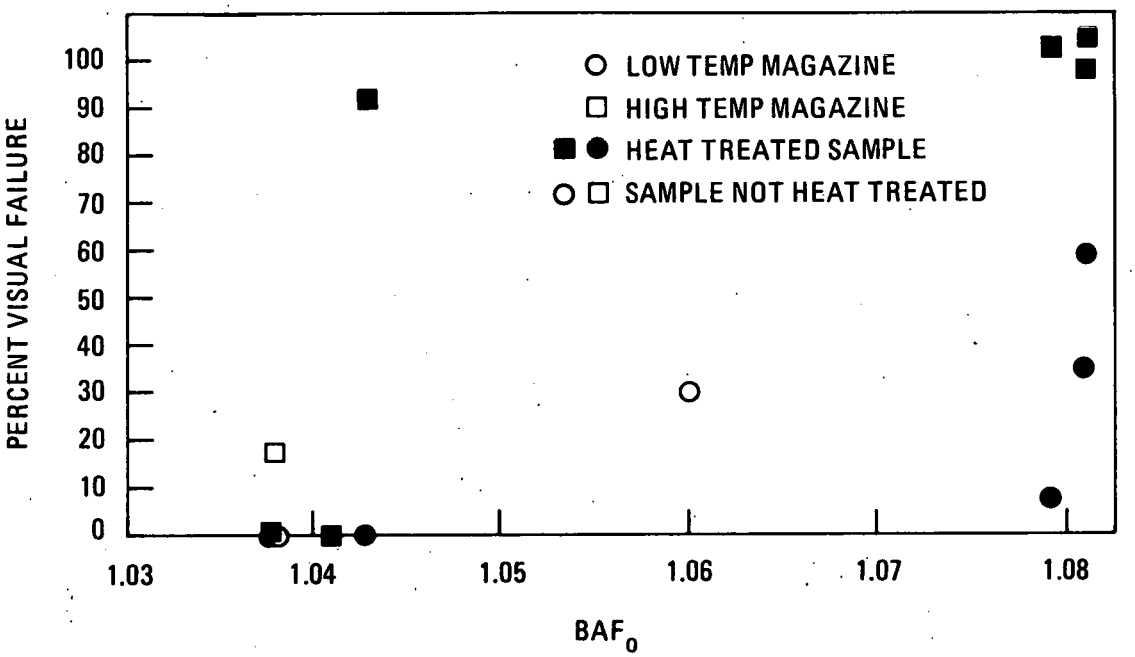

Fig. 5-23. Visual total coating failure versus anisotrophy

5-7. "Fuel Design Data Manual, Issue C," General Atomic Company, unpublished data.

5-8. Scott, C. B., "Evaluation of BISO and TRISO Coated ThO_2 Fuel Particles Irradiated in HFIR Capsules HT-12 Through HT-15 and HT-17 Through HT-19," ERDA Report GA-A13557, General Atomic Company, October 1977.

6. SUMMARY AND CONCLUSIONS

The HT capsule irradiation tests are performed to evaluate fertile particle coating designs. The data obtained from these accelerated tests can be used in performance model studies. The results of the HT-31 and HT-33 capsule irradiation tests are summarized as follows:

1. TRISO and BISO ThO_2 fuel fabricated in the 240-mm-diameter coater performs as well during irradiation as does fuel fabricated in the 127-mm-diameter coater.

2. The BISO and TRISO fuel showed no significant fission product release or failure up to a burnup of 7.5% FIMA at 1250°C for 2800 h. At 1250°C from 7.5% to 9.0% FIMA the BISO particles showed some failure, while the TRISO particles showed no failure or fission product release. At particle surface temperatures of about 1500°C, both TRISO and BISO fuel showed very high failure levels.

3. Two BISO samples from the high-temperature magazine showed zero total coating failure, but showed very high diffusional release of their cesium inventory.

4. No significant correlation between failure and the TRISO OPyC variables of active coating gas ratio, coating rate, anisotropy, density, or microporosity could be determined.

5. Anisotropy was the only OPyC variable that appeared to affect the failure of the BISO particles.

6. The effect of heat treatment alone on BISO OPyC performance could not be determined.

7. There was no discernible difference in the irradiation performance of the TRISO coatings of the 450-μm kernel particles and the larger 500-μm kernel particles.

8. The TRISO pressure vessel performance is consistent with the pressure vessel performance predicted by stress modeling.

9. Calculated in-pile kernel migration coefficients (KMCs) for TRISO ThO_2 particles from HT-31 were found to be in excellent agreement (within a factor of 1.5) with out-of-pile KMC values for BISO ThO_2 particles.

10. A white phase of metallic silicon was found in the lenticular flaws of the SiC in some of the TRISO batches after irradiation, but this did not affect the irradiation performance of these batches.

11. The shrinkage of BISO particles caused by irradiation is in qualitative agreement with predictions, but are about 50% greater than the predicted values.

7. ACKNOWLEDGMENTS

The author would like to thank the many people at ORNL and GA who assisted in the capsule irradiation and the postirradiation examination work, in particular, C. A. Young for the planning and execution of the postirradiation examinations; K. R. Thoms for in-reactor operation and the operating history; M. J. Kania and A. M. Howard for thermal analysis; E. L. Ryan and the staff of the High Radiation Experiment Laboratory for capsule disassembly and visual examination; E. L. Long for his invaluable help in coordinating GA's capsule work at ORNL; W. E. Simpson for hot cell metallography; the staff of the hot cell for postirradiation examination work; T. B. Crockett for the burnup analysis; J. S. Greenwood for the fission gas release measurements; P. R. Macy for the long-term heating test; C. E. Kaufman for density measurements; C. A. Young, C. L. Smith, B. F. Myers, W. J. Kovacs, O. M. Stansfield, J. W. Ketterer, and W. J. Scheffel for technical assistance; S. J. Helfrich for data reduction; and B. A. Yalof and R. E. Maze for editing of the manuscript.

GENERAL ATOMIC COMPANY
P. O. BOX 81608
SAN DIEGO, CALIFORNIA 92138